



UNIVERSITÀ
DEGLI STUDI
DI PADOVA

Sede Amministrativa: Università degli Studi di Padova

Dipartimento di Scienze Biomediche

CORSO DI DOTTORATO DI RICERCA IN: SCIENZE BIOMEDICHE SPERIMENTALI

CICLO: XXX

**EFFECTS OF PRESENILIN 2 MUTATIONS ASSOCIATED WITH
FAMILIAL ALZHEIMER'S DISEASE ON MITOCHONDRIAL
BIOENERGETICS**

Coordinatore: Ch.mo Prof. Paolo Bernardi

Supervisore: Ch.ma Prof.ssa Paola Pizzo

Co-Supervisore: Dott. Riccardo Filadi

Dottoranda: Alice Rossi

Index

Summary.....	5
--------------	---

Riassunto.....	7
----------------	---

Introduction

1. Alzheimer's Disease.....	11
1.1 The pathology.....	11
1.2 The γ -secretase complex.....	13
1.3 Presenilins.....	15
1.4 Amyloid Precursor Protein.....	17
1.5 The amyloid cascade hypothesis for AD.....	19
1.6 The hyper-phosphorylated tau hypothesis for AD.....	20
2. Ca²⁺ homeostasis.....	21
2.1 Plasma membrane.....	22
2.2 Endoplasmic Reticulum.....	24
2.3 Golgi Apparatus.....	27
2.4 Acidic Compartments.....	28
2.5 Mitochondria.....	29
2.5.1 Mitochondria Calcium Uniporter (MCU).....	30
2.5.2 Other proteins involved in mitochondrial Ca ²⁺ uptake.....	35
2.5.3 Mitochondrial Ca ²⁺ efflux.....	36
2.5.4 Physiological consequences of mitochondrial Ca ²⁺ uptake.....	37
2.6 ER-mitochondria cross-talk: microdomains and mitochondria associated membrane.....	39
2.6.1 ER-mitochondria tethering and diseases.....	42
2.7 The Ca ²⁺ hypothesis for AD.....	43
3. Bioenergetics.....	47
3.1 Brain metabolism: neurons/astrocytes differences and their metabolic coupling.....	47
3.2 Glucose metabolism.....	51
3.2.1 Glycolysis.....	52
3.2.2 Pentose Phosphate pathway.....	53
3.3 Mitochondrial metabolism.....	53
3.3.1 TCA cycle and oxidative phosphorylation.....	53
3.3.2 Glutamine pathway.....	56

3.3.3	The role of Ca ²⁺ in mitochondria metabolism regulation.....	57
3.4	Substrates and mitochondria.....	60
3.4.1	Voltage Dependent Anion Channel.....	60
3.4.2	Hexokinase.....	62
3.4.3	The Mitochondrial Carrier System.....	64
3.5	AMPK.....	68
3.6	Mitochondrial dysfunctions and Alzheimer’s Disease.....	70
 Aim of the work		 73
 Results		
1.	FAD-linked PS2 mutants, but not PS1, affect mitochondrial ATP production..	75
2.	The FAD-linked PS2-T122R mutant does not impair glycolysis.....	81
3.	Mitochondrial defects caused by FAD-linked PS2 mutants are partly due to Ca ²⁺ dysregulation.....	83
4.	FAD-linked PS2 mutants, but not PS1, affect mitochondrial functionalities.....	85
5.	FAD-linked PS2 mutants induce the detachment of Hexokinase1 from mitochondria.....	87
6.	FAD-PS2-induced Hexokinase1 detachment from mitochondria contributes to mitochondrial impairment.....	90
7.	The FAD-PS2-T122R mutant causes mitochondrial pyruvate import defect and cytosolic pyruvate accumulation.....	97
 Discussion		 99
 Materials and Methods		 107
 References		 117

Summary

Alzheimer's Disease (AD) is a neurodegenerative disorder of the central nervous system. It is mainly sporadic, however, a little percentage of cases is inherited (Familial AD, FAD) and due to autosomal dominant mutations on three different genes, coding for Amyloid Precursor Protein (APP), Presenilin 1 (PS1) and Presenilin 2 (PS2). Presenilins, mainly localized at Endoplasmic Reticulum (ER) membranes, are the catalytic core of the γ -secretase complex, although several γ -secretase-independent activities of PSs, such as modulation of neurites outgrowth, apoptosis, autophagy, synaptic functions and regulation of Ca^{2+} homeostasis, have been described.

Ca^{2+} , a key intracellular second messenger, is involved in multiple cellular functionalities. Interestingly, alterations in Ca^{2+} homeostasis have been proposed as an early event in different neurodegenerative diseases, including AD. Notably, FAD-PS mutants have been reported to be directly involved in these dysregulations. In our lab, it has been previously showed that PS2 expression, both WT and, more potently, FAD mutants (such as PS2-T122R), but not PS1, decreases the ER Ca^{2+} content, mainly by inhibiting SERCA pump activity. Moreover, PS2 increases ER-mitochondria physical and functional coupling, favouring the process of ER to mitochondria Ca^{2+} transfer. However, due to its effect on ER $[\text{Ca}^{2+}]$, which results in a lower amount of available Ca^{2+} within the ER, its expression dampens mitochondrial Ca^{2+} rises upon cell stimulation.

Based on the well-established role of Ca^{2+} on mitochondrial metabolism, here we investigate the possible effects on mitochondrial functionalities of the complex balance between alterations in ER Ca^{2+} content and increased ER-mitochondria coupling, induced by FAD-PS2 mutants expression. A neuroblastoma cell line (SH-SY5Y) grown in a medium containing galactose, as a substitute of glucose, has been used. This growth condition enhances mitochondrial metabolism and results in an excellent experimental protocol to visualize possible mitochondrial defects.

Lower total cellular ATP levels were measured in FAD-PS2-T122R expressing cells, grown either in glucose- or galactose-containing medium, with the reduction more evident in the latter condition, thus suggesting possible mitochondrial defects induced by PS2 expression.

In order to investigate how Ca^{2+} dysregulation induced by PS2 could influence mitochondrial metabolism, we stimulated mitochondrial ATP production inducing ER Ca^{2+} release, followed by mitochondria Ca^{2+} uptake, using both bradykinin, as a maximal IP3R stimulation, and Fetal Calf Serum (FCS), as a more physiological stimulus. In both conditions, a reduction in mitochondrial ATP production, measured by a mitochondrial luciferase-based ATP probe, has been observed in cells expressing FAD-PS2, but not PS1. The defects in ATP synthesis were observed in SH-SY5Y, MEF, HT22 cells and in cortical neurons from PS2-N141I transgenic (Tg) mice (PS2.30H), by employing FRET-based ATP probes (ATeam 1.03) specifically targeted to the mitochondrial matrix or the nucleus. We also evaluated the glycolytic flux in these cells, by both employing a cytosolic luciferase-based ATP probe and measuring the extracellular medium acidification, but we did not observed any difference in these two parameters in FAD-PS2 expressing cells, compared to controls.

In order to understand the mechanism through which PS2 causes the observed mitochondrial dysfunction, we firstly considered the marked Ca^{2+} dysregulation induced by PS2 expression. We thus decided to modulate Ca^{2+} handling in control cells, to mimic the ER Ca^{2+} depletion caused by PS2 expression. We used two different approaches: i) treating control cells with a SERCA pump inhibitor (Cyclopiazonic acid, CPA), to partially reduce the ER Ca^{2+} content, or ii) overexpressing a mutated-MICU1 ($\text{MICU1}^{\text{mut}}$), a component of the mitochondrial Ca^{2+} uniporter complex. Although both approaches were able to reduce the capacity of control cells to produce ATP, for similar mitochondrial Ca^{2+} uptake in control and PS2-expressing cells, a lower mitochondrial ATP production in FAD-PS2 expressing-cells compared to CPA-treated

or MICU1^{mut} expressing controls was still observed. Taken together, these results suggest that part of the FAD-PS2-induced defects in mitochondrial metabolism is due to a reduced ER Ca²⁺ content and, consequently, mitochondrial Ca²⁺ uptake, negatively regulating the Ca²⁺-dependent mitochondrial metabolism. However, additional mechanisms, induced by FAD-PS2, are likely involved in mitochondrial dysfunctions. We thus evaluated the respiratory chain activity measuring the oxygen consumption rate (OCR): both basal and maximal OCR were reduced in FAD-PS2, but not in FAD-PS1, expressing cells. Moreover, a reduced mitochondrial ATP-linked respiration was measured in PS2-T122R expressing cells, while no difference was found in the proton leak.

Since the expression levels of the ATP synthase and the respiratory chain complexes were not affected by FAD-PS2 expression, and isolated mitochondria from WT and PS2-N141I Tg mice did not reveal substantial differences in mitochondrial respiratory activity, we reasoned that the impairment in ATP production observed in intact cells is not due to defective mitochondria *per se*, but likely depends on the cellular environment.

Importantly, for a proper mitochondrial metabolism, the right amount of substrates produced through glycolysis in the cytosol has to reach the mitochondrial matrix to support the TCA cycle and the respiratory chain activity. Hexokinase1 (HK1), the enzyme that catalyses the first step of glycolysis converting glucose to glucose 6-phosphate, seems to be involved in the modulation of the mitochondrial substrates import, since HK1 interaction/detachment with/from mitochondria can modulate mitochondrial substrates permeability. Firstly, we measured a reduced HK1-mitochondria co-localization in FAD-PS2 expressing SH-SY5Y cells, in FAD-PS2 patient-derived fibroblasts and in primary cortical neurons from FAD-PS2-N141I Tg mice, compared to controls. By mimicking the FAD-PS2 effect on HK1-mitochondria interaction treating control cells with Clotrimazole, a drug capable to detach HK1 from mitochondria, a reduced mitochondrial ATP production was measured; however, the impairment on ATP production induced by clotrimazole was less marked than that caused by FAD-PS2 expression. These results indicate that, although the detachment of HK1 from mitochondria plays a pivotal role in causing mitochondrial defects upon FAD-PS2 expression, the PS2-induced Ca²⁺ dysregulation, described above, may additionally contribute to the overall mitochondrial impairment. These results have been confirmed also by a genetic approach. We down-regulated the expression of endogenous HK1, by specific siRNAs, and we rescued HK1 protein level by over-expressing siRNA-resistant full-length- (FL-HK1) or truncated- (Tr-HK1) HK1. This latter protein lacks the mitochondrial binding domain, but still conserves the catalytic activity. We found that, upon endogenous HK1 silencing, mitochondrial ATP production is strongly reduced. Interestingly, while the re-expression of FL-HK1 was able to completely rescue the reduced ATP production, the Tr-HK1 was unable to do it, again confirming that the detachment of HK1 from mitochondria is involved in the mitochondrial impairment caused by FAD-PS2.

Related to HK1 and its role in the regulation of mitochondrial substrates permeability, an increase in the cytosolic amount of pyruvate was measured in FAD-PS2 expressing cells, compared to controls, employing a cytosolic FRET-based pyruvate probe, Pyronic. Importantly, by pharmacologically blocking mitochondrial pyruvate carrier (MPC), the protein responsible for mitochondrial pyruvate uptake, with two different drugs, UK5099 and Pioglitazone, no differences were anymore detected between control and FAD-PS2 expressing cells, suggesting that FAD-PS2 is acting on this pathway.

Overall, we have showed that FAD-PS2 mutants decrease cellular ATP levels, in particular mitochondrial ATP production, by two different mechanisms: 1) causing Ca²⁺ dysregulation, mainly decreasing the ER Ca²⁺ content, and thus the amount of Ca²⁺ available for mitochondrial Ca²⁺ uptake; 2) inducing the detachment of HK1 from mitochondria, likely affecting the availability of substrates (*i.e.*, pyruvate) for mitochondria. Further experiments will be aimed at: i) evaluate the impact of the PS2-dependent strengthened ER-mitochondria

coupling on the reported mitochondrial defects; ii) defining the molecular mechanism through which FAD- PS2 mutants affect HK1 intracellular distribution; iii) evaluate the impact of these alterations on the onset/progression of the AD phenotype.

Riassunto

La malattia di Alzheimer è un disturbo neurodegenerativo del sistema nervoso centrale. È, principalmente, una malattia sporadica; tuttavia in una piccola percentuale di casi è ereditata e dovuta a mutazioni autosomiche dominanti in tre diversi geni, che codificano per la Proteina Precursore dell'Amiloide (APP), per Presenilina1 (PS1) e per Presenilina2 (PS2). Le preseniline, principalmente localizzate nella membrana del reticolo endoplasmatico (RE), costituiscono la porzione catalitica del complesso enzimatico della γ -secretasi. Le stesse, oltre ad essere fondamentali per l'attività di questo complesso enzimatico, hanno molte funzioni che sono indipendenti dalla γ -secretasi; tra queste, la modulazione della crescita dei neuriti, dell'apoptosi, dell'autofagia, delle funzioni sinaptiche e dell'omeostasi del Ca^{2+} .

Il Ca^{2+} è un secondo messaggero intracellulare fondamentale, coinvolto in molteplici funzionalità cellulari; alterazioni dell'omeostasi del Ca^{2+} sono state proposte come eventi precoci in diverse malattie neurodegenerative, tra cui la malattia di Alzheimer. In particolare, è stato dimostrato che mutazioni in PS2 associate a forme familiari di Alzheimer (FAD) sono direttamente coinvolte in queste alterazioni. Nel nostro laboratorio è stato precedentemente dimostrato che l'espressione di PS2, sia della forma WT ma soprattutto delle forme mutate associate a FAD (come PS2-T122R), ma non di PS1, riduce il contenuto di Ca^{2+} nel RE principalmente inibendo l'attività della pompa SERCA. PS2, inoltre, aumenta la vicinanza fisica e funzionale di RE e mitocondri, favorendo il processo di trasferimento di Ca^{2+} tra i due organelli; tuttavia, a causa del suo effetto sulla $[Ca^{2+}]$ nel RE, che ha come conseguenza una minore quantità di Ca^{2+} disponibile per il rilascio nel citosol, la quantità di Ca^{2+} che entra nei mitocondri, dopo stimolazione, è ridotta.

Sulla base del ruolo fondamentale svolto dal Ca^{2+} nella regolazione del metabolismo mitocondriale, nel lavoro presentato in questa tesi abbiamo esaminato i possibili effetti sulla funzionalità mitocondriale del complesso equilibrio tra alterazioni del contenuto di Ca^{2+} nel RE e l'aumento della vicinanza tra RE e mitocondri, indotti dall'espressione di forme mutate di PS2 legate a FAD. Per svolgere questo studio abbiamo utilizzato una linea cellulare di neuroblastoma (SH-SY5Y), cresciuta in un terreno contenente galattosio, invece di glucosio. Infatti, le cellule cresciute in un terreno che contiene galattosio aumentano il metabolismo mitocondriale, rendendo così questo protocollo sperimentale ottimale per evidenziare eventuali difetti mitocondriali.

In cellule esprimenti FAD-PS2-T122R, cresciute in un terreno contenente glucosio o galattosio, sono stati misurati livelli totali di ATP cellulare minori rispetto a quelli di cellule di controllo. La riduzione di questo parametro era più evidente in cellule cresciute in terreno contenente galattosio, suggerendo possibili difetti mitocondriali indotti da PS2.

Per studiare come la deregolazione del Ca^{2+} , causata dall'espressione di PS2, possa influenzare il metabolismo mitocondriale, abbiamo indotto il rilascio di Ca^{2+} dal RE, a cui segue un aumento di Ca^{2+} nei mitocondri che conseguentemente stimola la produzione di ATP mitocondriale. A tal fine abbiamo utilizzato sia bradichinina, come stimolo massimale del recettore IP3, sia siero fetale di vitello (FCS), contenente fattori che inducono una stimolazione più fisiologica dello stesso recettore. In entrambe le condizioni, è stata osservata una riduzione nella produzione di ATP mitocondriale, misurata utilizzando luciferasi (in particolare la sonda mitocondriale), in cellule esprimenti FAD-PS2, ma non in cellule che esprimevano FAD-PS1. I difetti nella sintesi di ATP sono stati osservati in cellule SH-SY5Y, MEF,

HT22 e in neuroni corticali di topi FAD-PS2-N141I (Tg, PS2.30H), utilizzando anche sonde per l'ATP basate su FRET (ATeam 1.03), contemporaneamente espresse nella matrice mitocondriale e nel nucleo. Abbiamo anche valutato se l'espressione di FAD-PS2 potesse influenzare la glicolisi; per fare questo, abbiamo espresso in cellule una luciferasi citosolica, per valutare l'ATP prodotta nel citoplasma, e abbiamo misurato l'acidificazione del mezzo extracellulare, come indice di glicolisi. Per entrambe i parametri, non abbiamo osservato alcuna differenza tra cellule esprimenti FAD-PS2 o di controllo.

Per comprendere il meccanismo attraverso il quale PS2 causa la disfunzione mitocondriale osservata, data la nota deregolazione dell'omeostasi del Ca^{2+} indotta da PS2, abbiamo innanzitutto deciso di simulare la deplezione di Ca^{2+} nel RE causata dall'espressione di PS2 nelle cellule di controllo. Abbiamo usato due approcci diversi: da un lato abbiamo trattato le cellule di controllo con un inibitore della pompa SERCA (acido ciclopiazonico, CPA) per ridurre il contenuto di Ca^{2+} nel RE, dall'altro abbiamo sovraespresso una forma mutata di MICU1 (MICU1^{mut}). In entrambi i casi abbiamo ottenuto una riduzione nell'entrata di Ca^{2+} nel mitocondrio, mimando perfettamente il difetto causato dall'espressione di FAD-PS2. Come atteso, il trattamento con CPA e l'overespressione di MICU1^{mut} riducono notevolmente la produzione di ATP rispetto alle cellule di controllo non trattate. Ciononostante, a parità di Ca^{2+} che entra nel mitocondrio in cellule esprimenti o meno FAD-PS2, abbiamo misurato una minore produzione di ATP mitocondriale in cellule esprimenti forme mutate di PS2, rispetto ai controlli trattati con CPA o esprimenti MICU1^{mut}. Tali risultati suggeriscono che i difetti nel metabolismo mitocondriale indotti dall'espressione di FAD-PS2 solo almeno in parte riconducibili alla riduzione del contenuto di Ca^{2+} nel RE, e quindi al suo ingresso nei mitocondri. Tuttavia, sono probabilmente coinvolti meccanismi aggiuntivi nelle disfunzioni mitocondriali osservate. Abbiamo, quindi, valutato l'attività della catena respiratoria misurando la velocità nel consumo di ossigeno (OCR). È stato così possibile osservare che sia il consumo di ossigeno a basale che il massimo consumo di ossigeno sono ridotti in cellule esprimenti FAD-PS2, ma non FAD-PS1. Inoltre, in cellule esprimenti PS2-T122R è stata misurata una riduzione della respirazione mitocondriale legata alla produzione di ATP. Tuttavia, poiché i livelli di espressione dell'ATP sintasi e dei complessi della catena respiratoria non variano, in seguito all'espressione di PS2, e dato che misure di respirazione in mitocondri isolati da topi WT e PS2-N141I Tg non hanno rivelato differenze sostanziali, la riduzione nella produzione di ATP osservata in cellule intatte non è verosimilmente dovuta ad un'alterazione intrinseca nell'attività della catena respiratoria. Questo suggerisce che i difetti riscontrati possano dipendere dall'ambiente cellulare, piuttosto che da un difetto intrinseco degli stessi mitocondri.

Per un corretto metabolismo mitocondriale, la giusta quantità di substrati prodotti nel citoplasma attraverso la glicolisi deve raggiungere la matrice mitocondriale per supportare il ciclo di Krebs e l'attività della catena respiratoria. L'esochinasi 1 (HK1), enzima che catalizza la prima reazione della glicolisi, convertendo il glucosio in glucosio 6-fosfato, sembra anche modulare l'ingresso dei substrati nei mitocondri, poiché l'interazione/distacco di HK1 con/dai mitocondri può modulare la permeabilità mitocondriale ai substrati. Abbiamo misurato una riduzione nella co-localizzazione tra HK1 e mitocondri in cellule SH-SY5Y esprimenti FAD-PS2, in fibroblasti da pazienti FAD con mutazioni in -PS2 e in neuroni corticali da topi transgenici FAD-PS2. Il trattamento di cellule di controllo con clotrimazolo, una sostanza nota per avere la capacità di indurre il distacco di HK1 dai mitocondri, si è rivelato capace di ridurre la colocalizzazione tra HK1 e mitocondri a un livello simile a quello causato da PS2, mimandone così l'effetto. In seguito a questo trattamento, cellule di controllo mostravano una ridotta produzione di ATP mitocondriale, rispetto a cellule non trattate; tuttavia, l'effetto del clotrimazolo sulla produzione di ATP era meno evidente rispetto alla diminuzione causata dall'espressione di FAD-PS2. Questo significa che, anche se il distacco di HK1 dai mitocondri svolge un ruolo importante nel determinare i difetti mitocondriali osservati in seguito a

espressione di FAD-PS2, la disfunzione nell'omeostasi del Ca^{2+} , descritta in precedenza, contribuisce anch'essa alla diminuzione complessiva dell'attività mitocondriale. Questi risultati sono stati confermati anche con un approccio genetico. Abbiamo abbattuto l'espressione di HK1 endogena, mediante specifici siRNAs e abbiamo sovra-espresso la forma intera di HK1 (FL-HK1) o la forma tronca di HK1 (Tr-HK1), proteina quest'ultima che manca del dominio di legame mitocondriale ma che presenta ancora l'attività catalitica. Il silenziamento della proteina endogena causa una notevole riduzione nella produzione di ATP mitocondriale; la ri-espressione di FL-HK1 è in grado di recuperare completamente il difetto nella produzione di ATP, mentre quella di Tr-HK1 no. Questi risultati confermano nuovamente che il distacco di HK1 dai mitocondri è coinvolto nella manifestazione dei difetti mitocondriali osservati in seguito all'espressione di FAD-PS2. Relativamente a HK1 e al suo ruolo nella regolazione della permeabilità mitocondriale ai substrati, in cellule esprimenti PS2 è stato misurato un aumento nella quantità di piruvato nel citoplasma. È importante notare come il blocco farmacologico della proteina responsabile del trasporto del piruvato all'interno del mitocondrio (MPC) con due diversi farmaci, UK5099 e Pioglitazone, annulli le differenze tra le cellule esprimenti FAD-PS2 e i controlli, indicando che l'espressione di FAD-PS2 agisce anche su questa via metabolica.

In questo lavoro, abbiamo mostrato che forme mutate di PS2 legate a FAD diminuiscono i livelli cellulari di ATP, in particolare la produzione di ATP mitocondriale, con due diversi meccanismi: 1) causando una deregolazione dell'omeostasi del Ca^{2+} , principalmente diminuendo il contenuto di Ca^{2+} nel RE, e quindi il conseguente ingresso di Ca^{2+} nel mitocondrio; 2) inducendo il distacco di HK1 dai mitocondri, influenzando così la disponibilità di substrati (per es., piruvato) per i mitocondri. Ulteriori esperimenti saranno finalizzati a: i) valutare l'impatto dell'aumento della vicinanza tra RE e mitocondri causato dall'espressione di PS2 sui difetti mitocondriali riportati; ii) definire il meccanismo molecolare attraverso il quale FAD-PS2 induce il distacco di HK1 dai mitocondri; iii) valutare l'eventuale impatto di queste alterazioni nella progressione del fenotipo AD.

Introduction

1. Alzheimer's Disease

1.1 The pathology

Alzheimer's Disease (AD) is a devastating neurodegenerative disorder of the central nervous system. Nowadays, it represents the most common cause of dementia afflicting over 35 million people in the world (Forner S *et al.*, Rev Trends Neurosci 2017).

Old age is the strongest risk factor for developing AD, however environmental factors, diet and metabolic dysfunctions are progressively becoming more important in the onset of the pathology (Förstl H and Kurz A, Eur Arch Psychiatry Clin Neurosci 1999).

Although many efforts have been carried out to uncover the causes of this disease, currently no effective therapies are available and palliative treatments are used to partially slow down the progression of dementia symptoms (Holtzman DM *et al.*, Sci Trans Med 2011).

AD is characterized by a slow loss in memory and other cognitive abilities. The time course of the disease is about 7-10 years and it culminates in death; in details, the following features mainly characterize its development (Förstl H and Kurz A, Eur Arch Psychiatry Clin Neurosci 1999; Holtzman DM *et al.*, Sci Trans Med 2011) :

- (1) in the early stage of AD (lasting 2-5 years): recent memory impairment and mild cognitive deficits, such as changes in attention and problem-solving abilities;
- (2) in the moderate stage (lasting 2-4 years): long-term memory impairment and loss of the ability to operate independently; impairments in the basic activities of daily living (such as bathing or dressing);
- (3) in the severe stage (after 5-10 years from the first symptoms): learning deficits, language dysfunction, loss of the ability to recognize familial faces, hallucinations, aggressive behaviour, ambulatory regression, aphasia and impairment of daily living.

AD is divided, based on the age of onset, in the most common "late onset" (LOAD) cases that affects > 65 year old patients, and "early onset" cases (EOAD), that represent less than 5 % of AD cases and arise in 30-60 year old people. Among the EOAD cases, the 15 % are familial forms of AD (FAD); FAD cases represent less than 1 % of total AD and they are due to autosomal dominant mutation in three genes coding for Amyloid Precursor Protein (APP),

Presenilin 1 (PS1) and Presenilin2 (PS2). Mutations in PS1 are associated with more severe phenotype.

AD was described for the first time about 100 years ago (in 1906) by Alois Alzheimer, a German neurologist, who published the analysis of the brain of a woman suffering of FAD. Post-mortem analysis of brain specimens coming from AD patients revealed that, from a macroscopic point of view, the cortex, especially at the fronto-temporal cortex and parietal lobe, is characterized by a moderate atrophy, while a more severe atrophy damages the hippocampus (Figure 1). The loss of brain tissue is generally associated with a dilation of the lateral ventricles. Additional studies using different neuroimaging techniques (such as 18F-FDG PET, able to reveal brain regional glucose hypo-metabolism) and fluid biomarkers suggest that AD could be detected pre-clinically, although to date there is not yet consensus on their diagnostic use (Perrin RJ *et al.*, Nature 2009).

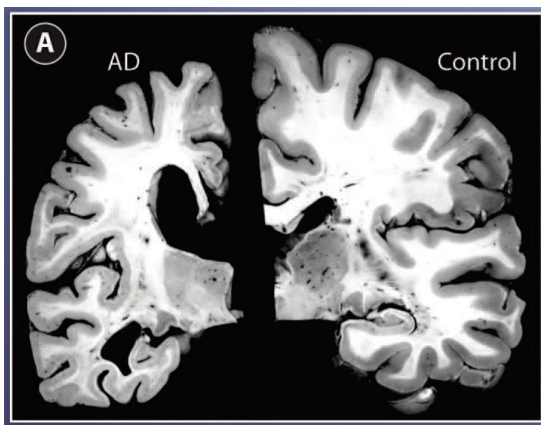


Figure 1 Post mortem brain section from an AD patient (left) compared with that of a cognitively normal individual (right). Modified from David M. Holtzman., 2011.

On the other hand, from a microscopic point of view, the hallmarks of AD are two: neurofibrillary tangles (NFTs) and senile plaques (Figure 2).

NFTs are abnormal fibrous inclusions within the perikaryal cytoplasm of some neurons but, most commonly, they are found along dystrophic axons that surround senile plaques. They are made of abnormal, 10 nm in diameter, thick fibrils, occurring in pairs and organized in a helical fashion, with a regular periodicity of 80 nm. They are mainly formed by the microtubule-associated protein tau, together with other proteins such as ubiquitin, cholinesterases and beta-amyloid (Perl DP, Mt Sinai J Med 2010). Tau binds tubulin and stabilizes microtubules. In AD, tau hyper-phosphorylation causes its dissociation from microtubules, increasing its tendency to self-aggregate. Data strongly suggest that neurofibrillary pathology contributes to

neuronal dysfunction and correlates with the clinical progression of AD (Holtzman DM *et al.*, Sci Trans Med 2011).

Senile plaques, or amyloid plaques, are brain extracellular accumulations of A β peptides, deriving from APP processing that assume beta-sheet configuration and form insoluble fibrils, eventually constituting large aggregates. In addition to these extracellular amyloid-like structures, in AD brains insoluble plaques of α -synuclein and huntingtin are reported as well. The central core of amyloid plaques is made by different proteins, such as heparin sulphate glycoproteins, apolipoprotein E and complement proteins (Perl DP, Mt Sinai J Med 2010). The plaques are often surrounded by dystrophic neurites, microglia and reactive astrocytes (cells involved in the inflammatory response). Whether these latter cells are actively involved in the pathogenesis of the disease is still a matter of intense debate. Nowadays, a consensus has formed around the idea that the inflammatory processes, mediated by glial cells, can aggravate the intrinsic amyloid toxicity.

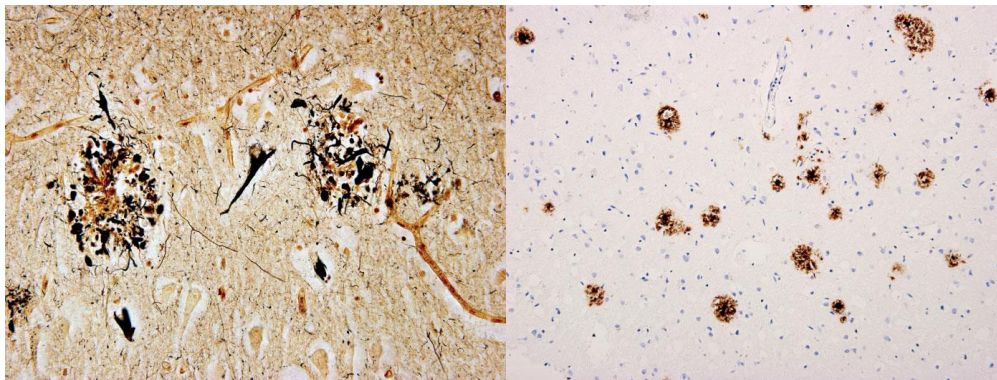


Figure 2 (left) Two amyloid plaques surrounded by dystrophic neurites and a neurofibrillary tangle between them in the cortex of an AD patient; (right) Immuno-histochemical techniques allow to visualize amyloid plaques (modified from Perl DP, Mt Sinai J Med 2010).

1.2 The γ -secretase complex

γ -secretase is a large enzymatic complex made by four different integral membrane proteins; it is the enzyme responsible for the generation of A β peptides from the cleavage of the C-terminal fragment of APP. γ -secretase is an aspartyl-protease that cleaves different substrates, with low specificity (Tolia A and De Strooper B, Semin Cell Div Biol 2009). In addition to APP, it cleaves Notch, Delta1, E- and N-cadherins, CD44, ErbB4 and the β 2 subunit of the voltage dependent Na⁺ channel (McCarthy JV *et al.*, Cell Mol Life Sci 2009).

γ -secretase is made by four components that form a complex with a stoichiometry 1:1:1:1. Presenilin (either PS1 or PS2) is the catalytic core of the γ -secretase (see below) while

Nicastrin (NCT), Anterior Pharynx-defective 1 (Aph-1) and Presenilin Enhancer-2 (Pen-2) have structural functions (Tolia A and De Strooper B, *Semin Cell Div Biol* 2009) (Figure 3).

NCT is a type I glycoprotein (80-130 kDa depending on the glycosylation state) with a trans-membrane (TM) domain that allows its interaction with the other components of the enzyme, Aph-1 and PSs (Yu G *et al.*, *Nature* 2000). During the maturation process, the ecto-domain of NCT undergoes conformational changes that allow the protein to be incorporated into the γ -secretase complex and the initial binding of the enzyme to substrates. Aph-1, is a 30 kDa protein with 7 TM domains, a luminal N-terminus and a cytosolic C-terminus. Two variants of the protein, Aph-1a and Aph-1b, are present in humans that, together with the two forms of PS, make the composition of the γ -secretase complex highly variable. In Aph-1 TM4, there is a GxxxG motif essential for its interaction with Pen-2 and PS. Aph1 interacts with immature NCT and PS to form a relatively stable pre-complex which is then translocated from the ER/cis-Golgi to the trans-Golgi, for further maturation. The role of this component is not yet clear and it appears to be a structural/scaffold protein necessary for the proper assembly of the complex (Lee *et al.*, *J Biol Chem* 2002).

Pen-2 is a 10 kDa small hairpin-like protein with two TM domains and both the N- and C-termini toward the ER luminal side. The interaction of Pen-2 with PS occur through the N-terminus, while the C-terminus and the TM1 domain are necessary for endo-proteolysis and the following activation of PS, even if the mechanism is unknown (Luo WJ *et al.*, *J Biol Chem* 2003). The crystallization of the purified γ -secretase complex has not been obtained yet since γ -secretase is a membrane-embedded protein complex harbouring at least 19 membrane-spanning domains (De Strooper B *et al.*, *Cold Sp Harb Perspect Med* 2012). However, human γ -secretase complexes have been purified and analyzed by EM and 3D reconstruction; its 3D structure at 48Å resolution occupied a volume of 560 x 320 x 240 Å with a low-density space containing multiple pores, which may house the catalytic site (De Strooper B *et al.*, *Cold Sp Harb Perspect Med* 2012).

The formation of the γ -secretase complex occurs through different steps. An initial sub-complex is made by the interaction of NCT and Aph-1 within the ER membranes (De Strooper B *et al.*, *Cold Sp Harb Perspect Med* 2012); this first complex interacts with another sub-complex formed by PS and Pen-2, where the proteolytic cleavage of PS1 or PS2 occurs in order to form the active enzyme (Kim J *et al.*, *J Cell Biol* 2007). A large amount of γ -secretase complexes is formed within the cell but less than 10 % is active and reaches its final destinations, plasma membrane (PM) and endosomes. Moreover, the enzyme can move to

PM or endosomes only after NCT glycosylation, that occurs in the Golgi apparatus (Kaether C *et al.*, Traffic 2006; Chyung JH *et al.*, J Biol Chem 2005).

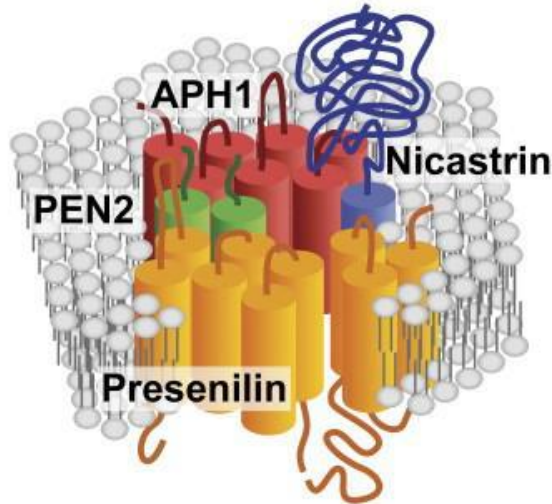


Figure 3 Schematic representation of the γ -secretase complex (Parks *et al.*, Trends Genet 2007).

Given the pivotal role of γ -secretase in AD pathogenesis, being the producer of A β peptides, many attempts have been performed to develop γ -secretase inhibitors. However, the majority of the inhibitors, though able to reduce the cleavage of APP, showed toxic side effects due to their low substrates specificity (De Strooper B *et al.*, Cold Sp Harb Perspect Med 2012). Knowing the structure of γ -secretase is still a primary goal in AD research because it will allow scientists to design effective and selective inhibitors or modulators that can rescue to normality the abnormal APP cleavage.

1.3 Presenilins

PS1 and PS2, identified in the middle '90s (Levy-Lahad E *et al.*, Science 1995; Sherrington R *et al.*, Nature 1995), are homologous (65 % identity), 50 kDa TM proteins encoded by the genes *PSEN1*, on chromosome 14, and *PSEN2*, on chromosome 1, respectively. Presenilins are mainly located in the ER and GA membranes but also, although less abundantly, in PM and endosomes; moreover, recently PSs have been reported to be localized also in mitochondria associated membranes (MAM) (Area-Gomez E *et al.*, AM J Path 2009; Filadi R *et al.*, Cell Rep 2016; Leal N *et al.*, J Cell Mol Med 2016). PSs are highly expressed in brain, although their expression is detectable in most adult human tissues (Brunkan AM and Goate AL, J of Neurochem 2005).

Functionally, PS1 and PS2 are the catalytic core of the γ -secretase complex, since enzymatic activity of the complex is abolished upon both PSs knockout (KO) in MEF cells (Herreman A *et al.*, Nat Cell Biol 2000). From the structural point of view, they are constituted by 10 hydrophobic domains and 9 TM domains, with the N-terminus of the protein facing the cytosol and the C-terminus located in the lumen of the organelle.

The N-terminal (NTF, 30kDa) and the C-terminal fragment (CTF, 20kDa) of PS are the two catalytically active parts within the γ -secretase complex; the two fragments are generated by the autocatalytic cleavage within the 7 TM domain during the incorporation of PS in the complex.

Essential for the activity of γ -secretase are two aspartate residues located into the TM domains 6 and 7; mutation of one of these aspartate residues into an alanine, leads to the complete inactivation of the enzyme (Kimberly WT *et al.*, J Biol Chem 2000). Though the cleavage of PS is autocatalytic, PS maturation needs other molecular partners and the process is saturable. The accumulation of the non-mature form of PS, called full length (FL) PS, leads to its proteasomal degradation; in fact, FL-PSs have a very short half-life (around 1.5 h), compared to the mature form (24 h; Kim TW *et al.*, J Biol Chem 1997).

PS mutated forms play a pivotal role in most of FAD cases; in details, more than 150 autosomal dominant mutations in PS1 (Figure 4) and 14 in PS2 are associated with FAD onset.

In agreement with the finding that PSs form the catalytic core of the γ -secretase, which cleaves APP generating toxic A β peptides, first studies showed that FAD-linked PS mutants were associated with an increased activity, generating more A β , in different cell models and in transgenic mice carrying FAD-PS mutations (Scheuner D. *et al.*, Nat Med 1996; Citron M. *et al.*, Nat Med 1997). This original idea has been challenged by other studies reporting, in FAD-PS expressing models, a lower enzymatic activity, with an increase in the A β 42/A β 40 ratio, due mainly to a drop in the production of A β 40 (Florea C, *et al.* Bioch Biophys Acta 2008; Shimojo M *et al.*, Neurosci Res 2007; Walker ES *et al.*, J Neurochem 2005; Xia D *et al.*, Neuron 2015).

Thus, although an intense debate is still running on this issue, the first hypothesis of gain-of-function FAD-PS mutations has been revised in a loss-of-function view: FAD-PSs decrease total production of A β , due to the less precise cleavage of APP, altering the physiological balance of the process, and causing an increased A β 42 and a decreased A β 40 generation.

In addition to their well-defined catalytic role within the γ -secretase complex, PSs are known to have pleiotropic, γ -secretase-independent functions, primarily in regulating Ca²⁺ homeostasis, but also in protein trafficking, cell adhesion and autophagy (De Strooper B and Annaert W Ann Rev Cell Dev Biol 2010; De Strooper B *et al.*, Cold Sp Harb Perspect Med 2012).

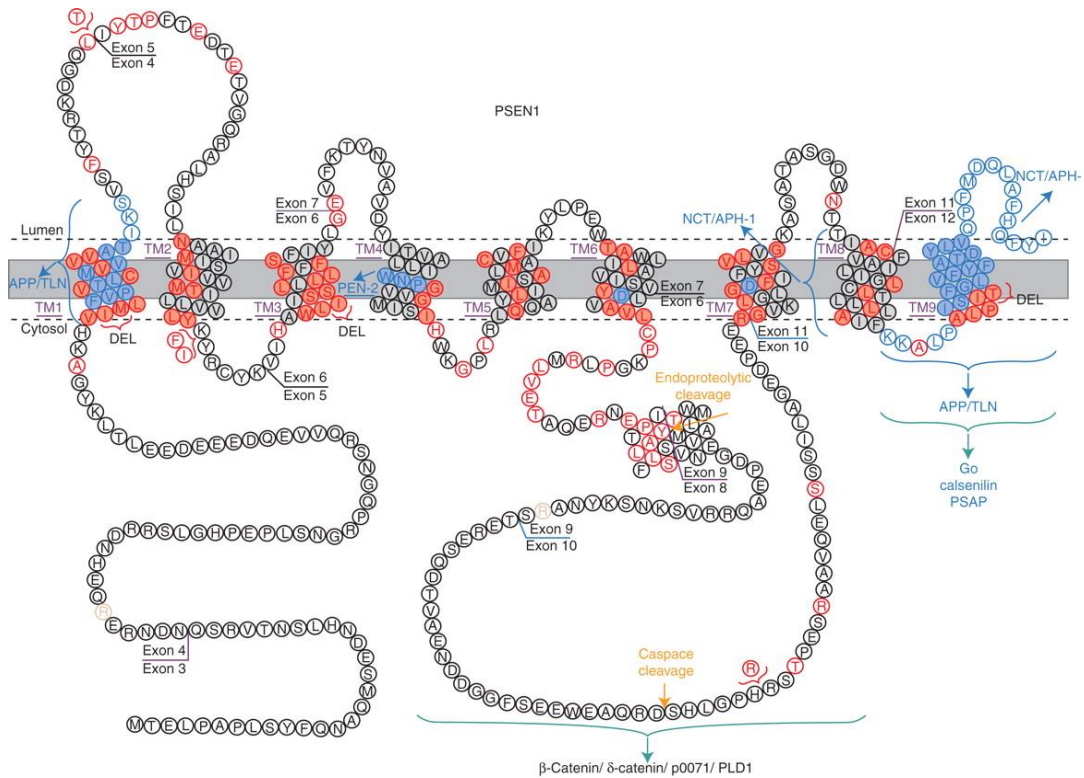


Figure 4: Schematic representation of PS1 sequence and topology. In red, aa whose mutations are associated to FAD; in blue, those involved in protein-protein interactions (De Strooper B. *et al.*, Cold Sp Harb Perspect Med 2012).

1.4 Amyloid Precursor Protein (APP)

The amyloid precursor protein (APP) is a single TM domain protein of the type I family with an extracellular/luminal N-terminus and a cytosolic C-terminus.

The APP encoding gene is localized on the long arm of chromosome 21, it consists of 18 exons and undergoes tissue-specific splicing, generating different isoforms, ranging from 365 to 770 aa.

APP undergoes post-translational modifications in the Golgi apparatus including O- and N-glycosylation, with only 10 % of the protein being found in PM (the protein is also recycled through endocytosis; Thinakaran G. and Koo E.H., J Biol Chem 2008).

Several functions of APP has been proposed (Thinakaran G. and Koo E.H., J Biol Chem 2008); here some of them are reported:

- the extracellular soluble domain of APP (APP α), generated upon APP cleavage by α -secretase, modulates neurites growth, synaptogenesis and the growth of other cell types, such as fibroblasts (Hung AY *et al.*, PNAS 1992);

- based on the similarities with Notch (another substrate of γ -secretase), a well-known transmembrane receptor involved in a large variety of cellular signalling and neurogenesis, APP can function as a receptor as well; a specific ligand, TAG-1, has been found (Ma QH *et al.*, Nat cell biol 2008);
- axonal transport, mediated by APP interaction with kinesin-1 (Kamal A *et al.*, Neuron 2000);
- gene transcription regulated by AICD, the APP intra-cellular domain formed after APP cleavage by γ -secretase (Zhang Y *et al.*, PNAS 2007);
- cell migration (Herms J *et al.*, EMBO J 2004).

APP, being the substrate of different enzymes, can be differentially cleaved leading to different products; in details, APP processing can follow two different pathways (Figure 5): the non-amyloidogenic and the amyloidogenic pathway (for reviews, see Zheng H. and Koo E.H., Mol Neurodegen 2006; Thinakaran G. and Koo E.H., J Biol Chem 2008). The non-amyloidogenic pathway is the most common: APP is firstly cleaved by α -secretase within the region corresponding to the A β fragment, thus preventing its formation; an N-terminal fragment (sAPP α) is released in the extracellular/luminal space, while a C-terminal part (C83) remains inserted to the membrane (α -stub).

On the contrary, in the amyloidogenic pathway, β -secretase (BACE1) cleaves APP preserving the entire A β peptide and releasing a soluble fragment (sAPP β) with unknown functions. The cleavage of APP by the β -secretase generates also a membrane-inserted C-terminal peptide, called C99 (β -stub). C83 (coming from non-amyloidogenic pathway) and C99 (formed through the amyloidogenic pathway) can be further cleaved by γ -secretase: while the cleavage of C83 produces the release of the extracellular, non-pathogenic peptide p3 and the intracellular AICD, the C99 cleavage generates amyloidogenic A β peptides (released in the extracellular space) and again AICD.

However, the cleavage operated by the γ -secretase is not highly precise and can produce A β peptides of different length (from 49 to 38 aa). The most abundant is A β 40 and about 10 % is represented by A β 42, more hydrophobic and more prone to oligomerization.

FAD-APP mutations are mainly localized near the sites of secretases cleavage, thus altering their activity and promoting the amyloidogenic pathway. These considerations, together with the fact that mutations inside the A β peptide sequence favour its aggregation, and that APP overexpression (for example in Down Syndrome, due to trisomy 21) is associated to an early

onset of AD symptoms, give strong genetic support to the amyloid cascade hypothesis for AD pathogenesis.

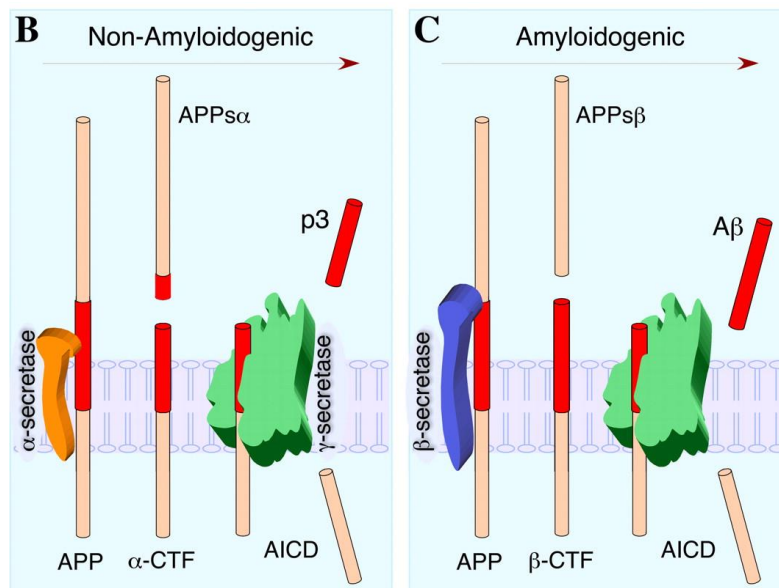


Figure 5 The two alternative pathways for APP maturation.
From Thinakaran G. and Koo E.H., J Biol Chem 2008.

1.5 The amyloid cascade hypothesis for AD

As already described above, Familial Alzheimer's Disease (FAD) is due to autosomal dominant mutations on three genes coding for APP, PS1 and PS2. The amyloid cascade hypothesis (Figure 6) proposes that the neurodegeneration observed in AD is due to a series of events depending on the altered processing of APP and subsequent production of A β peptides caused by mutations on these three genes (Hardy and Selkoe, Science 2002). In particular, APP, PS1 and PS2 mutations promote the APP amyloidogenic pathway leading to an increase in the amount of A β 42 produced, or at least to changes in the ratio A β 42/A β 40 in favour of the first, more toxic peptide (Haass C and Selkoe DJ, Nat Rev Mol Cell Biol 2007). Indeed, different studies have demonstrated that A β 42 is more prone to oligomerization, starts to aggregate and then is followed by A β deposition and formation of fibrils found in amyloid plaques (Chen Y.R. and Glabe, C.G., J Biol Chem 2006).

In contrast, it has been showed that dementia and pathology progression do not correlate with the number of amyloid plaques; moreover, the plaques have been found also in the brain of old healthy subjects, suggesting that the toxic form involved in synaptic dysfunctions are A β -soluble oligomers, and not the insoluble fibrils (Haass C and Selkoe DJ, Nat Rev Mol Cell Biol 2007). In details, the level of soluble A β corresponds to the degree of cognitive

impairments and soluble A β oligomers inhibit long term potentiation (LTP), a process involved in memory formation (Walsh DM *et al.*, Nature 2002), though the causal link is still largely unknown.

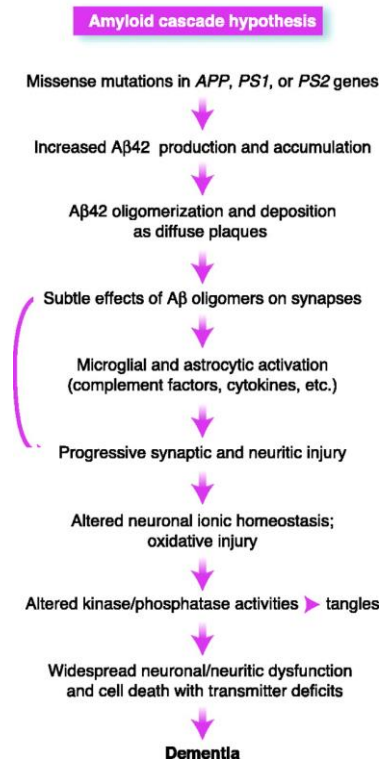


Figure 6 The amyloid cascade hypothesis for AD. From Hardy J. and Selkoe D.J., Science 2002

Different mechanisms have been proposed to explain the pathogenic activity of A β (Parihar M.S. and Hemnani T., J Clin Neurosci 2004; Fiala JC, Acta Neuropathol 2007; LaFerla F.M. *et al.*, Nat Rev Neurosci 2007; Gandy S, J Clin Invest 2005; Querfurth H.W. and LaFerla F.M, N Engl J Med 2010). Among them: alteration of Ca²⁺ handling, mitochondrial and energy metabolism dysfunctions, formation of cationic channels on plasma membrane, cellular oxidative stress due to ROS production, cytoskeletal and axonal transport alterations, inflammatory processes, increase susceptibility to pro-apoptotic and pro-necrotic stimuli.

1.6 The hyper-phosphorylated tau hypothesis for AD

AD belongs to a group of neurodegenerative diseases collectively designated as "tauopathies", characterized by the hyper-phosphorylation and aggregation of the tau protein (Martin L *et al.*, Neurochem Int 2011).

Tau, identified in 1975 (Weingarten MD *et al.*, PNAS 1975), is a microtubule-associated protein able to stabilize the cytoskeleton. It is made of four regions: an acidic region in the N-terminal part, a proline-rich region, a microtubule-binding domain and a C-terminal region. Different kinases and phosphatases can modulate the phosphorylation state of tau; phosphorylation is the basic mechanism by which tau function is regulated, since it specifically promotes tau self-aggregation (Martin L, *Neurochem Int* 2011).

According to the “tau-hypothesis”, tau phosphorylation is one of the first event that causes tau filament formation, then developing in aggregates and masses within nerve cell bodies (known as neurofibrillary tangles). This process leads to cytoskeleton destabilization, impairing axonal growth, vesicles and organelles transport, nervous signal propagation along the nerve network (LaPointe NE *et al.*, *J Neurosci Res* 2009). This hypothesis is supported by the fact that alterations in the expression and/or activity of tau kinases, such as GSK3 β , CDK5, DYRK1A, p38 and CK1, have been reported in brains of AD patients, suggesting that one or several of them could be involved in tau hyper-phosphorylation (Chung SH, *BMB Rep* 2009).

2. Ca²⁺ homeostasis

Ca²⁺ is the most important intracellular second messenger that plays a pivotal role in the regulation of several cellular processes such as proliferation, differentiation, muscle contraction, migration, survival, synaptic transmission, secretion, motility, membrane excitability, apoptosis and gene transcription. The capability of this small molecule to modulate such a big range of functions depends on the development, by different cell types, of specific Ca²⁺ signalling mechanisms that are maintained by a highly complex Ca²⁺ signalling toolkit. The toolkit is made by different components, such as channels, pumps, antiporters and Ca²⁺ binding proteins that cooperate in maintaining the cell Ca²⁺ homeostasis; the components have different role and distribution within the cell (Berridge MJ, *Bioch Soc Trans* 2012) (Figure 7). The Ca²⁺ signal is generated by the cells using internal and external sources of Ca²⁺. In details, in resting conditions, in excitable and non-excitable cells, the cytosolic Ca²⁺ concentration is kept around 100 nM, depending on different cell types, while the extracellular Ca²⁺ level is in the millimolar range (1.8 mM). Upon different kinds of stimuli, the cytosolic Ca²⁺ can rise up to 1-3 μ M due to Ca²⁺ release from the intracellular stores or Ca²⁺ influx through the plasma membrane.

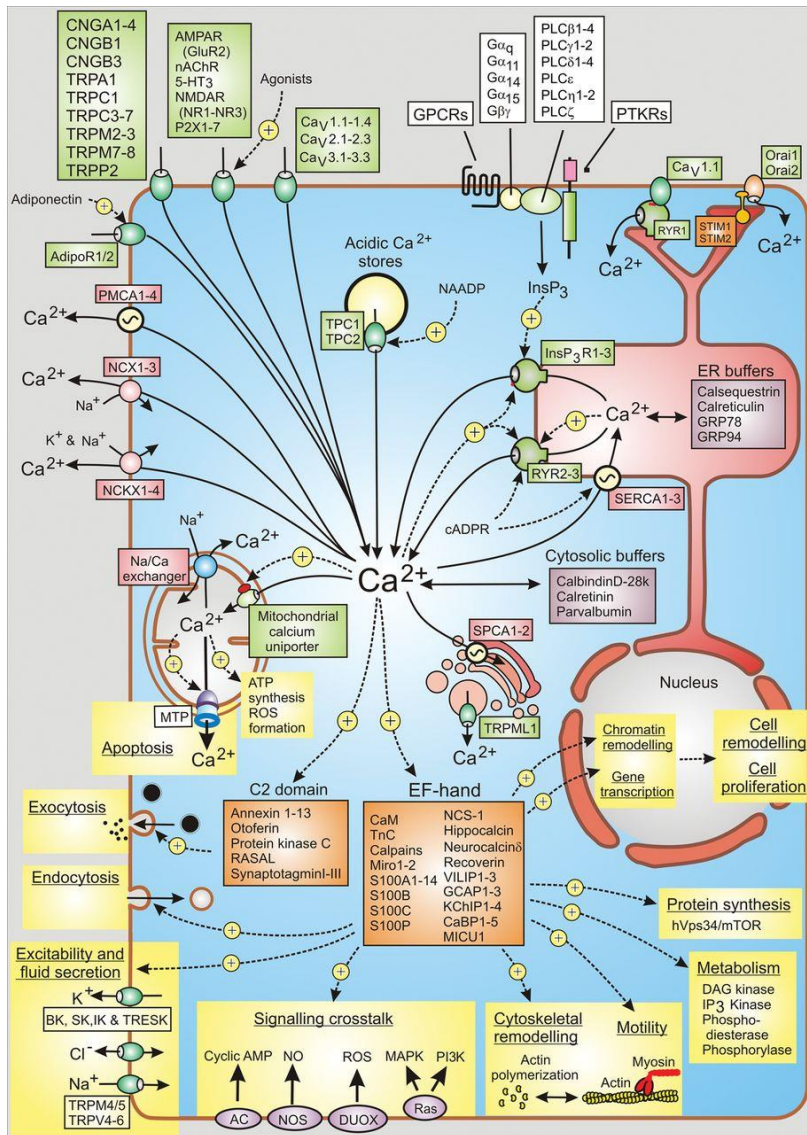


Figure 7 The Ca^{2+} signalling toolkit. Michael J. Berridge *Biochem. Soc. Trans.* 2012; 40:297-309

2.1 Plasma membrane

The PM is the barrier that divides the intracellular and extracellular space, allowing the maintenance of different functions and compositions of the two compartments. However, due to the presence of different types of channels with a different distribution throughout the PM, the two compartments are in a highly regulated connection and the PM allows the transmission of signals from the extracellular environment to the cytosol (Rizzuto R and Pozzan T, *Physiol Rev* 2006). Several of these signals are mediated by Ca^{2+} that can enter in the cytoplasm thanks to the large electrochemical gradient across the PM. These channels could be distinguished on the basis of their ionic selectivity and the mechanism for their

activation/opening (Berridge MJ *et al.*, Nat Mol Cell Biol 2003); we can distinguish ligand-gated Ca^{2+} channels and voltage-operated Ca^{2+} channels (VOCCs; Figure 7).

Ligand-gated Ca^{2+} channels are characterized by a lower selectivity for Ca^{2+} , compared to VOCCs. They are divided into four subgroups: (1) Receptor-operated Ca^{2+} channels (ROCCs or ROCs); they have an extracellular binding-domain for their ligand, either hormones or neurotransmitters, that trigger channels opening and thus Ca^{2+} entry. Among them, NMDA-R and AMPA-R are activated by their physiological ligand glutamate and have a crucial role in neurons. Depending on their subcellular localization (soma or synapses) and the amount of Ca^{2+} that they allow to enter, they could generate different signals, such as LTD (long term depression) or LTP (long term potentiation) (Wojda U *et al.*, IUBMB Life 2008). (2) G-protein-Operated Ca^{2+} channels (called G-protein-coupled receptors, GPCRs); their activity is coupled with the action of G-proteins. In the resting state, the α subunits of the G-protein binds guanosine diphosphate (GDP); upon receptor stimulation, the GDP is released and a guanosine triphosphate (GTP) molecule, from the cytoplasm, takes its place; at this point, the G-protein dissociates in a cytosolic $\text{G}\alpha\text{-GTP}$ and a membrane-bound $\text{G}\beta\gamma$ dimer. These subunits are the active forms of the G-protein, capable to transmit the signal to specific membrane associated effectors, such as enzymes and ion channels. GPCRs generate IP3 through phospholipase C (PLC) activation, thus triggering Ca^{2+} release from ER through IP3Rs (Berridge MJ *et al.*, Nat Mol Cell Biol 2003). (3) Second-messenger Operated Ca^{2+} channels (SMOCs) are activated by second messengers, such as cAMP, cGMP, IP3, diacylglycerol (DAG), arachidonic acid and Ca^{2+} itself, produced or released after activation of G proteins or enzyme-coupled receptors (Clapham DE, Cell 2007). (4) Store-Operated Ca^{2+} channels (SOCCs or SOCs) are important for Ca^{2+} entry in response to ER Ca^{2+} depletion. The proteins that modulate this process have been recently identified: STIM and Orai. While Orai forms channels in the PM (Prakriya M *et al.*, Nature 2006; Yeromin AV *et al.*, Nature 2006), STIM is the protein that “senses” the $[\text{Ca}^{2+}]$ into ER lumen. After ER depletion, STIM1 changes its distribution, forms clusters on ER membrane and interacts with Orai in PM, allowing Ca^{2+} entry (Roos J. *et al.*, JCB 2005; Liou J. *et al.*, Current Biol 2005) (Figure 7).

Voltage Operated Ca^{2+} Channels (VOCCs) play a crucial role in excitable cells, like neurons, since their opening is regulated by membrane depolarization, which transforms electrical signals into chemical signals. VOCCs are a complex family of channels comprising different subtypes; their open probability is voltage- dependent and they have a very high selectivity for Ca^{2+} in physiological condition (Catterall, Cold Spring Harb Perspect Biol 2011). In the nervous system, they control a broad array of functions including neurotransmitter release, neurite

outgrowth, synaptogenesis, neuronal excitability, differentiation and plasticity. VOCCs are present also in other cell types, such as cardiac and smooth muscle cells, where their activation initiates contraction directly by increasing cytosolic $[Ca^{2+}]$ and indirectly by activating the Ca^{2+} induced Ca^{2+} release (CICR) mechanism (see below) (Catterall W A, Cold Spring Harb Perspect Biol 2011).

Finally, Ca^{2+} ATPases are also located at the PM; they are essential to control Ca^{2+} signals and to guaranty the specificity required to modulate cell functions, avoiding excessive and dangerous stimulation. During a typical Ca^{2+} transient, the increase in cytosolic Ca^{2+} concentration is balanced by a process that reduces it; this latter is mediated by pumps and exchangers that remove the Ca^{2+} from the cytosol, in order to rescue resting conditions. The PM Ca^{2+} ATPases (PMCA) and the Na^+/Ca^{2+} exchangers (NCX) are the two main players that mediate this process (Berridge MJ *et al.*, Nat Mol Cell Biol 2003). The first one, PMCA, is a ubiquitous PM protein that catalyses the active transport of Ca^{2+} out of the cell, by hydrolysing ATP (Ca^{2+} : ATP stoichiometry is 1:1). Due to its high Ca^{2+} affinity, it controls $[Ca^{2+}]_{cyt}$ at resting state (Carafoli E, FEBS J 2005). The NCX is an electrogenic antiport located in the PM; it exchanges 3 moles of Na^+ for 1 mole of Ca^{2+} and due to its low Ca^{2+} affinity, but high transport rate, it constitutes the principal Ca^{2+} extrusion system in excitable cells (Rizzuto R and Pozzan T, Physiol Rev 2006)(Figure7).

2.2 Endoplasmic Reticulum

The Endoplasmic Reticulum (ER) is a very complex organelle made of membrane-enclosed sacs and tubules, known as cisternae, that form a membranes network diffused throughout the cytosol, from the perinuclear region to cell periphery, contacting several other organelles. A special type of ER, known as Sarcoplasmic Reticulum (SR), can be found in muscle cells. Three main regions can be detected: Rough ER, Smooth ER and the nuclear envelope. The ER has several essential functions in the cell; beyond being important for proteins folding and synthesis, and their transport to the final location, it represents the most important intracellular Ca^{2+} store of the cell, playing a crucial role in Ca^{2+} homeostasis and Ca^{2+} signalling. To this end, it contains Ca^{2+} binding proteins, for Ca^{2+} storage, pumps and channels, located in the ER membranes, for Ca^{2+} uptake and Ca^{2+} release, respectively (Zampese E and Pizzo P, Cell Mol Life Sci 2012)(Figure7).

About the ER Ca^{2+} content, it has been reported, employing different techniques, that depending on the cell type, the Ca^{2+} concentration can range from 200 μ M up to 1-3 mM (Meldolesi J and Pozzan T, Trend Bioche Sci 1998; De la Fuente S *et al*, cell calcium 2013). ER

Ca²⁺ concentration lower than 100 μM has been also measured in unstimulated cells, but most of the cell types have an ER Ca²⁺ content in the range of 300-800 μM (Zampese E and Pizzo P, Cell Mol Life Sci 2012). Alterations in ER Ca²⁺ content can modify its activity inducing ER stress, the Unfolded Protein Response (UPR) and, eventually, cell death.

The steady-state ER Ca²⁺ content is dynamic and results from the equilibrium between the ER Ca²⁺ uptake and its release. To maintain its Ca²⁺ concentration, ER takes up Ca²⁺ through the SERCA pump. This is a 110 kDa TM protein that can mediate the uptake of two ions of Ca²⁺ using the energy of a molecule of ATP. In mammals, SERCA pump can be encoded by three different genes (*ATP2A1*, *ATP2A2*, *ATP2A3*) and can exist in different isoforms. Different drugs are able to block its activity: Thapsigargin (Tg) blocks SERCA pump in an irreversible way (Thestrup T *et al.*, Nat Methods 1990), while Cyclopiazonic acid (CPA) and 2,5-di-(ter-butyl)-1,4-benzohydroquinone (t-BHQ) block the pump with a reversible mechanism (Seidler NW *et al.*, J Biol Chem 1989, Oldershaw KA and Taylor CW, FEBS lett 1990).

On the other side, the ER Ca²⁺ release is mediated by the activity of two channels located in the ER membranes: inositol 1,4,5-trisphosphate Receptors (IP3Rs) and Ryanodine Receptors (RyRs).

IP3Rs are a family of Ca²⁺ release channels that are ubiquitously expressed and mainly localized in the ER, but also present in the Golgi apparatus and nuclear envelope of all cell types. In mammals, three different genes encode for three IP3Rs and different isoforms have been identified, differently expressed depending on the development and differentiation state of the cell (Mak DO and Foskett K, Cell Calcium 2015). IP3R is a ligand-gated ion channel that release Ca²⁺ from intracellular stores inducing cytosolic Ca²⁺ rises (Mak DO and Foskett K, Cell Calcium 2015). In details, IP3R is activated by its physiological ligand, IP3. IP3 is generated in the plasma membrane by enzymes of the PLC family; PLC hydrolyses the plasma membrane phosphatidylinositol 4,5-bisphosphate producing the inositol 1,4,5-trisphosphate (IP3) and diacylglycerole (DAG). At this point, IP3 diffuses from the PM to the ER throughout the cytosol. Once reached the ER, it binds its receptor in the ER membranes allowing its opening and thus Ca²⁺ release (Foskett JK *et al.*, Physiol Rev 2007).

Structurally, IP3Rs are 260 kDa molecules made of a short cytoplasmic C-terminus, a big NH2 cytoplasmic terminus that includes an IP3-binding domain and a regulatory domain; they present also a hydrophobic part containing 6 TM that forms the pore. IP3R channels are tetramers made by four IP3R molecules (Foskett JK *et al.*, Physiol Rev 2007). As mentioned above, IP3 is the most important ligand of IP3Rs but another molecule that is essential for the activity of IP3Rs is Ca²⁺ itself. In details, Ca²⁺ can regulate IP3Rs in a biphasic manner: at low

Ca²⁺ concentration, it favours the opening of the channel mediated by IP₃, while at high Ca²⁺ concentration the channel is inhibited. This Ca²⁺ activity allow IP₃R to generate local and then widespread Ca²⁺ signals due to the propagation of the signal between different IP₃R. This highly complex events contribute to the known Ca²⁺-induced Ca²⁺ release (CICR) mechanism, also important for the regulation of RyRs (Foskett JK *et al.*, *Physiol Rev* 2007 ; Zampese E and Pizzo P, *Cell Mol Life Sci* 2012).

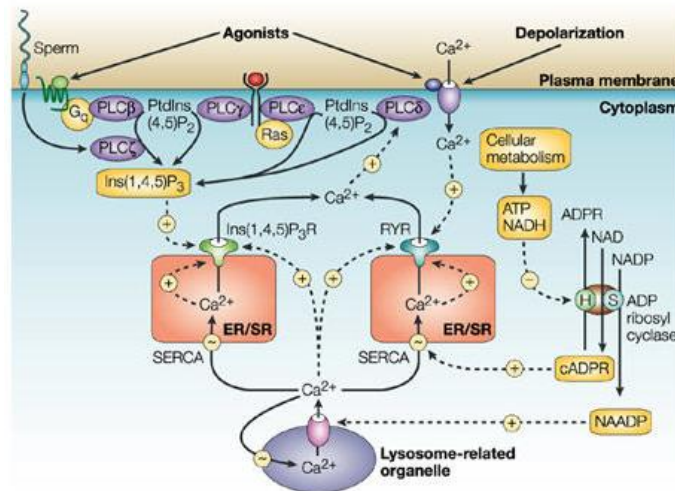


Figure 8: Endoplasmic Reticulum Ca²⁺ signalling.
Michael J. Berridge *Nature Reviews Molecular Cell Biology* 2003

In addition to IP₃R, intracellular store Ca²⁺ release can indeed be mediated by RyRs. Four RyRs assemble into a homo-tetramer that forms a channel of more than 2 MDa. Structurally, it consists of a transmembrane domain that forms the ion conducting pore, located in the C-terminus, and a big N-terminus domain that lies in the cytosol. This latter domain interacts with several proteins and molecules such as protein kinase A (PKA), calmodulin, Ca²⁺ and Mg²⁺ that modulate the opening of the channel. Again, Ca²⁺ is important, through the CICR mechanism, for the modulation of RyRs activity.

In mammals, three different genes encode for RyR1 (mainly expressed in skeletal muscle), RyR2 (predominantly expressed in heart, in Purkinje cells and in cortical neurons) and RyR3 (ubiquitously expressed at low levels). While in skeletal muscle RyR1 opening is primarily (or exclusively) due to the electromechanical coupling with the dihydropyridine receptor (DHPR), the major gating mechanism of RyR2 and RyR3 opening, fundamental in cardiac muscle cells, is CICR. In this latter case, the opening of RyRs is stimulated by the local Ca²⁺ increase, occurring in the proximity of PM-located VOCCs L-type Ca²⁺ channels (Fill M and Copello JA, *Physiol Rev* 2002).

Finally, a basal Ca^{2+} leak from the ER has a role in the maintenance of the steady state of ER Ca^{2+} concentration. However, despite its physiological relevance, the mechanism of ER Ca^{2+} leak remains elusive. In addition, RyRs and IP3Rs are known to undergo spontaneous activity, maybe contributing to the basal ER Ca^{2+} leak (Zampese E and Pizzo P, Cell Mol Life Sci 2012). Pivotal players in ER Ca^{2+} handling are a lot of different proteins located in or spanning in the ER lumen that act as Ca^{2+} buffer or chaperones, such as calreticulin (CRT), calnexin (CNX), calsequestrin (CSQ), glucose-related protein 78 (GRP78/Bip) and glucose-related 94 (GRP94). They all have between 1-50 Ca^{2+} binding sites and low affinity for the cation. In this way, they have two functions: they can buffer a large amount of Ca^{2+} and release it rapidly within the organelle, allowing its fast exit into cytoplasm, upon opening of Ca^{2+} releasing channels (Zampese E and Pizzo P, Cell Mol Life Sci 2012).

2.3 Golgi Apparatus

The Golgi Apparatus (GA) is an intracellular organelle that belongs to the secretory pathway; it has a crucial role in lipids and proteins modifications after their synthesis in the ER, directing them to their final destination within or outside the cell. To this aim, it contains several enzymes (such as glycosyltransferases, glycosidases, sulphatases and kinases) that properly modify proteins to their mature form. Structurally, it is made by three different compartments: *cis*-, *medial*- and *trans*-Golgi; they are all organized in flatten cisternae and their architecture depends on the balance of anterograde and retrograde vesicles trafficking between GA, ER and other cellular compartments (Pizzo P *et al.*, Cell Calcium 2011). Beyond being essential for proteins modifications, it has been reported that GA can store high amount of Ca^{2+} and that several of its functions, as well as enzymes contained in its lumen, are modulated by Ca^{2+} concentration (Pinton P *et al.*, EMBO J 1998; Pizzo P *et al.*, Cell Calcium 2011). Being a Ca^{2+} storage organelle, as ER, it contains Ca^{2+} releasing channels, pump for Ca^{2+} uptake and Ca^{2+} binding proteins (Zampese E and Pizzo P, Cell Mol Life Sci 2012).

For Ca^{2+} uptake, GA presents on its membranes two ATP-dependent pumps: the SERCA and the Secretory Pathway Ca^{2+} ATPase 1 (SPCA1), a protein ubiquitously expressed that contains, as SERCA, a Ca^{2+} binding domains located in the TM region. On the other side, Ca^{2+} release from the GA is mediated by IP3Rs and RyRs (see above). However, the above described pumps and channels have not a homogenous distribution in GA membranes; their different localization in the GA compartments characterizes the Ca^{2+} handling heterogeneity of the GA. The Ca^{2+} homeostasis of *cis*-GA is similar to that of ER, since IP3Rs, RyRs and SERCA are the

channels and the pump responsible for Ca^{2+} release and uptake, respectively; the Ca^{2+} concentration within this sub-domain is around 250 μM (Pizzo P *et al.*, Cell Calcium 2011). The medial-Golgi presents IP3Rs and RyRs, as Ca^{2+} release channels, and SERCA and SPCA1, as Ca^{2+} uptake pumps; its Ca^{2+} concentration is supposed to be lower than the ER [Ca^{2+}] but higher than the one of *trans*-Golgi, thus being about 250-300 μM (Wong AK *et al.*, J Mol Cell Biol 2013). Finally, the *trans*-Golgi presents only SPCA1 to take up Ca^{2+} , it is not sensitive to IP3 and presents an estimated Ca^{2+} concentration of 130 μM (Lissandron V *et al.*, PNAS 2010). The GA contains also Ca^{2+} -binding-proteins: CALNUC, is the most abundant and better characterized of the GA Ca^{2+} binding-proteins (Lin P *et al.*, J Cell Biol 1999); Cab45, a soluble protein important for vesicles sorting (Scherer PE *et al.*, J Cell Biol 1996); p45/NEFA, a luminal protein strongly associated to GA membranes (Karabinos A *et al.*, Mol Biol Evol 1996); Calumenin, a protein found also in the ER and in the secretory pathway, that interacts with SERCA and RyR2 modulating their activity (Jung DH *et al.*, Biochem Biophys Res Commun 2006).

2.4 Acidic Compartments

Beyond ER and GA, also acidic organelles, such as endosomes and lysosomes, are considered intracellular Ca^{2+} stores. The Ca^{2+} concentrations inside these organelles is heterogeneous, depending on the cell type: from 10-40 μM , in mast cell and chromaffin cell granules, up to 100-200 μM , in insulin granules; in newly-formed endosomes the Ca^{2+} content is thought to be similar to the extracellular Ca^{2+} concentration (1 mM). However, it rapidly decreases to 3 μM upon their acidification (Zampese E and Pizzo P, Cell Mol Life Sci 2012). Moreover, recently, some studies demonstrated that also peroxisomes can take up and store Ca^{2+} (Raychaudhury B *et al.*, Biochim Biophys Acta 2006; Drago I *et al.*, J Biol Chem 2008). The mechanisms by which acidic compartments take up and release Ca^{2+} are still unknown, even if some studies suggest that SERCA and SPCA pumps are used to take up the cation (Mitchell KJ *et al.*, J Cell Biol 2001). Moreover, the idea that the proton gradient is involved in Ca^{2+} homeostasis is well accepted, since $\text{Ca}^{2+}/\text{H}^+$ exchangers are present and indirect pathways involving Na^+/H^+ and $\text{Na}^+/\text{Ca}^{2+}$ exchangers have been also reported (Mahapatra NR *et al.*, J Biol Chem 2004; Krieger-Brauer HI *et al.*, J Neurochem 1983). Regarding Ca^{2+} release, different molecules such as IP3, cADPR (cyclic adenosine diphosphate-ribose), and also the RyRs activator, caffeine, have been proposed to mediate the process (Zampese E and Pizzo P, Cell Mol Life Sci 2012).

2.5 Mitochondria

Mitochondria are the powerhouse of the cell, since they provide the biggest amount of ATP required for all the cell functions. They are delimited by two membranes, the Outer Mitochondrial Membrane (OMM) that faces the cytosol and is quite permeable to ions and small molecules, and the Inner Mitochondrial Membrane (IMM) that is less permeable than the OMM and forms a lot of invaginations (known as cristae), leading to an increase of its surface. Between these two membranes, there is the Intermembrane Space (IMS), while the IMM encloses the matrix, where a lot of enzymes and proteins essential for mitochondrial functions (such as Krebs' cycle and programmed cell death) are located (Giacomello M *et al.*, Cell Death Differ 2007; Contreras L *et al.*, Biochim Biophys Acta 2010). Moreover, mitochondria are dynamic organelles. The shape and the size of mitochondria are regulated by two balanced processes: fusion and fission. Depending on the cellular phase, the energy demand and their damages, mitochondria can become smaller, after fission, or bigger, due to fusion processes. In order to sustain all the functions mentioned, mitochondria move throughout the cell thanks to their interaction with the cytoskeleton, mediated by specific kinesins and adaptor proteins, such as Milton and Miro (Zampese E and Pizzo P, Cell Mol Life Sci 2012).

Most of the mitochondrial functions described above are regulated by Ca^{2+} signals that reach both the IMS and the matrix of mitochondria thanks to the action of several proteins; that is why mitochondria are considered important players in cell Ca^{2+} homeostasis (Contreras L *et al.*, J Biol Chem 2012; Jouaville LS *et al.*, PNAS 2001).

The capability of mitochondria to take up Ca^{2+} has been described for the first time in the early '60s by several studies (De Luca HF and Engstrom G, PNAS 1961, Vasington FD and Murphy JV, J Biol Chem 1962) even if the molecular identity of the channel (Mitochondrial Calcium Uniporter, MCU), responsible for mitochondrial Ca^{2+} uptake, has been identified only recently (Baughman JM *et al.*, Nature 2011, De Stefani D *et al.*, Nature 2011). However, in addition to the Ca^{2+} uptake machinery, mitochondria are endowed with Ca^{2+} extrusion molecules that export Ca^{2+} outside the mitochondria and limit Ca^{2+} accumulation within the matrix (Figure 9).

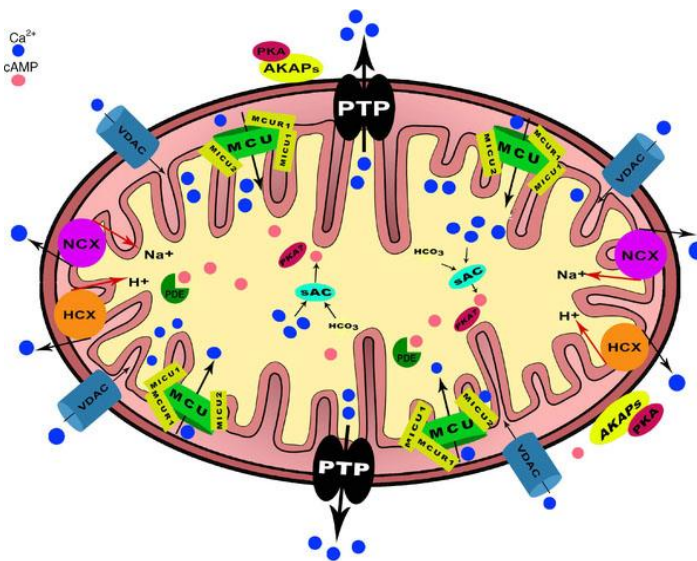


Figure 9 Mitochondrial Ca^{2+} toolkit. Di Benedetto G *et al.*, the Journal of Physiology 2014.

2.5.1 Mitochondrial Calcium Uniporter (MCU)

Despite the molecular identity of the MCU has been described only in last years, the capability of mitochondria to take up Ca^{2+} has been elucidated already in the '70s. Later, Mitchell proposed the chemiosmotic theory revealing the thermodynamic basis for mitochondrial Ca^{2+} uptake. Indeed, the generation, by the pumping of protons from the matrix to the IMS by the respiratory chain, of the electrochemical gradient ($\Delta\Psi$) across the IMM, negative inside the matrix (-180 mV), is the huge driving force that allows the mitochondrial Ca^{2+} accumulation in the matrix (Mitchell P and Moyle J, Nature 1967). The OMM is highly permeable to ions and molecules smaller than 5 kDa thanks to the presence on its surface of the Voltage Dependent Anion Channel (VDAC; see below). Thus Ca^{2+} can easily pass the OMM and reach the IMS. On the contrary, the IMM is impermeable, thus specialized channels and carriers are required to allow the uptake of ions and molecules (Bragadin M *et al.*, Biochemistry 1979). In 2011, two groups reveal the molecular nature of the MCU (Baughman JM *et al.*, Nature 2011; De Stefani D *et al.*, Nature 2011). This is a 40 kDa protein located in the IMM that loses its mitochondrial targeting sequence resulting in a 35 kDa protein. In mammals, it is ubiquitously expressed while it is not present in yeast. Once reconstituted into a planar lipid bilayer, it generates a Ca^{2+} current (Mammucari C *et al.*, Biochim Biophys Acta 2016; Patron M *et al.*, J Biol Chem 2013); moreover its downregulation reduces the mitochondrial Ca^{2+} uptake, while its overexpression increases it (De Stefani D *et al.*, Nature 2011). Structurally, it is made of two

highly conserved TM domains with the N- and C- termini facing the matrix and a small linker (DIME) between the two TM. The pore region of MCU is formed by eight helices and the negative electrostatic potential needed for cations permeability is due to a cluster of negatively charged aa found in the DIME region, in proximity of the pore (Raffaello A *et al.*, EMBO J 2013).

Due to the high driving force that allows mitochondria to take up Ca^{2+} , this organelle should accumulate large amounts of cation inside their matrix; however, the very low MCU affinity for Ca^{2+} (Kd 10-20 μM) guarantees that the mitochondrial Ca^{2+} concentration in living cells remains, at rest condition, similar to that of the cytosol. Based on these early measurements, it has been believed for long time that mitochondria could not take up considerable amount of Ca^{2+} in physiological conditions, since the Kd of MCU is much higher than the physiological cytosolic Ca^{2+} rises. This theory completely changed when it became possible to directly measure mitochondrial Ca^{2+} uptake in living cells using genetically encoded Ca^{2+} probes targeted to the mitochondrial matrix, such as mitochondrial-aequorin (Rizzuto R *et al.*, Nature 1992). By this tool, it has been shown that, upon modest cytosolic Ca^{2+} rises (1-2 μM), mitochondria can take up high amount of Ca^{2+} , reaching Ca^{2+} concentrations much higher than those in the cytosol (Rizzuto R *et al.*, Nature 1992). The discrepancy between the effective consensus at that time with these direct measurements has been solved by the finding that mitochondria are in close contact with the cell source of Ca^{2+} , such as ER and PM. Thus, being in close proximity to ER Ca^{2+} -releasing channels (IP3Rs and RyRs), or to Ca^{2+} entry from PM, mitochondria can sense high Ca^{2+} concentration microdomains and hence take up Ca^{2+} through MCU.

The MCU subunit is part of the so-called MCU complex (MCUC, figure 10), made of MCU but also by other proteins capable of modulating the activity, the Ca^{2+} affinity and (probably) the assembly of the channel in the mitochondrial membrane. MCUC is a complex with a molecular weight around 480 kDa (Baughman JM *et al.*, Nature 2011), composed by:

- MCUB. It is a 330 aa proteins (35 kDa) conserved among all species and structurally similar (50 %) to MCU. Although it is highly similar to MCU, it presents aa substitutions in the pore forming region that prevent MCUB to form a Ca^{2+} channel, thus acting as a dominant-negative subunits of the MCUC; in fact, MCUB overexpression dramatically reduces the mitochondrial Ca^{2+} uptake. However, MCUB : MCU ratio is highly variable between different tissue, depending on the type and the functions of the tissue; for example, in heart, where the mitochondrial Ca^{2+} transients are low, the MCUB : MCU

is higher than that of skeletal muscle (Mammucari C *et al.*, *Biochim Biophys Acta* 2016).

- EMRE. EMRE (Essential MCU Regulator), a 10 kDa protein, has been recently identified by SILAC-based quantitative mass spectrometry of affinity-purified MCUC. It is a protein with one TM domain in the IMM and a C-terminus enriched in aspartates (Sancak Y *et al.*, *Science* 2013). EMRE knock-out (KO) dramatically reduces MCU activity even if MCU expression levels are not altered. It was originally proposed that EMRE mediates the interaction of two regulators of the channel, MICU1 and MICU2 (see below), with MCU (Sancak Y *et al.*, *Science* 2013), since upon EMRE KO, MICU1 and MICU2 were not anymore immune-precipitated with MCU. Recently, EMRE has been proposed as a Ca^{2+} sensor of MCU on both sides of the IMM; the mechanism of action of EMRE requires the presence of both MICU1 and MICU2. Hence, EMRE is important because it protects mitochondria from both Ca^{2+} depletion and Ca^{2+} overload (Vais H *et al.*, *Cell Report* 2016).
- MICU. Three different isoforms have been identified; all of them are EF-hand containing proteins that play a crucial role in the modulation of MCU activity and thus mitochondrial Ca^{2+} uptake. (1) MICU1 is the first component of the MCUC that has been described, even before the MCU identification (Perocchi F *et al.*, *Nature* 2010). It is a 54 kDa protein localized in the IMS that physically interacts with MCU, regulating its activity. In details, MICU1 acts as a gatekeeper favouring or preventing mitochondrial Ca^{2+} uptake, depending on the cytosolic Ca^{2+} concentration. Indeed, MICU1 functions as a gatekeeper when the cytosolic Ca^{2+} amount is low, while it favours the channel activity when the cytosolic Ca^{2+} rises (Csordas G *et al.*, *Cell Met* 2013; Mallilankaraman K *et al.*, *Nat Cell Biol* 2012; Patron M *et al.*, *Mol Cell* 2014). The KO of MICU1 abolishes mitochondrial Ca^{2+} uptake, though overexpression does not result in a major effect on the rate and extent of Ca^{2+} uptake by the organelle (Perocchi F *et al.*, *Nature* 2010). The MICU1 EF-hands mutant loses the capability to activate the channel (Patron M *et al.*, *Mol Cell* 2014). (2) MICU2 is a 45 kDa protein ubiquitously expressed in mammalian tissues; 27 % of its sequence is identical to that of MICU1 and, as this latter, it is localized in the IMS. It physically interacts with MICU1, forming a heterodimer (through a disulfide bridge) that interacts with the DIME domain of MCU. The function of MICU2 depends on the presence of MICU1; indeed, the decrease of MICU1 protein expression reduces also the level of MICU2 and results in the absence of gatekeeping on MCU (Patron M *et al.*, *Mol Cell* 2014).

Functionally, MICU2 exerts an inhibitory effect on MCU channel activity in planar lipid bilayers and in intact HeLa cells at low Ca^{2+} levels. Thus, the heterodimer made by MICU1-MICU2 works as a gatekeeper in resting conditions, while increases in cytosolic Ca^{2+} concentration induce a conformational change of the dimer, causing the release of the MICU2-dependent inhibition and triggering MICU1-mediated stimulation of MCU activity (Patron M *et al.*, Mol Cell 2014).

(3) MICU3, as MICU1 and MICU2, belongs to the MICU family and presents two EF-hand domains, however, its function is still unknown. It is mainly expressed in the nervous system and in skeletal muscle (Mammucari C *et al.*, Biochim Biophys Acta 2016).

- MCUR1 (Mitochondrial Ca^{2+} Uniporter Regulator 1) is another recently discovered member of the complex. It is a 40 kDa protein with two TM domains and one coiled-coil region (Mallilankaraman K *et al.*, Nat Cell Biol 2012b). It has been shown to be important in the regulation of the uniporter activity (Mallilankaraman K *et al.*, Nat Cell Biol 2012b); its downregulation suppresses mitochondrial Ca^{2+} uptake while its overexpression increase it. Moreover, the silencing of MCUR1 causes defect in the assembly of cytochrome C oxidase and reduces mitochondrial membrane potential, thus impairing mitochondrial Ca^{2+} uptake (Paupe V *et al.*, Cell Metab 2015). However, the real function of MCUR1 has not been uncovered yet.

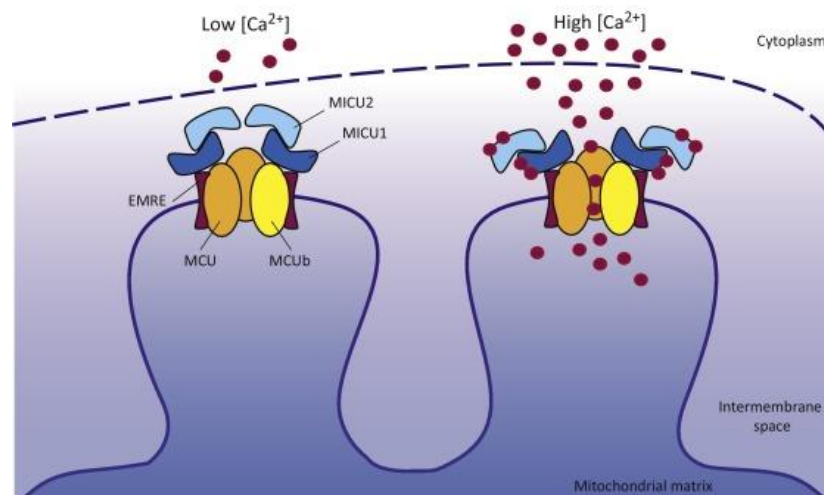


Figure 10 The Mitochondrial Calcium Uniporter Complex (MCUC).
Raffaello A. *et al.*, Trends in Biochemical Science 2016

Thus, mitochondrial Ca^{2+} import involves a high complex molecular system, conserved in its basic characteristics, but with regulatory mechanisms that have been probably added during

evolution. Moreover, a huge set of data demonstrates the involvement of mitochondrial Ca^{2+} uptake in many key aspects of cell physiology and pathology; however, the characterization of the MCU-KO mice produced unexpected results. Finkel and co-workers showed that MCU-KO mice are regularly born with a very mild phenotype; the animals are slightly smaller than their wild type littermates and have modest defects in metabolism (pyruvate dehydrogenase impairments) and skeletal muscle strength. They observed also that mitochondria, isolated from both skeletal and cardiac muscles, of MCU-KO mice are totally incapable of accumulating Ca^{2+} in an energy dependent manner. In MEFs from the same transgenic mice, Ca^{2+} release from intracellular stores causes no detectable increase in mitochondrial Ca^{2+} levels but, surprisingly, only a partial reduction in mitochondrial Ca^{2+} content at resting condition. Moreover, mitochondria from MCU-KO mice lack evidence for Ca^{2+} -induced permeability transition pore (PTP) opening but, unexpectedly, this modification does not seem to protect MCU-KO cells and tissues from cell death. Furthermore, while, as expected, the PTP inhibitor Cyclosporine A (CsA) provided significant protection against ischemia-reperfusion injury to WT hearts, this agent had no demonstrable effect on MCU-KO hearts. Thus, in the absence of MCU, alternative PTP- or Ca^{2+} -independent cell death mechanisms could emerge and become prevalent (Pan X *et al.*, Nature Cell Biol 2013). In the last years, others mouse models have been generated to better understand the role and the importance of MCU. Indeed, Anderson and co-authors generated a heart-specific transgenic mouse model that expresses a dominant-negative form of MCU (MCU^{D260Q, E263Q}, DN-MCU). As expected, heart mitochondria from DN-MCU mice are not able to take up Ca^{2+} and, more importantly, this mouse model has an evident phenotype. In physiological stress conditions, the MCU-dependent increased ATP production is essential to sustain SERCA activity to maintain ER Ca^{2+} homeostasis; accordingly, the heart of this mouse model presents impaired performance upon increase workloads. Moreover, again, the heart of DN-MCU mice is not protected from ischemia/reperfusion injury, as the mice previously described; importantly, this transgenic mouse model has the same genetic background of the MCU-KO mouse above described (Wu Y *et al.*, Nat Commun 2015; Rasmussen TP *et al.*, PNAS 2015). In the same period, two different groups evaluated the cardiac function using a conditional MCU-KO mouse model (Kwong JQ *et al.*, Cell Rep 2015). The decrease in the expression level of MCU (80%) leads to a strong reduction in the mitochondrial Ca^{2+} uptake; however, regarding the cardiac functions, the absence of MCU does not strongly affect heart activity. Contrary to the above described MCU-KO mouse model (Pan X *et al.*, Nature Cell Biol 2013), here, the lack of MCU strongly protects cardiac tissue from ischemia/reperfusion injury (Kwong JQ *et al.*, Cell Rep 2015; Luongo TS *et al.*, Cell Rep

2015). The same groups observed that basal mitochondria respiration of cardiomyocytes is unchanged while maximal respiration, upon FCCP addition or after increased workload, is affected; moreover, a decrease in the activity of the pyruvate dehydrogenase has been detected. With these results, they confirmed the crucial role of MCU in ATP production-cell energy demand coupling (Kwong JQ *et al.*, Cell Rep 2015).

On the existence of alternative mitochondrial Ca^{2+} uptake pathways, of interest are the recent observations, by Graier and co-workers, that up to 5 different Ca^{2+} currents can be identified in mitoplasts by electrophysiology (Jean-Quartier C *et al.*, Mol Cell Endocrinol 2012). In a more recent study, the same group observed that one of these currents (different from the one generated by MCU) is increased in mitoplast ablated of MCU (Bondarenko AI *et al.*, Pflugers Arch 2013). They suggested the existence of at least two different mitochondrial Ca^{2+} channel sets, one MCU-dependent and another, MCU-independent. As much as the existence of multiple mitochondrial Ca^{2+} influx pathways is fascinating (and could explain the mild phenotype of MCU-KO mice), it needs stressing that, in MCU-KO animals, either in isolated organelles or in living cells, Pan and co-authors did not find any evidence for energy dependent Ca^{2+} uptake.

2.5.2 Other proteins involved in mitochondrial Ca^{2+} uptake

Uncoupling proteins 2 and 3 (UCP2/3) are two proteins described to modulate the MCUC activity and thus mitochondrial Ca^{2+} uptake. The down-regulation of these proteins reduces mitochondria Ca^{2+} uptake while the over-expression increases it (Trenker M. *et al.*, Nat Cell Biol 2007). It has been proposed that these two proteins can modulate mitochondrial Ca^{2+} uptake only when Ca^{2+} is released from the ER (Waldeck-Weiermair M. *et al.*, Cell Calcium 2010). However, the real role of UCPs has still to be clarified since it has been observed that isolated mitochondria from UCP2-KO or UCP3-KO mice take up Ca^{2+} normally (Brookes P.S. *et al.*, Nat Cell Biol 2008).

Letm1 has been proposed, in 2009, to be a mitochondrial $\text{H}^+/\text{Ca}^{2+}$ electrogenic antiport, with high Ca^{2+} affinity (Jiang D. *et al.*, Science 2009). Purified Letm1 reconstituted into liposomes mediates a Ruthenium Red-sensitive mitochondrial Ca^{2+} uptake. However, others challenged this idea, proposing that Letm1 is probably a H^+/K^+ antiporter, since in MEFs the Letm1-KO phenotype could be rescued by nigericin, a bona fide H^+/K^+ ionophore (Nowikovsky K. *et al.*, 2012). Thus, the role of Letm1 in mitochondrial Ca^{2+} uptake is still under investigation. Anyway, a recent RNAi-based screening, that permitted the identification of MCUR1

(Mallilankaraman K *et al.*, Nat Cell Biol 2012b), confirmed a role for Letm1 in mitochondrial Ca^{2+} handling, since its silencing induces a decreased Ca^{2+} uptake into the organelles.

2.5.3 Mitochondria Ca^{2+} efflux

In order to maintain mitochondrial Ca^{2+} homeostasis, the capability of mitochondria to take up high amount of Ca^{2+} has to be balanced by mitochondrial Ca^{2+} release (Figure 9).

NCX. The first idea that a mitochondrial $\text{Na}^+/\text{Ca}^{2+}$ exchanger (NCX) could exist, came in the early '70s, when it has been observed that, in isolated mitochondria, upon addition of Na^+ to the external solution, a consequent release of Ca^{2+} occurred (Hoppe UC, FEBS let 2010). Moreover, this release was not inhibited by Ruthenium Red, thus suggesting that it is mediated by a mechanism distinct from the one responsible for Ca^{2+} uptake. However, the direction and the amplitude of ion movements were dependent on Na^+ and Ca^{2+} concentrations in cytosolic and mitochondrial matrix environments (meaning that it could work also in a reverse mode, extruding Na^+ and taking up Ca^{2+}). NCX has an important role in excitable tissues, such as heart, brain and skeletal muscle. In 1992, a 110 kDa protein was purified from bovine heart mitochondria; when reconstituted in liposomes, it catalysed a $\text{Na}^+/\text{Ca}^{2+}$ and Na^+/Li^+ exchange (NCLX) (Li W. *et al.*, J Biol Chem 1992). In 2010, Sekler and co-workers demonstrated that the NCLX (until that moment considered an isoform of the PM $\text{Na}^+/\text{Ca}^{2+}$ exchanger family) is the elusive mitochondrial $\text{Na}^+/\text{Ca}^{2+}$ antiport (Palty R. *et al.*, PNAS 2010). Indeed, they found that:

- NCLX is located in the IMM.
- It can be blocked by CGP-37157.
- NCLX-KO reduces the Na^+ -dependent Ca^{2+} efflux in isolated mitochondria.

The stoichiometry of the NCLX-mediated exchange is still under debate, although it seems to be 3 Na^+ : 1 Ca^{2+} ratio.

mHCX. $\text{H}^+/\text{Ca}^{2+}$ antiporter is another protein located in mitochondria and important for the efflux of Ca^{2+} in non-excitable cells, even if less is known about it, compared to NCLX. Although in 1998 a 55-66 kDa protein has been purified by affinity chromatography, the molecular identity of this protein has not been yet revealed.

mPTP. It has been proposed that Ca^{2+} could efflux from mitochondria through the permeability transition pore (mPTP; for a review see Bernardi P, Physiol Rev 1999), though the role of PTP in the mitochondrial Ca^{2+} efflux is debated (De Marchi E *et al.*, Cell Calcium 2014).

On one hand, PTP has been reported to undergo transient openings, in both isolated mitochondria and intact cells, thus allowing mitochondrial Ca^{2+} release when the matrix Ca^{2+} concentration is higher than in the external medium. This phenomenon contributes to organelle Ca^{2+} homeostasis, acting as a rapid, pro-survival Ca^{2+} -induced Ca^{2+} release mechanism without causing dramatic and irreversible PT (Rasola A. and Bernardi P., Cell Calcium 2011). On the other hand, the importance of the PTP in the Ca^{2+} efflux from mitochondria has been challenged by De Marchi and co-authors, showing that PTP is a dispensable element for mitochondria Ca^{2+} release (De Marchi E et al., Cell Calcium 2014).

2.5.4 Physiological consequences of mitochondrial Ca^{2+} uptake

The capability of mitochondria to take up Ca^{2+} is essential not only for mitochondria *per se* but also for the whole cell, since Ca^{2+} regulates several mitochondrial activities that are important for many cellular aspects (Figure 11).

Indeed, it has been well described the role of mitochondrial Ca^{2+} uptake in the following functions:

- Mitochondrial metabolism. It is known since '90s that Ca^{2+} has a pivotal role in the regulation of mitochondrial metabolism (see below);
- Cell death. It is well known that mitochondrial Ca^{2+} uptake, in particular mitochondrial Ca^{2+} overload, can mediate cell death, by both necrosis and apoptosis. On one side, an exaggerated mitochondrial Ca^{2+} influx disturbs the proton gradient across the IMM, inducing necrosis; on the other side, an excessive amount of mitochondrial Ca^{2+} can sensitize the organelle to apoptotic stimuli. At resting conditions, physiological Ca^{2+} rises in the mitochondria do not induce the opening of PTP; however, when coupled with apoptotic stimuli, such as ceramide, mitochondrial Ca^{2+} rises favour the opening of PTP, the release of cytochrome C in the cytosol and thus the activation of the apoptotic cascade (Rasola A and Bernardi P, Cell Calcium 2011). Of note, important in the apoptosis Ca^{2+} -dependent stimulation is ER-mitochondria interaction. Indeed, VDAC1, located in the OMM forms a bridge with the IP3R, located in the ER, through their interaction with GRP75; this bridge is essential for ER-mitochondria Ca^{2+} transfer and, importantly, is enhanced upon apoptotic stimuli (De Stefani D *et al.*, Cell death different 2012). Furthermore, also Fis1, a mitochondrial fission protein, can be an apoptotic signal; it can interact with the ER protein Bap31, inducing its cleavage into a

pro-apoptotic complex p20Bap31. This complex stimulates ER-mitochondria Ca^{2+} transfer and the recruitment of procaspase-8, stimulating apoptosis.

- ER stress. The reduction in ER Ca^{2+} content can induce impairments in ER activity, accumulation of unfolded proteins that activates ER stress and the so called “unfolded protein response” (UPR) (Verfaillie T *et al.*, Cancer Lett 2013). In this context, the ER-mitochondria coupling plays an important role; in the early stage of ER stress, ER undergoes conformation changes and mitochondria change their distribution within the cells, positioning around the ER and increasing ER-mitochondria contact sites, thus favouring ER-mitochondria Ca^{2+} shuttling. The increased Ca^{2+} rises in mitochondria stimulate mitochondrial metabolism and thus ATP production. The increase in ATP production seems to be an attempt of the cell to solve stress conditions, supplying with more ATP enzymes located in the ER and involved in UPR (Bravo R *et al.*, J Cell Sci 2011). Under stress condition, the ER-mitochondria Ca^{2+} transfer is favoured also by ER proteins such as Sigma1R. At rest condition, it is associated with Bip/GRP78 in the ER lumen; upon ER stress signals, it dissociates from Bip and it moves to MAM (see below) where it promotes Ca^{2+} transfer from ER to mitochondria.
- Mitochondrial shape. Ca^{2+} influences also the shaping of the organelles by activating the mitochondrial shaping protein, Drp1, through its calcineurin-driven dephosphorylation, occurring after $[\text{Ca}^{2+}]_c$ rises (Cribbs JT and Strack S, EMBO Rep 2007).
- Autophagy. It is a pathway that regulates the quality and the homeostasis of the whole cell. It is present both at resting conditions and mainly upon stimulation, such as under nutrients deprivation and low cellular energy. It has been showed that the constitutive IP3 mediated ER-mitochondria Ca^{2+} transfer is essential to sustain cell bioenergetics; a reduction in this Ca^{2+} shuttling causes mitochondrial impairments that leads to lower ATP levels. The energy stress condition causes an increase in the phosphorylated form of AMPK and consequently autophagy activation. Thus, the absence of the constitutive ER-mitochondria Ca^{2+} transfer causes AMPK activation and mTOR inactivation, and the increase in the autophagy markers LC3II and LC3 puncta (Cardenas C *et al.*, Cell 2010 ; Bootman MD *et al.*, Cell Calcium 2017).

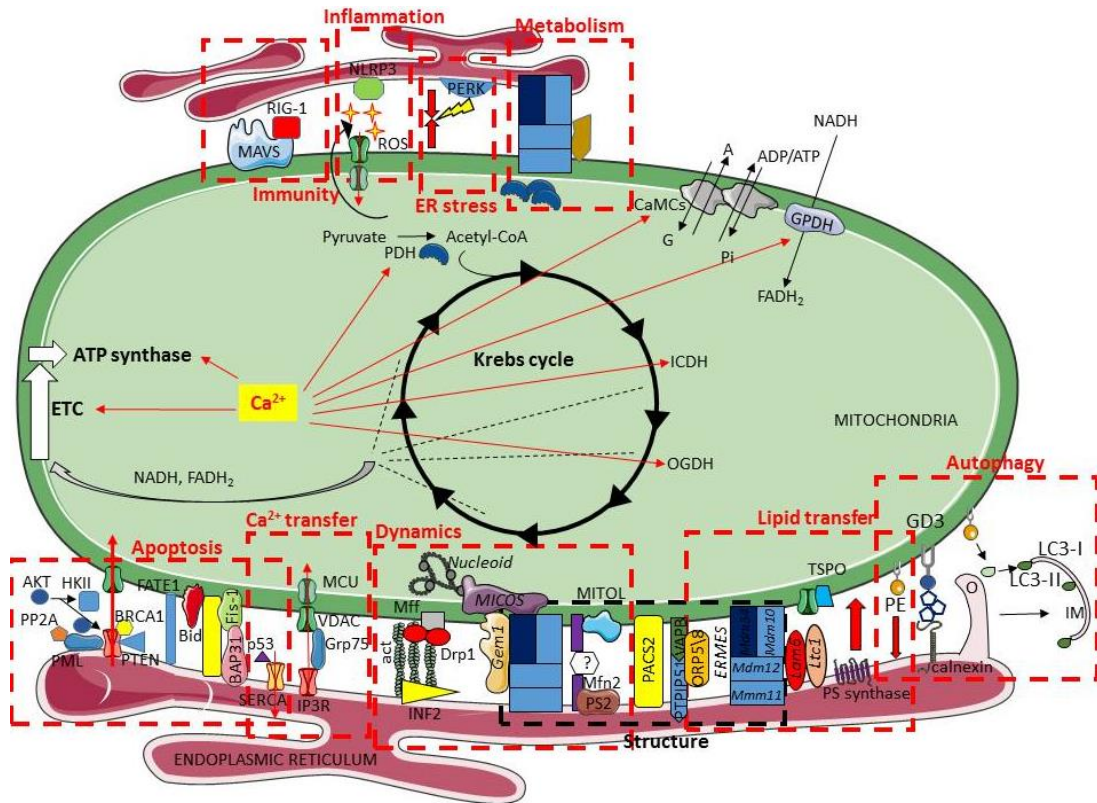


Figure 11 : ER-mitochondria contact sites. Representation of the main proteins involved in ER-mitochondria tethering and their functions. Red-dotted squares indicate specific functions sustained by the ER-mitochondria interaction; in the black-dotted square are represented proteins that have been implicated in the structure of the ER-mitochondria interface. Modified from Filadi R *et al.*, Mitochondrial Ca^{2+} handling and behind: the importance of being in contact with other organelles. Molecular Basis for Mitochondrial Signaling. T.K. Rostovtseva. Switzerland, Springer(2017).

2.6 ER-mitochondria crosstalk: Ca^{2+} microdomains and Mitochondria Associated Membranes

Even if, as described above, the affinity of MCU is low, mitochondria can take up high amount of Ca^{2+} since they are located in close contact with the Ca^{2+} releasing intracellular stores (mainly ER) or with the PM (Rizzuto R and Pozzan T , *Physiol Rev* 2006). Thus, when ER or PM Ca^{2+} channels open, Ca^{2+} flows out of the store, or passes the PM, and spread in the cytosol (where the Ca^{2+} concentration is lower), generating, in front of the channels mouth, high Ca^{2+} concentration microdomains that are sensed by the nearby mitochondria, allowing the activity of MCU and thus mitochondrial Ca^{2+} uptake. These observations lead to the “ Ca^{2+} microdomain hypothesis”. Generally, a microdomain is a localized region within the cell whose composition is different from that of the surrounding area. The Ca^{2+} microdomain hypothesis

has been confirmed by different approaches; through electron and fluorescence microscopy, in different cell types, it has been shown that there are regions of close proximity between ER and mitochondrial membranes (Csordas G *et al.*, EMBO J 1999; Rizzuto R *et al.*, Science 1998; Gilibert JA *et al.*, EMBO J 2000). Moreover, the existence of Ca²⁺ microdomains has been directly confirmed using Cameleon Ca²⁺ probes targeted to the OMM (Giacomello M *et al.*, Mol Cell 2010); these experiments have proved the existence of small OMM regions where, upon stimulation of Ca²⁺ release from the ER, [Ca²⁺]_i reaches values as high as 15–20 μM. Altogether, these data support the conclusion that microdomains of high [Ca²⁺]_i are sensed by mitochondria that are present in close proximity to IP3Rs and RyRs in ER or SR membranes (Giacomello M *et al.*, Mol Cell 2010; Korzeniowski *et al.*, Cell Calcium 2009).

Structurally, the first observation of the existence of sites of contacts between ER membranes and the OMM revisits more than 50 years ago (Robertson JD, Prog Biophys Mol Biol 1960; Ruby *et al.*, 1969; Morré DJ *et al.*, Protoplasma 1971), but the significance of these appositions has been revealed only recently. In details, an ER fraction that is attached to mitochondria can be biochemically isolated as mitochondria-associated membranes (MAM), a fraction enriched in enzymes that are involved in lipid synthesis, including phosphatidylserine (PS) synthase (Stone SJ and Vance JE, J Biol Chem 2000). The distance between ER and mitochondria in MAM have been measured to be 10–30 nm. This distance is close enough to suggest that the two organelles are tethered together by proteins located on the apposed membranes (Rowland AA and Voeltz GK, Nat Rev Mol Cell Biol 2012).

The distance between ER and mitochondria is important for the regulation of Ca²⁺ transfer; in particular, it has been shown that decreasing the distance between the two organelles, or increasing the surface of contact, favours the Ca²⁺ transfer from ER to mitochondria (Csordas G *et al.*, J Cell Biol 2006) (Figure 12).

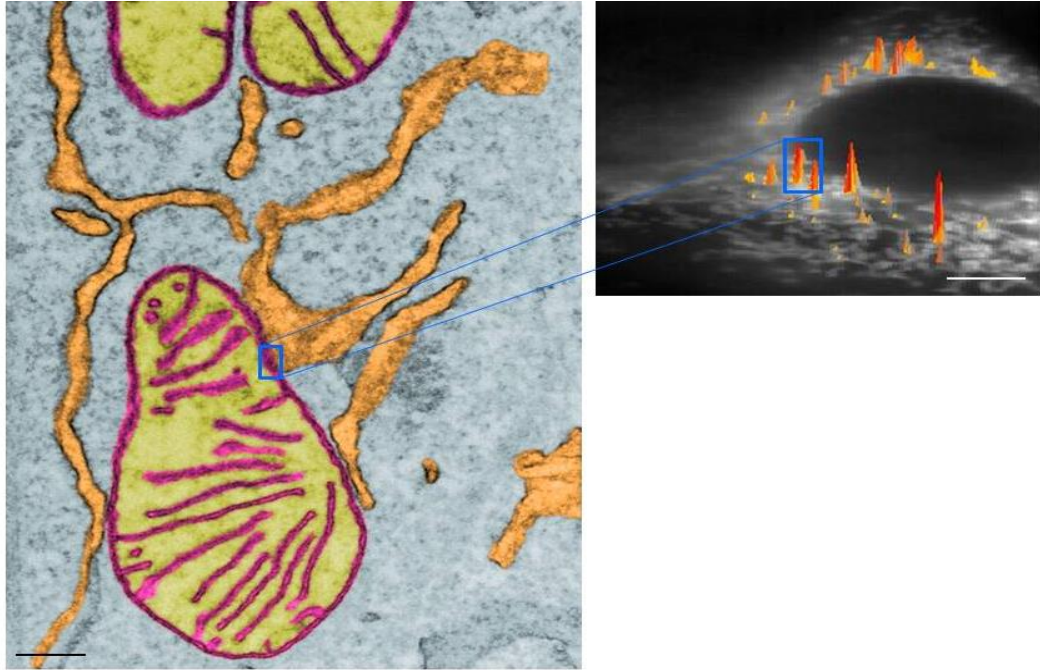


Figure 12 ER-mitochondria juxtaposition. (Left) EM image of a wt MEF showing several close appositions between ER (orange) and OMM (purple). Scale bar: 100 nm. The juxtaposition between the two opposing membranes allows the generations of high $[Ca^{2+}]$ domains on OMM upon Ca^{2+} release from ER-located Ca^{2+} channels. (Right) A neuroblastoma cell (SH-SY5Y) transiently expressing the OMM-targeted cameleon Ca^{2+} probe N33-D1cpv. Yellow-to-red spikes indicate the generation of high $[Ca^{2+}]$ microdomains in OMM regions, upon IP₃-mediated ER Ca^{2+} release. Image modified from Filadi *et al.*, "Endoplasmic Reticulum Stress in Health and Disease", P. Agostinis, A. Samali (eds), 2012 Springer Science+Business Media Dordrecht.

Many are the molecular components identified in MAM that play a crucial role in the regulation of contact sites between ER and mitochondria (Figure 11); here some of them are commented. One of the proteins that received a lot of attention is Mitofusin2 (Mfn2). It is a protein enriched in MAM, located in both ER membrane and OMM, reported to modulate the ER-mitochondria tethering. Originally, it was proposed to be an ER-mitochondria tether, since, upon Mfn2-KO, a decrease in the ER-mitochondria co-localization was observed (De Brito and Scorrano 2008). However, later, we and other groups (Filadi R *et al.*, PNAS 2015, Leal N *et al.*, J Cell Mol Med 2016, Cosson C *et al.*, Plos One 2012, Wang PT *et al.*, J cell sci 2015; Cieri D *et al.*, Cell Death Diff 2017) have demonstrated, using several techniques, that Mfn2-KO or Mfn2-KD increases contact sites between the two organelles instead of reducing them, as previously reported.

Beyond Mfn2, other proteins are involved in the regulation of ER-mitochondria tethering. Among them, IP3R, GRP75 and VDAC are three proteins that form a complex that functionally

modulates ER-mitochondria Ca^{2+} coupling: IP3R, localized in the ER, interacts with VDAC1, located in the OMM, through the presence of the cytosolic chaperone GRP75 (Szabadkai G. *et al.*, J Cell Biol 2006).

Also the Familial Alzheimer's Disease-linked Presenilin2 have been reported, by our group, to be enriched in MAM and increase ER-mitochondria contact sites, both from a physical and a functional point of view. Both the wt and the mutated PS2 acts in the same way, although PS2 mutants seems to be more effective (Zampese E *et al.*, PNAS 2011; Kipanjula M *et al.*, Aging cell 2012,). Recently, we have also demonstrated that PS2 increases ER-mitochondria contact sites in a Mfn2-dependent way: PS2 sequesters Mfn2, blocking its negative effects on ER-mitochondrial tethering (Filadi R *et al.*, Cell Rep 2016).

The ER-mitochondria physical and functional coupling has been shown to be positively modulated by an ER protein, VAPB, and an OMM protein, PTPIP51 (De Vos KJ *et al.*, Hum Mol Genet 2012). Also, the ER stress related protein kinase RNA-like ER kinase (PERK) is involved in ER-mitochondria contact sites regulation, independently from its function in ER stress. Recently, a new modulator of ER-mitochondria contact sites has been discovered. Hirabayashi *et al.* described PDZD8 as an ER protein enriched in MAM and essential for ER-mitochondria physical and functional coupling (Hirabayashi Y *et al.*, Science 2017).

All the proteins mentioned above, and many others, are located in this particular regions of contact between ER and mitochondria. Here, they have both a physical role, maintaining the ER-mitochondria coupling structure, and a functional role. Regarding this latter, they not only regulate Ca^{2+} shuttling between the two organelle, as already described, but also other important cellular functions, such as lipids synthesis and trafficking, autophagy, UPR, organelles dynamics and biogenesis (Figure 11).

2.6.1 ER-mitochondria tethering and diseases

Alzheimer's Disease (AD). AD is characterized by several early alterations in many cellular functions, such as Ca^{2+} homeostasis, autophagy, lipids metabolism, mitochondrial dynamics and ROS production. PS1 and PS2 have been found enriched in MAM (Area Gomez E *et al.*, J Am Pathol 2009). It has been also demonstrated that both WT and, more efficiently, FAD-PS2 mutants favour the ER-mitochondria Ca^{2+} transfer by increasing ER-mitochondria coupling, in different AD models (cell lines expressing mutated PS2, cortical neurons from PS2-N141I transgenic mice and FAD-PS2 patient-derived fibroblasts; Zampese E *et al.*, PNAS 2011, Kipanjiula M *et al.*, Aging Cell 2012; Area Gomez E *et al.*, EMBO J 2012), while PS1 does not impact on this aspect. Recently, our group has shown that PS2 increases ER-mitochondria

contact sites by sequestering Mfn2 and blocking its negative effect on ER-mitochondria tethering (Filadi R *et al.*, Cell Rep 2016). Moreover, by increasing ER-mitochondria contacts, downregulating Mfn2, γ -secretase activity results affected, causing an alteration in the A β production process (Leal N *et al.*, J Cell Mol Med 2016). Altogether, these results suggest that MAM may represent a novel AD therapeutic target.

Parkinson's Disease (PD). PD is a progressive neurodegenerative disorder characterized by loss of dopaminergic neurons. It is well known that mitochondrial dysfunctions are involved in the PD pathogenesis; it is mainly sporadic, however a little percentage of cases are due to mutations on genes coding for different proteins, such as PINK or Parkin (Cali T *et al.*, Biofactors 2011). The overexpression of wt Parkin has been shown to increase ER-mitochondria contact sites and thus ER-mitochondria Ca²⁺ transfer and ATP production, while the KO of the same proteins causes mitochondrial fragmentation (Cali T *et al.*, Biochim Biophys Acta 2013). Another protein involved in PD is DJ1; when overexpressed, DJ1 increases contact sites between the two organelles, by inhibiting the activity of the tumor suppressor protein p53. Moreover, while the wt DJ1 translocates to the mitochondrial matrix, to sustain ATP levels upon nutrient deprivation, when pathogenically mutated, it is not able to do it (Cali T *et al.*, Hum Mol Genet 2015). Finally, also α -synuclein is enriched in MAM, increasing the ER-mitochondria coupling (Cali T *et al.*, J Biol Chem 2012); on the contrary, when mutated, it dissociates from MAM, altering the ER-mitochondria connection.

Amyotrophic Lateral Sclerosis (ALS). ALS is a motor neuron disease associated with frontotemporal dementia. The 50 % of the cases are due to mutations on three genes coding for TDP-43, FUS and C9ORF72 that accumulate in the nucleus and cytosol of neurons and glia. Overexpression of both wt and mutants of TDP-43 and FUS causes a reduction in the physical and functional ER-mitochondria coupling, thus affecting mitochondria activity (Stoica R *et al.*, Nat comm 2014; Stoica R *et al.*, Embo Rep 2016), through the disruption of the VAPB-PTPIP51 ER-mitochondria tether complex. Indeed, other ALS-linked mutated proteins, such as G93AhSOD1 and Sigma1R, have been shown to affect the ER-mitochondria communication, decreasing the number of contact sites and their functions.

2.7 The Ca²⁺ hypothesis for AD

Due to the observation that amyloid plaques and neurofibrillary tangles appear only in the late stage of the pathology, the idea that additional mechanisms can be responsible for the

development of the disease has emerged. Indeed, a central role for Ca^{2+} dys-homeostasis in early stages of the pathology has been proposed, leading to the formulation of the “ Ca^{2+} hypothesis”.

In 1988, for the first time, Khachaturian hypothesized that alterations in Ca^{2+} homeostasis are responsible for the neurodegeneration observed in AD. After few years, other data confirmed the role of Ca^{2+} in the AD pathology: studies performed in fibroblasts from still asymptomatic but FAD-PS expressing patients, reported an increased IP3-mediated Ca^{2+} release from the ER, suggesting that alterations in Ca^{2+} homeostasis could be early events in AD pathogenesis (Ito E *et al.*, PNAS 1994; Etcheberrigaray R *et al.*, Neurobiol Dis 1998). In the following years, several studies have confirmed these results (Honarnejad K and Herms J., Int J Biochem Cell Biol 2012); in details:

- FAD-PS1 expressing models (cell lines and neurons from transgenic mice) display an increased ER Ca^{2+} release upon stimulation (Chan SL *et al.*, J Biol Chem 2000; Guo Q *et al.*, Neurorep 1996; Stutzmann JE *et al.*, J Neuroscience 2006)
- FAD-PS1 and FAD-PS2 mutations potentiate ER Ca^{2+} release from RyRs, probably due to increased expression levels of the RyR (Chan SL *et al.*, J Biol Chem 2000);
- FAD-PS1 and FAD-PS2 mutations increase ER Ca^{2+} release via IP3Rs (Ito E *et al.*, PNAS 1994; Guo Q *et al.*, Neurorep 1996) ;
- wt PS holoproteins form passive Ca^{2+} leak channels on planar lipid bilayers and FAD-PS mutants impair this leak activity, leading to an increased ER Ca^{2+} content (Tu H *et al.*, Cell 2006).

Altogether, these data support the “calcium overload” hypothesis for AD, sustaining that the ER Ca^{2+} overload is the first cause of exaggerated Ca^{2+} release from the ER, mitochondrial Ca^{2+} overload, altered APP processing and kinase activities, cell death and neurodegeneration (La Ferla FM, Nat Rev Neurosci 2002).

Later, the Ca^{2+} overload hypothesis has been challenged. Indeed, different results, here listed, came out:

- Expression of FAD-PS2 mutants (PS2-T122R, PS2-M239I, PS2-N141I, PS2-D366A) reduces ER Ca^{2+} release upon stimulation; the effect of PS2 mutants has been shown in different cell lines but also in cortical neurons from PS2-N141I transgenic mice, compared to WT, and in fibroblasts from FAD-PS2 patients (Zatti G *et al.*, Neurobiol

- Dis 2004; Giacomello M *et al.*, *Neurobiol Dis* 2005; Zatti G *et al.*, *Cell Calcium* 2006; Brunello L *et al.*, *J Cell Mol Med* 2009; Kipanyula MJ *et al.*, *Aging cell* 2012);
- In FAD-PS1 (PS1-A246E, PS1-M146L, PS1-L286V, PS1-P117L) expressing cells, both cell lines and fibroblasts from patients, the ER Ca²⁺ release is unchanged or reduced (but to a lower extent compared to FAD-PS2) (Zatti G *et al.*, *Cell Calcium* 2006);
 - Direct ER Ca²⁺ measurements, performed by both a FRET-based Ca²⁺ probe, ERD4 and an ER-Aequorin, confirmed the data just described; the ER Ca²⁺ content is reduced in FAD-PS2 (PS2-T122R, PS2-M239I, PS2-N141I, PS2-D366A) expressing cells, while it is unchanged, or slightly reduced, in FAD-PS1 (PS1-A246E, PS1-M146L, PS1-L286V, PS1-P117L) expressing cells (Zatti G *et al.*, *Cell Calcium* 2006; Kipanyula MJ *et al.*, *Aging cell* 2012).
 - Foskett's group similarly found no evidence of ER Ca²⁺ overload due to the expression of PS1 or PS2 mutants; moreover they showed that the "apparent" Ca²⁺ overload previously described is due to exaggerated Ca²⁺ release following modulation of the IP3R's gating by PS mutants (Cheung, *et al.* 2010).

Regarding the mechanism by which PSs alter Ca²⁺ signalling, it has been demonstrated that they physically interact with SERCA2b (Green KN *et al.*, *J Gen Physiol* 2008); in particular, in our lab it has been demonstrated that PS2 expression does not alter SERCA expression levels but it inhibits its activity (Brunello L *et al.*, *J Cell Mol Med* 2009). Moreover, in cells expressing different FAD-PS2 mutants, no changes and an increase in the expression levels of IP3R and RyR, respectively, have been detected (Brunello L *et al.*, *J Cell Mol Med* 2009; Kipanyula MJ *et al.*, *Aging cell* 2012). A slight increase in basal Ca²⁺ leakage through IP3Rs and RyRs, upon PS2 over-expression, has been also observed (Brunello L *et al.*, *J Cell Mol Med* 2009), with a reduced response to IP3-linked stimuli, but an increased response to caffeine (a RyR activator) (Kipanyula MJ *et al.*, *Aging cell* 2012).

Due to the discrepancy between these data and those sustaining the Ca²⁺ overload hypothesis, some attempts to uncover the PSs role in Ca²⁺ homeostasis have been performed using MEF cells double KO for both PS1 and PS2. However, inconsistent results have been obtained, describing either attenuated (Kasri NN *et al.*, *Cell Calcium* 2006) or amplified (Tu H. *et al.*, *Cell* 2006) Ca²⁺ release from the ER.

In addition, it has been shown that PS2, in particular FAD-PS2 mutants, but not PS1, favours ER to mitochondria Ca^{2+} transfer, upon similar ER Ca^{2+} release, due to its ability to increase ER-mitochondria contacts (Zampese E *et al.*, PNAS 2011; Filadi R *et al.*, Cell Rep 2016).

The link between Ca^{2+} dys-homeostasis and AD is also sustained by the fact that alterations in CCE have been also described:

- PS1-M146L overexpression in MEF and HeLa cells reduces CCE (Zatti G *et al.*, Cell Calcium 2006);
- PS1-M146V reduces CCE in fibroblasts from transgenic mice (Leissring MA, *et al.*, J Cell Biol 2000);
- PS1-A246E; PS1-L286V, PS1dE9 and PS1-P117L decreases CCE when overexpressed in different cell types (Zatti G *et al.*, Cell Calcium 2006; Smith IF *et al.*, Brain res 2002);
- PS2-T122R reduces CCE in HeLa (Zatti G *et al.*, Cell Calcium 2006), HEK293T cells and human FAD fibroblasts (Giacomello M. *et al.*, Neurobiol Dis 2005);
- PS2-N141I decreases CCE in HeLa cells (Zatti G *et al.*, Cell Calcium 2006), MEFs and primary neurons from transgenic mice (Yoo AS, *et al.*, Neuron 2000);
- PS2-M239I decreases CCE in HeLa but not in human fibroblasts (Zatti G *et al.*, Cell Calcium 2006; Zatti G. *et al.*, Neurobiol Dis 2004).

The molecular mechanism by which this Ca^{2+} entry pathway is affected by FAD-PSs expression is not clear.

Of note, a connection between alterations in Ca^{2+} handling and APP processing has been reported; in particular, some works showed an increase in both cytosolic $[\text{Ca}^{2+}]$ and $\text{A}\beta$ production (Bojarski L. *et al.*, Biochim Biophys Acta 2008). $\text{A}\beta$ has been showed to form low conductance cationic channels in PM permeable to Ca^{2+} , interfering with NMDA and AMPA receptors activity, affecting LTP (Haass and Selkoe, Nat Rev Mol Cell Biol 2007; Querfurth H.W. and LaFerla F.M, N Engl J Med 2010). $\text{A}\beta$ oligomers can also induce ER Ca^{2+} release in different way: (a) enhancing the sensitivity and gating of IP3Rs and RyRs (Demuro A and Parker I, J Neurosci 2013; Oules B *et al.*, J Neurosci 2012); (b) Increasing the expression of RyRs (Supnet C *et al.*, J Biol Chem 2006); (c) altering the IP3/DAG pathway, by destabilizing the phosphatidylinositol-4, 5-bisphosphate metabolism (Berman DE *et al.*, Nat Neurosci 2008).

On this aspect, in our lab, measuring cytosolic and ER Ca^{2+} levels, it has been recently showed that: the acute application of $\text{A}\beta_{42}$ (monomers or oligomers) at physiological levels (0.5-1 μM) does not cause neither Ca^{2+} influx nor Ca^{2+} release. Moreover, the incubation of cortical

neurons with A β 42 oligomers causes a reduction in Ca²⁺ release mediated by IP3-generating agonists, while an increase in Ca²⁺ release through RyRs (Lazzari C *et al.*, *Neurobiol Aging* 2015). Altogether, the data described above suggest that in AD there is a link between the “amyloid cascade hypothesis” and the “Ca²⁺ hypothesis”, likely being both at the basis of AD pathogenesis.

3. Bioenergetics

Each cell, part of tissues or organs in the body, sustains a huge amount of functions essential for its healthy and for organs or tissues activity. Most of these functions require energy. Thus, every cell has to produce high amounts of energy to carry out its work. Indeed, cells use organic food molecules, such as fats, proteins and sugars that are processed by several different pathways, to produce energy.

The most abundant energy molecule is ATP, adenosine 5'-triphosphate. It is made of adenine (nitrogen base), ribose and three phosphate groups that bind the sugar; the bond between the last two phosphate groups is a high-energy bond. ATP is produced by many pathways in the cell such as glycolysis, citric acid cycle (Tricarboxylic Acid Cycle, TCA cycle, also known as Krebs' cycle), oxidative phosphorylation, fatty acid pathway, pentose phosphate pathway, urea cycle and beta-oxidation. Depending on the tissues, cells favour one pathway instead of another. Excesses of energy are stored by the cell in energy-enriched molecules, like glycogen and lipids (Clarke DD and Sokoloff L, *Intermediary metabolism* 1999).

3.1 Brain metabolism: neurons/astrocytes differences and their metabolic coupling

One of the organs that requires a high amount of energy for its function is the brain. Although it represents only the 2% of the body mass, its energy demand is around 20% of whole body. The brain's cell types are highly heterogeneous and consequently they have different metabolic profiles. Indeed, while neurons use mainly mitochondria (TCA cycle and oxidative phosphorylation) to produce ATP, in astrocytes, glycolysis is predominant. The metabolism of other cell types, such as oligodendrocytes and microglia, has not been characterized yet.

Many reasons justified the metabolic differences between neurons and astrocytes (Figure 13). Below, some of them are listed:

- Pyruvate Dehydrogenase (PDH) activity. PDH is the enzyme that converts pyruvate, entered in the mitochondria, to acetyl-CoA. The active/inactive state of this enzyme is regulated by a kinase (PD kinase, PDK), that through the phosphorylation of the enzyme made it inactive, and by a phosphatase (PD phosphatase, PDP), that activates the enzyme by de-phosphorylating it. In astrocytes, it has been demonstrated that the PDK expression levels are high, the degree of PDH-P is elevated, thus favouring the inactive form of the protein, hence justifying the glycolysis upregulation in these cells (Halim ND *et al.*, *Glia* 2010; Zhang S *et al.*, *Nutr Metab* 2014).
- 6-phosphofructo2-kinase/fructose-2,6-biphosphatase 3 (Pfkfb3). It is a potent activator of the glycolytic enzyme phosphofructokinase-1 (PFK1) and thus an important regulator of glycolysis. In neurons, but not in astrocytes, this enzyme is constantly subjected to degradation by proteasome, justifying the slow glycolysis of these cells (Bolanos JP *et al.*, *J Trends Neurosci* 2010; Herreno-Mendez A *et al.*, *Nat Cell Biol* 2009).
- In neurons, low levels of Pfkfb3 justify the fact that these cells process glucose not through glycolysis but mainly through the pentose phosphate pathway (PPP); this is the main pathway used by the cell to produce NADPH, a reducing equivalent that neurons use as scavenger for reactive oxygen species (ROS), highly produced by the neurons' oxidative activity. Thus, neurons use glucose mainly to sustain their antioxidant status instead of energy production (Magistretti PJ and Allaman I, *Neuron* 2015).
- Pyruvate kinase (PK). It is the enzyme that converts phosphoenolpyruvate to pyruvate, becoming an important regulator of glycolysis. Neurons express the isoform 1 of the enzyme (PKM1), while astrocyte the isoform 2 (PKM2). Moreover, while astrocytes are able, upon high energy demand, to upregulate glycolysis through PKM2, neurons are not (Magistretti PJ and Allaman I, *Neuron* 2015).

Altogether, the differences described above suggest that astrocytes and neurons have complementary metabolic pathways.

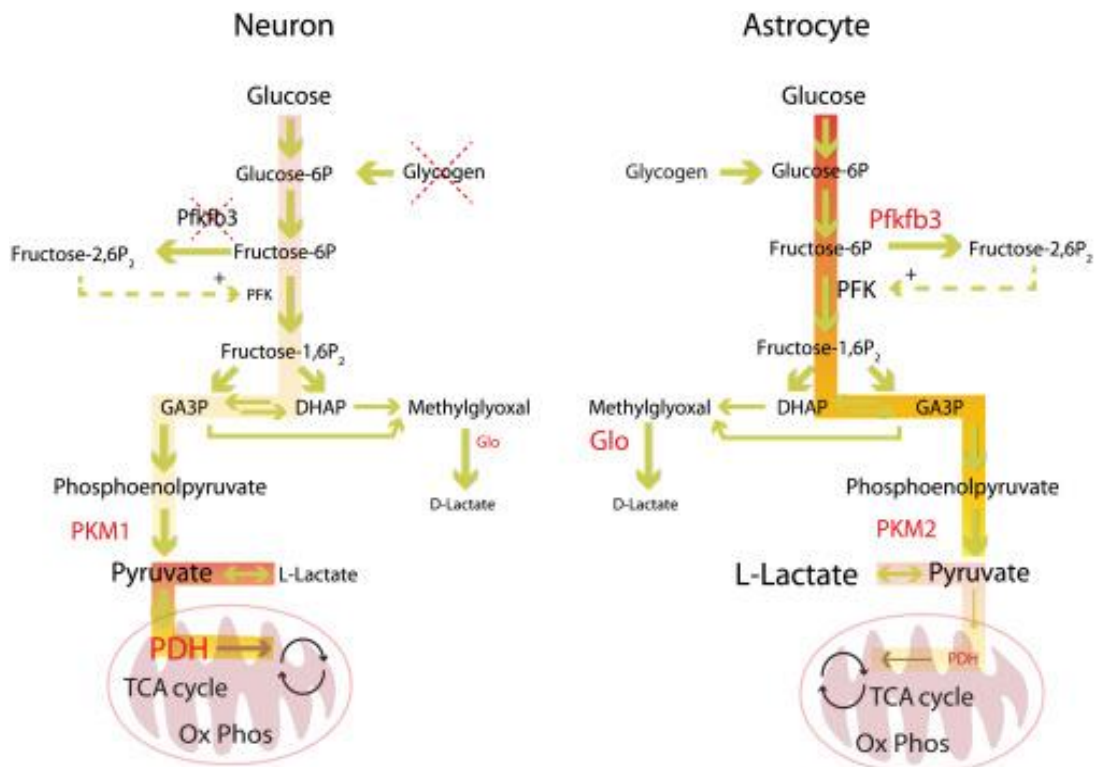


Figure 13 Features that underlie the differences in metabolic profiles between neurons and astrocytes (Magistretti PJ and Allaman I, Neuron 2015)

Indeed, neurons produce ATP, essential for all their functions, in particular synaptic activity, mainly through the TCA cycle and the oxidative phosphorylation, occurring in mitochondria, by utilizing pyruvate and lactate produced through glycolysis or coming from astrocytes (see below). Moreover, they mainly utilize glucose to produce, through the PPP, the reducing equivalents used as ROS scavengers. On the other side, astrocytes produce energy mainly using glucose that undergoes glycolysis; through this process, they produce a high amount of pyruvate and lactate, then transported to neurons. In details, the upregulation of glycolysis in astrocytes is induced by the uptake of glutamate once released in the synaptic space by neurons. Astrocytes glutamate uptake is a process that consumes ATP, thus inducing the uptake of glucose, through the GLUT1 transporter, and glycolysis. The upregulation of this last process leads to an increase in lactate production, metabolite that is then transferred to neurons, to sustain mitochondrial metabolism. Hence, the mechanism that allows the coupling of these two metabolic pathways is called astrocyte-neuron lactate shuttle (ANLS), mediating the link between synapses activity and energy demand (Figure 14; Magistretti PJ and Allaman I, Neuron 2015).

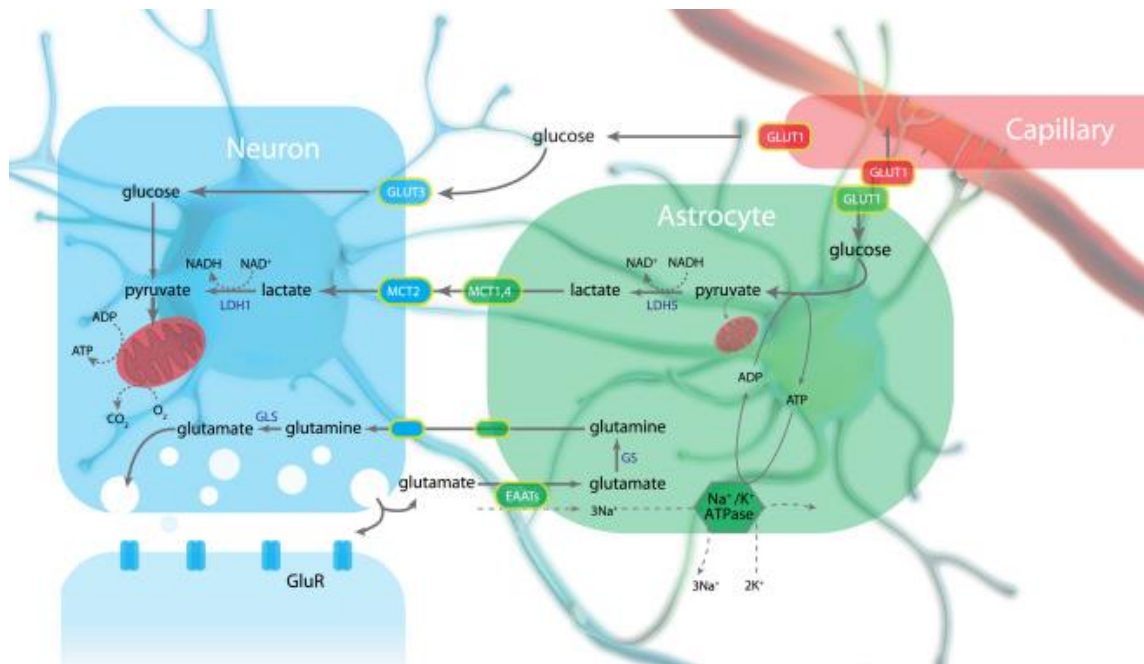


Figure 14 Schematic representation of the Astrocyte-Neuron Lactate Shuttle (Magistretti PJ and Allaman I, Neuron 2015).

As mentioned above, the excess of energy produced by cells is kept as glycogen or lipids; indeed, glycogen metabolism plays a crucial role in neuronal activity, sustain their energy demand. In conditions in which neurons need high levels of ATP, astrocytes convert glycogen into glucose inducing glycolysis, and thus lactate production. Lactate is then transferred to neurons and used to produce ATP (review Falkowska A *et al.*, Int J Mol Sci 2015).

The oxidation of fatty acids is a pathway highly used by several types of cells (liver, kidney, heart) to produce ATP; however, it seems that brain does not use this process to make energy. In particular, it has been proposed that brain does not use fatty acids for three main reasons (Schonfeld P and Reiser G, J Cereb Blood Flow Metab 2013):

- they do not easily cross the blood brain barrier (BBB);
- low enzymatic capacity for fatty acids degradation by brain's mitochondria beta-oxidation; the low level of fatty acids oxidation is due to: (I) low enzymatic activity; (II) low rate of translocation across the IMM;
- High mitochondrial side effects and high ROS production.

Finally, another energy source that can be used by neurons comes from ketone bodies. Under prolonged fasting conditions, ketone bodies can be used by the cell to produce ATP, replacing glucose. They can cross the BBB thanks to the monocarboxylate transporters (MCT1-2); they can then be converted to acetyl-CoA and used for energy production through the TCA cycle

and the oxidative phosphorylation. Moreover, the use of ketone bodies as energy source is not coupled with side effects, as for fatty acids, and with ROS production (review Schonfeld P and Reiser G, *J Cereb Blood Flow Metab* 2013).

Considering the neuronal metabolic system just described, in the following paragraph the main bioenergetics processes that can occur in this cell type will be described: glucose metabolism (glycolysis and pentose phosphate pathway) and mitochondrial metabolism (TCA cycle, oxidative phosphorylation, glutamine pathway).

3.2 Glucose metabolism

Neurons take up glucose through the glucose transporter GLUT3 ($K_d = 2-5$ mM); beyond glucose, it can transport also 2-deoxyglucose and galactose (JI Bell *et al.*, *J Biol Chem* 1993). The first step of glucose metabolism is the irreversible conversion of glucose in glucose 6-phosphate (G6P) through its phosphorylation in carbon 6 by hexokinase 1 (HK1), the brain hexokinase isoform (Cardenas ML *et al.*, *Biochim Biophys Acta* 1998). Thus, HK is a cytosolic enzyme that becomes firmly associated with mitochondria when it catalyses the first step of the glucose metabolism ($G \rightarrow G6P$). In physiological conditions, an equilibrium exists between the soluble and the bound protein; indeed, its activity is regulated by both energy demand and the amount of G6P produced. An increase in G6P amount inhibits, by a feedback mechanism, HK1 activity, inducing the detachment of the enzyme from mitochondria, while an increase in energy demand stimulates its bound state. Hence, G6P is an important element in neuronal glucose metabolism since it represents a common substrate for glycolysis, pentose phosphate pathway and glycogenolysis (mainly by astrocytes) (Figure 15).

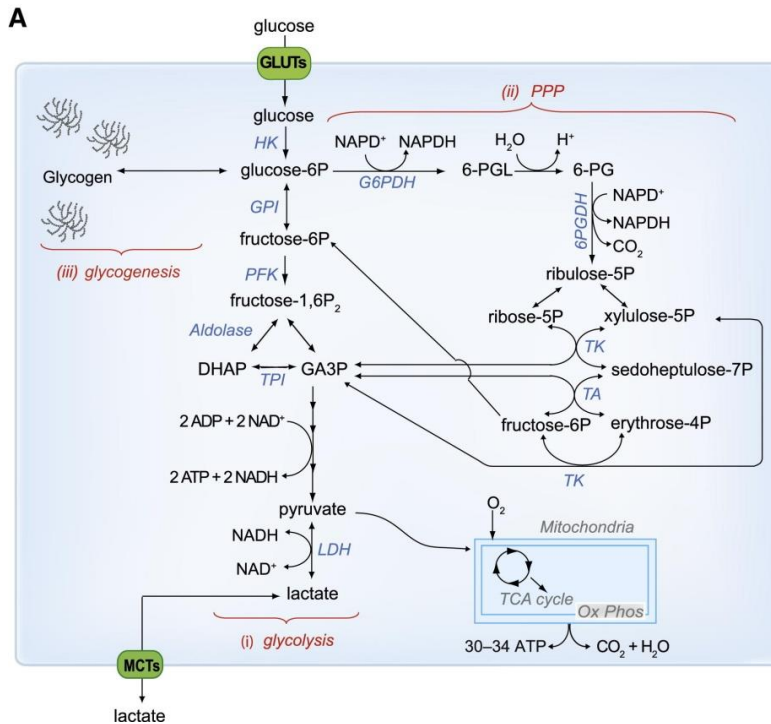


Figure 15 Schematic representation of glucose metabolism in neurons
Belanger M *et al.*, Cell Met 2011

3.2.1 Glycolysis

Glucose 6-phosphate can undergo glycolysis to produce two molecules of pyruvate through an 8 steps catabolic process that involves 9 different enzymes, with a net production of 2 molecules of ATP and 2 reduced nicotinamide adenine dinucleotide (NADH) cofactors.

Among the 9 enzymes that catalyse the whole process, phosphofruktokinase (PFK) is the most important in the regulation of the pathway; it is the enzyme that irreversibly converts fructose 6-phosphate into fructose-1,6-biphosphate (F1,6BP) and it is highly regulated by the concentration of different substrates and molecules. ATP, Mg²⁺ and citrate are the molecules that inhibit its activity, while AMP is the molecule that activates the enzyme that thus senses the ATP/AMP ratio.

Another essential enzyme in the regulation of glycolysis is Pyruvate Kinase (PK) that catalyses the second irreversible reaction of glycolysis. It converts phosphoenolpyruvate into pyruvate, producing ATP. PK is inhibited by the allosteric binding of ATP, reducing glycolysis rate when energy charge is high (Berg JM, Tymoczko JL, Stryer L, Biochemistry 5th edition 2002).

At this point, pyruvate, produced through glycolysis can follow two different pathways: (1) it can be converted in lactate by lactate dehydrogenase (LDH); (2) it can cross the OMM and be

transported by the mitochondrial pyruvate carrier in the mitochondrial matrix. Here, it is converted in acetyl-CoA, thus sustaining the TCA cycle and mitochondrial metabolism.

3.2.2 Pentose Phosphate Pathway

Alternatively to glycolysis, G6P can be metabolized by the pentose phosphate pathway (PPP), known also as hexose monophosphate shunt, highly active during brain development, reaching a peak during myelination. It can be divided in two parts: (1) the oxidative phase, in which G6P is oxidized into ribose-5-phosphate (R5P), producing two molecules of NADPH essential for many reductive reactions (needed for example for cholesterol, lipid and nucleotide synthesis). R5P is incorporated in DNA, ATP, RNA, NAD and Coenzyme A. (2) The non-oxidative phase, in which the excess of R5P is used to produce F6P and glyceraldehyde-3-phosphate, two intermediates of the glycolysis pathway (Berg JM, Tymoczko JL, Stryer L, Biochemistry 5th edition 2002). The rate limiting step of PPP is the glucose-6-phosphate dehydrogenase (G6PDH) enzyme that, in the oxidative phase of the pathway, converts G6P into 6-phosphogluconolactone. G6PDH activity is inversely proportional to the NADPH/NADP ratio.

3.3 Mitochondrial metabolism

In eukaryotic cell, mitochondria are responsible for the production of the major amount of energy. From one molecule of glucose, mitochondria are able to produce 34 molecules of ATP. The main neuronal pathways that contribute to energy production in mitochondria are: TCA cycle, oxidative phosphorylation and glutamine pathway (Berg JM, Tymoczko JL, Stryer L, Biochemistry 5th edition 2002).

3.3.1 TCA cycle and oxidative phosphorylation

By glycolysis, glucose is converted into pyruvate, the essential substrates for mitochondrial bioenergetics. Indeed, pyruvate, once produced in the cytosol, can firstly cross the OMM (through VDAC) and then the IMM thanks to the presence, on this membrane, of the specialized mitochondrial pyruvate carrier (MPC, described below). Once entered in the mitochondrial matrix, pyruvate is converted to Acetyl-CoA, producing a molecule of NADH, by pyruvate dehydrogenase (PDH), to finally enter in the TCA cycle (Figure 16; Cooper GM *et al.*, The cell: a molecular approach 2nd edition 2000).

The PDH complex plays a crucial role in the regulation of the energy production by mitochondria, since its activity is highly regulated by specific pyruvate dehydrogenase kinases

(PDK) and phosphatase (PDP), that can phosphorylate or dephosphorylate the E1 subunit of the complex, respectively. In particular, when PDH is phosphorylated, by PDK, is inactive, while when it is dephosphorylated, by PDP, it becomes active. Again, the activity of PDK and PDP is allosterically regulated by the concentration of different molecules and metabolites. In details, NADH and Acetyl-CoA, the products of the reaction catalysed by PDH, induce the activity of PDK, while this latter is inhibited by pyruvate and ADP; on the other hand, PDP is stimulated by Mg^{2+} and Ca^{2+} , while it is inhibited by NADH (Roche TE and Hiromasa Y Cell Mol Life Sci 2007).

Once produced, acetyl-CoA reacts with oxaloacetate, to produce citrate, and then undergoes 8 enzymatic reactions forming again an oxaloacetate molecule, producing three NADH and one reduced flavin adenine dinucleotide coenzyme (FADH). Beyond PDH complex, other two enzymes of the TCA cycle, α -ketoglutarate dehydrogenase and isocitrate dehydrogenase, are regulated by mitochondrial matrix Ca^{2+} concentration (see below). Due to the fact that one molecule of glucose forms two molecules of pyruvate that can enter in TCA cycle, the final products from one molecule of glucose are 10 molecules of NADH, 2 FADH, 2 ATP and 2 guanosine triphosphate (GTP) (Cooper GM *et al.*, The cell: a molecular approach 2nd edition 2000).

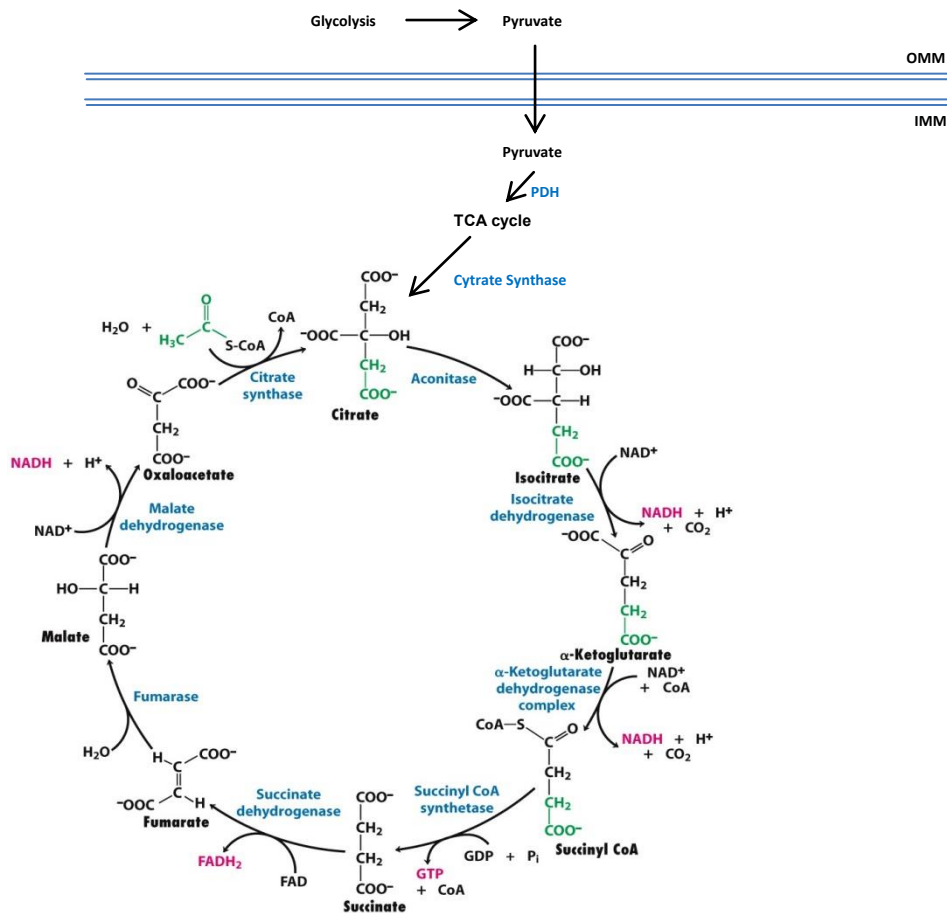


Figure 16: Tricarboxylic Acid Cycle scheme.
 Modified from Freeman WH, Biochemistry, Seventh Edition 2012

Reduced coenzymes (NADH and FADH₂), produced during the TCA cycle, together with oxygen, are now used by the respiratory chain. The respiratory chain (known also as electron transport chain, ETC) is composed by a set of four protein complexes; all these protein complexes are located in the cristae of the IMM. Indeed, electrons, donated by NADH and FADH₂, flow through the four carriers of the respiratory chain. In details, electrons, entered in the respiratory chain through the complex I, are transferred to flavin mononucleotide and then, through an iron-sulfur carrier, to coenzyme Q (also known as ubiquinone), that transfers them from complex I to complex III; here electrons are carried, by cytochrome C, to complex IV, where they are finally transferred to O₂ reduced to H₂O. Among the four electron transport chain complexes, there is also the complex II whose substrate is succinate; FADH₂ donates electrons to complex II and then transferred to complex III through coenzyme Q, located in the IMM. The electrons transport is coupled with the passage of protons from the matrix to the

mitochondrial intermembrane space, thus creating an electrochemical gradient (negative in the matrix) that constitutes the driving force for protons movement back to the matrix across the IMM. The passage of protons from the intermembrane space to the matrix is coupled to the synthesis of ATP from ADP and P_i by the F_0F_1 complex of the ATP synthase.

Thus, the final outcome of the total glycolytic aerobic processing of one molecule of glucose is 36 molecules of ATP (Figure 17; Lodish H *et al.*, Molecular Cell Biology 4th edition 2000).

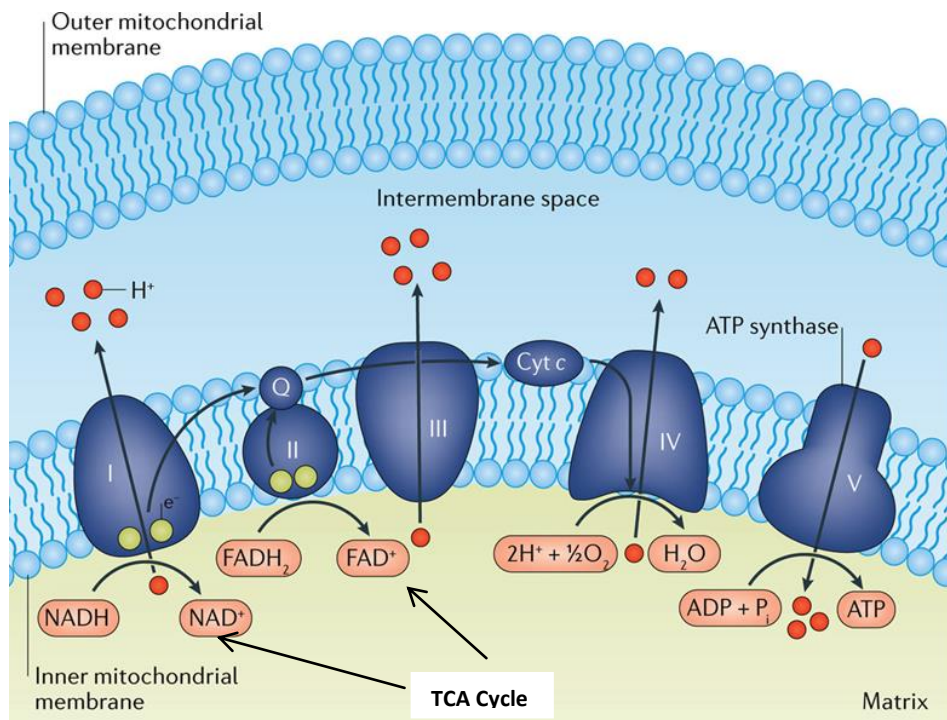


Figure 17 Mitochondrial energy metabolism and oxidative phosphorylation. Modified from Chow J *et al.*, Nat. Rev. Endocrinol 2016

3.3.2 Glutamine pathway

Glutamine is an aminoacid that plays important roles in many metabolic and signalling pathways. Glutamine can enter in the cells through a specific transporter; once inside, it can contribute to several processes, such as nucleotide biosynthesis (to support protein folding and trafficking) or be converted into glutamate, by glutaminase (GLS), contributing to glutathione synthesis, or sustain mitochondrial metabolism. In details, glutamine enters in mitochondria by a transporter that, despite its importance, has not been identified yet. Once in the matrix, a glutaminase can covert it into an ammonium ion and glutamate, converted by glutamate dehydrogenases into α -ketoglutarate that, in turn, enters in the TCA cycle, to generate ATP through production of NADH and FADH₂.

3.3.3 The role of Ca²⁺ in mitochondria metabolism regulation

Bioenergetics homeostasis and mitochondrial functionality are two essential features aim at providing energy to the cells, in particular to excitable ones such as neurons, mainly relying on mitochondrial metabolism. Ca²⁺, a second messenger responsible for the regulation of many physiological processes in the cell, plays a pivotal role in the regulation of mitochondrial activity, metabolism and energy production. The increase in mitochondrial matrix Ca²⁺ levels stimulates organelle activity and ATP synthesis (Jouaville JS *et al.*, PNAS 1999). On the other hand, it has been demonstrated that buffering cytosolic or mitochondrial matrix Ca²⁺ blocks the increase in metabolism induced by the Ca²⁺ stimulations (Wiederkehr A *et al.*, Cell Metab 2011). Moreover, in the last years, the Foskett's group has demonstrated that a constitutive, serum-induced Ca²⁺ transfer from ER to mitochondria is important for maintaining mitochondrial energy metabolism; the inhibition or the absence of the physiologic Ca²⁺ transfer causes a decrease in the ATP levels, an increase in the AMPK phosphorylation and a strong autophagy activation (Cardenas C *et al.*, Cell 2010). The mechanisms by which Ca²⁺ accumulation in the mitochondrial matrix modulate energy metabolism are multiple (Figure 11). Ca²⁺ acts both at the intermembrane space, regulating the activity of substrates carriers, and in the matrix, stimulating the TCA cycle, NADH formation and thus respiratory chain activity; the result is an increase in ATP production. On the contrary, mitochondrial Ca²⁺ overload can induce apoptosis and cell death signalling, through the opening of the PTP and the release of Cytochrome C.

In 1970, four mitochondrial dehydrogenases have been showed to be regulated by Ca²⁺. One of these, the FAD-glycerol phosphate dehydrogenase (GPDH), is located in the IMM and sense Ca²⁺ in the intermembrane space, while the others are three enzymes that catalyse reactions of the TCA cycle and sense matrix Ca²⁺ concentration: pyruvate dehydrogenase (PDH), isocitrate dehydrogenase (ICDH) and oxoglutarate dehydrogenase (OGDH) (Denton RM, Biochim Biophys Acta 2009).

FAD-glycerol phosphate dehydrogenase (GPDH) transfers reducing equivalents from NADH, produced by glycolysis, to the ETC, as FADH₂; it is activated by Ca²⁺ (K_D = 0,1 μM), presenting a Ca²⁺ binding motif that lies in the intermembrane space; moreover, it has been demonstrated that its activation increases ATP levels (Hansford R.G. *et al.*, Biochem Biophys Res Comm 1967; Garrib A *et al.*, J Biol Chem 1986).

Pyruvate dehydrogenase complex (PDH) converts pyruvate into acetyl-CoA, allowing TCA cycle activation. Its activity is regulated by a kinase and a phosphatase. Ca²⁺ binds (K_D = 1 μM) the

phosphatase, increasing its activity, that leads to the de-phosphorylation of PDH, making it active (Linn TC *et al.*, PNAAS 1969; Teague WM *et al.*, Biochemistry 1982; Turkan A *et al.*, Biochemistry 2004).

Isocitrate dehydrogenase (ICDH) and *oxoglutarate dehydrogenase* (OGDH) catalyse two reactions of the TCA cycle; they are both regulated by Ca^{2+} through the direct binding of the ion; this binding induces an increase in the affinity of the enzymes for their substrates (K_D 20-30 μM ; K_D 1 μM respectively; Denton RM *et al.*, Biochem J 1978).

The Ca^{2+} stimulation of the TCA cycle dehydrogenases leads to an increase in NADH levels that will result in a higher activity of the respiratory chain, rising mitochondrial metabolism and ATP production. It has been well demonstrated that increases in cytosolic Ca^{2+} , followed by rises in mitochondrial Ca^{2+} , cause an increase in cellular NADH auto-fluorescent signal; the stimulation towards higher NADH levels by Ca^{2+} is a consequence of an increased mitochondrial metabolism (Jouaville JS *et al.*, PNAS 1999; Pitter JG *et al.*, Cell Calcium 2002).

If the role of Ca^{2+} in stimulating the TCA cycle enzymes is known since many years, only recently it has been reported that Ca^{2+} can act regulating directly the ETC and the F_1F_0 ATP synthase. In 2000, Balaban and co-workers, using heart isolated mitochondria, suggested that Ca^{2+} can directly regulate F_1F_0 ATP synthase (Territo PR *et al.*, Am J Cell Physiol 2000). Moreover, later in 2013, the same group suggests that an increase in mitochondrial Ca^{2+} concentration stimulates the activity of the respiratory chain: using isolated skeletal muscle mitochondria, they measured the effect of Ca^{2+} on ETC activity, founding that $\sim 1 \mu\text{M}$ Ca^{2+} causes a two-fold increase in the velocity of the complexes activity, in particular of complex I, II and III (Glancy B *et al.*, Biochemistry 2013).

Beyond modulating mitochondrial metabolism inside the matrix, Ca^{2+} can also regulate the shuttle of nucleotides, metabolites and cofactors. Indeed, there are specific mitochondrial carriers (MC), localized in the IMM, that exchange nucleotides, substrates and metabolites between cytosol and mitochondria. Among them, there are the Calcium-binding Mitochondrial Carriers (CaMCs): L-CaMCs (Long Calcium-dependent mitochondrial carriers) and S-CaMCs (Short Calcium-dependent mitochondrial carriers). Both carriers sense the Ca^{2+} concentration in the intermembrane space, by the presence of EF-hand Ca^{2+} binding domains, localized in their N-terminal fragments that face the intermembrane space (Del Arco A *et al.*, J Biol Chem 2004 ; Satrustegui J *et al.*, Physiol Rev 2007).

L-CaMCs are aspartate/glutamate transporters (AGC), belonging to the Malate-Aspartate Shuttle (MAS). They catalyse the exchange of a glutamate (from the cytosol) for an aspartate plus a proton (from mitochondria) and, being part of MAS, they allow the entry into

mitochondria of a molecule of NADH that can contribute to metabolism (Palmieri L *et al.*, EMBO J 2001). The role of AGC in the substrates transport was known since several years but only recently, thank to structural studies, it has been shown that even if AGC presents several EF-hand domains, the only one that is important for the Ca^{2+} regulation is the EF-domain located in the N-terminal fragment, faced to the intermembrane space. It has been also demonstrated that AGC is activated by low Ca^{2+} concentration, since its K_D is around 300 nM. Since the affinity of AGC for Ca^{2+} is higher than the affinity of MCU (see above), even tiny Ca^{2+} signals can induce the entering of NADH and metabolites into mitochondria. This event can stimulate ETC and ATP production independently of considerable Ca^{2+} rises within the matrix (C. Thangaratnarajah *et al.*, Nat Commun 2014; Pardo B *et al.*, J Biol Chem 2006).

S-CAMCs are ATP-Mg/ P_i carriers that catalyse the exchange of ATP and ADP for one phosphate across the IMM, thus modulating the levels of adenine nucleotides (AdN, AMP+ADP+ATP) inside mitochondria. Due to their function, these carriers can modulate several cell functionalities, such as mitochondrial metabolism and oxidative phosphorylation. It has been shown that a defect or the absence of these carriers in different tissues can induce an impairment in energy production (Amigo I *et al.*, J Biol Chem 2013; RP Anunciado – Koza J *et al.*, J Biol Chem 2011). The activity of the ATP-Mg/ P_i carrier is regulated by Ca^{2+} since it presents EF-hand calcium binding domains, homologous to those of calmodulin, in its N-terminal part, facing the intermembrane space and sensing the cytosolic Ca^{2+} concentration; its K_D is between 1.5-3 μM , much higher than the one of AGC. For this reason, these carriers are considerably activated only upon strong increases in cytosolic Ca^{2+} , resulting in the regulation of AdN levels in mitochondria (Haynes R, J Biol Chem 1986; Nosek MT, J Biol Chem 1990).

Overall, Ca^{2+} plays a crucial role in the stimulation of mitochondrial metabolism and ATP production. Energy produced by mitochondria is essential for the cell functionality, particularly for that cells that need a high amount of energy to work properly, such as neurons. Indeed, defects in the mitochondria Ca^{2+} uptake, due to an impairment in the MCU complex, a decrease in the ER Ca^{2+} levels or a disruption of ER-mitochondria tethering (causing lower ER-mitochondria Ca^{2+} transfer) could lead to detrimental effects on mitochondrial metabolism, that are not able to support the energy demand of the cell; these impairments are often features of many pathologies (Figure 11).

3.4 Substrates and mitochondria

Mitochondrial substrates (pyruvate, glutamate, succinate, citrate ect.) availability plays also a pivotal role in regulating mitochondrial activity since they sustain most of the pathways involved in ATP production. Indeed, metabolites and substrates can easily cross the permeable OMM thanks to the presence, on its surface, of VDAC (Colombini M, Nature 1979). On the contrary, the transport of metabolites and substrates, from the intermembrane space to the mitochondrial matrix, is mediated by specific carrier located in the IMM. Therefore, a cross-talk between mitochondria and the whole cell is essential to sustain the health of the cell.

3.4.1 Voltage Dependent Anion Channel (VDAC)

In mammals, three homologous genes have been found to encode three different isoforms of VDAC, VDAC1, VDAC2 and VDAC3, sharing 70% of identity. They are expressed in most tissues but the specific role of each isoform is not clear yet; however, some studies suggest that the three different isoforms have distinct physiological roles. For example, the KO of VDAC1 causes defects in skeletal and cardiac muscle, while the absence of VDAC3 impairs heart activity (Anflous-pharayra K *et al.*, Biochim Biophys Acta 2010). Moreover, the silencing of both VDAC1 and 2 causes reduce respiratory capacity, while the VDAC1 and 3 absence inhibits growth and VDAC2-KO causes male sterility (Wu S *et al.*, Biochim Biophys Acta 1999; Sampson MJ *et al.*, J Biol Chem 2001).

VDAC, also known as mitochondrial porin, is a mitochondrial gatekeeper channel of 30-35 kDa, located in the OMM; it controls the enter and the exit in and outside mitochondria of molecules (metabolites, substrates and ions), up to 5 kDa; in this way, it allows the coupling between mitochondria and cytosol. Due to its exchange role, VDAC mediates the enter into mitochondria of substrates such as pyruvate, citrate, malate and NADH, essential to sustain mitochondrial metabolism, and the exit of new formed molecules, such as ATP. In fact, it has been reported that VDAC downregulation reduces metabolites exchange between mitochondria and cytosol, altering energy metabolism, thus making VDAC essential for ATP production (Abu-Hamad S *et al.*, PNAS 2006). Similar results have been obtained inducing the closure of the channel (Holmuhamedov E and Lemasters JJ, Arch Biochem Biophys 2009).

Beyond being important for metabolites exchange, VDAC has other several functions; among them, it is involved in the apoptosis pathway, regulating cell fate through its interaction with apoptotic proteins; it regulates the transport of lipids and cholesterol inside mitochondria; it mediates the release of ROS from mitochondria and it has a role in ER-mitochondria Ca^{2+}

transfer, being part of the functional IP3R-GRP75-VDAC complex located in MAM (Shoshan-Barmatz V and Mizrachi D, Front Oncol 2012; Figure 18).

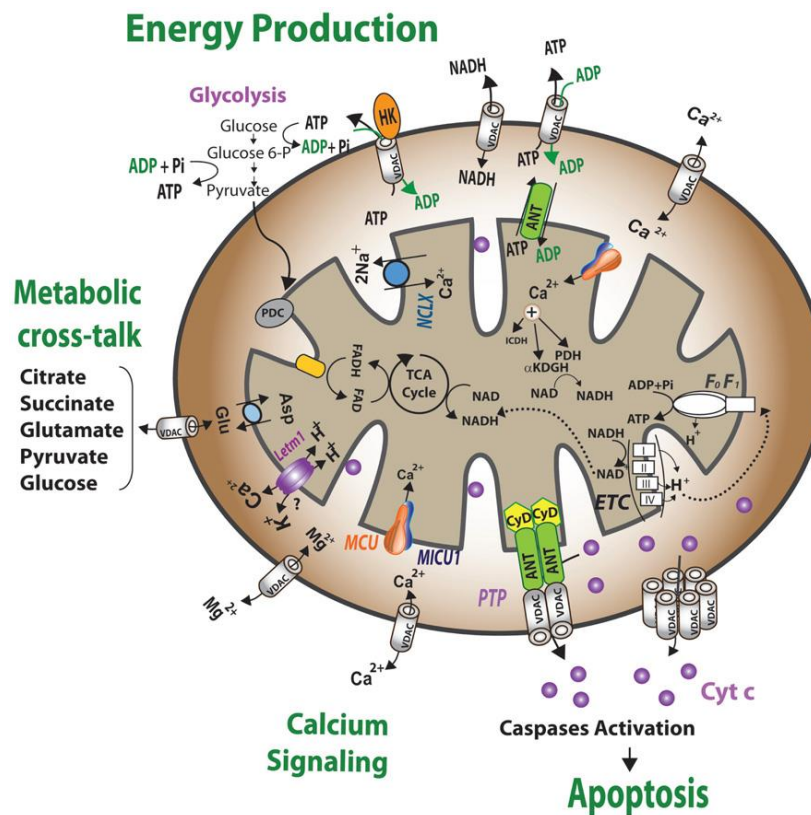


Figure 18 Schematic representation of VDAC1 as a multi-functional channel and convergence point for a variety of cell survival and cell death signals. Shoshan-Barmatz V and Mizrachi D, Front Oncol 2012

The 3D structure of VDAC has been obtained using X-ray crystallography and NMR techniques; it is a 283 aa polypeptide with a transmembrane organization. It is formed by 19 β -strands that are organized in a barrel; the N-terminal region, made of 25 aa, is highly dynamic and located in the channel pore; moreover, this part has been suggested to be essential for the VDAC interaction with several proteins important for channel activity regulation. The pore diameter of the channel has been proposed to be about 3-3.8 nm (Shoshan-Barmatz V and Mizrachi D, Front Oncol 2012; V Shoshan-Barmatz *et al.*, Cell Calcium 2017).

VDAC can interact with many proteins involved in several processes; among them, it can interact with Hexokinase and Adenine Nucleotide Translocase (ANT), both important for allowing the correct communication between cytosol and mitochondria.

3.4.2 Hexokinase

In mammals, four hexokinase (HK) isoforms have been identified; they are highly homologous but differently expressed in different tissues, with HK1 being the one expressed in the brain. It is a 100 kDa protein, essential for glucose metabolism and for regulating cytosolic and mitochondrial metabolism. In details, HK is the enzyme that catalyses the first step of glycolysis converting glucose into glucose 6-phosphate, consuming one molecule of ATP. It is a cytosolic protein that can dynamically associate with mitochondria during the reaction that converts glucose in glucose 6-phosphate. Its binding to mitochondria is mainly regulated by a feedback mechanism, mediated by the amount of glucose 6-phosphate produced; other processes and pathological conditions can also modulate its binding to the organelle (Pastorino JG and Hoek JB, *J Bioenerg Biomembr* 2008).

It is well established that HK interacts with the OMM; furthermore, several studies suggest that its binding happen through a specific interaction with VDAC (Abu-Hamad S *et al.*, *J Biol Chem* 2008; Arzoine L *et al.*, *J Biol Chem* 2009; Pastorino JG and Hoek JB, *J Bioenerg Biomembr* 2008; Shoshan-Barmatz V and Mizrachi D, *Front Oncol* 2012; Neumann D *et al.*, *PMC Biophys* 2010). Moreover, it has been suggested that HK association/dissociation to/from VDAC modulates the open or closed state of the VDAC channel; in this way, HK binding to mitochondria regulates metabolites, substrates, ATP and ADP exchange between cytosol and mitochondria and their metabolism. However, the precise mechanism through which HK regulates the mitochondrial (VDAC) permeability is still unclear (Figure 19; Robey RB and Hay N, *Oncogene* 2006; Shoshan-Barmatz V and Mizrachi D, *Front Oncol* 2012).

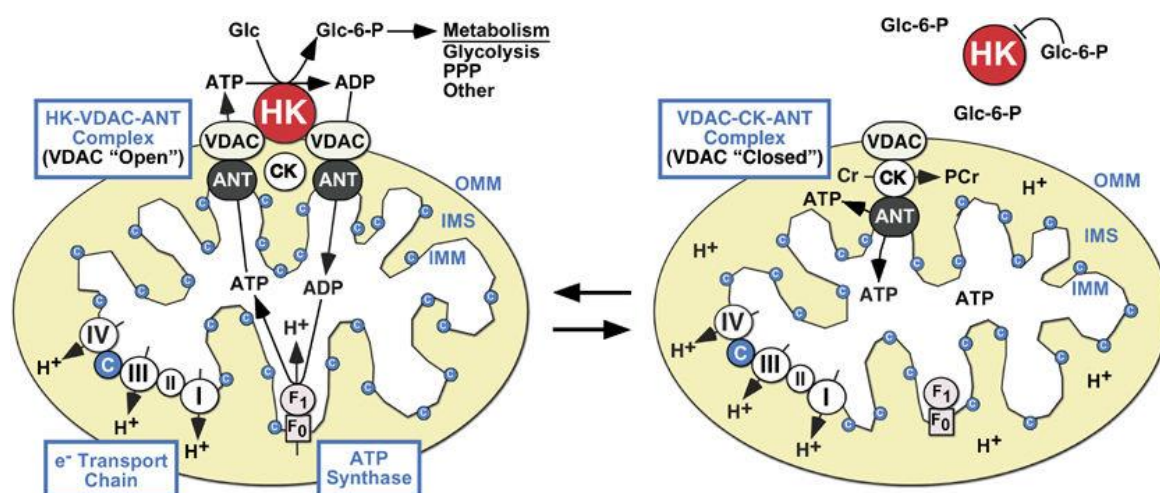


Figure 19 Scheme of Hexokinase-mitochondria interaction. Robey RB and Hay N, *Oncogene* 2006

The C- and the N- terminal domains of HK are both important for protein functionality since the C-terminus represents the catalytic part of the enzyme and the N-terminal domain has been described to be essential for its OMM binding. In particular, this latter domain possesses 15 aa that mediate the HK-mitochondria interaction; indeed, it has been showed that a peptide, that correspond to the N-terminal part of the protein, can displaced HK from mitochondria (Pastorino *et al.*, J Biol Chem 2002) and that a HK form, lacking the N-terminal domain, cannot associate with mitochondria, remaining diffused in the cytosol (Sun L *et al.*, Mol Cell Biol 2007). However, it is not well established how the N-terminal domain of HK can interact with VDAC; it has been proposed that it inserts in the membrane bilayer interacting with one or more of the TM domains of VDAC (Xie GC and Wilson JE, Arch Biochem Biophys 1988). Indeed, mutations on glutamate 72 of VDAC reduce the HK binding to mitochondria (Zaid H *et al.*, Cell Death Diff 2005). In addition, HK binds to OMM, particularly to the OMM-IMM contact sites; here, VDAC forms a complex with both HK, facing the cytosol, and the adenine nucleotide translocate (ANT) located in the IMM. The HK-VDAC-ANT complex is essential for the ATP/ADP exchange between mitochondrial matrix and cytosol; indeed, ATP produced by mitochondria through the respiratory chain exits in the cytosol to be used by HK, to convert glucose in glucose 6-phosphate. The reaction catalysed by HK produces one molecule of ADP that has to enter back in mitochondria and be converted, by the ATP synthase, in ATP. Thus, the ATP/ADP cycle is guarantee by the HK-VDAC-ANT complex (Brdiczka DG *et al.*, Biochim Biophys Acta 2005).

In pathologic conditions, alterations in the activity of some proteins, such as Akt, Gsk3 and PKA, can modulate the VDAC-HK interaction, inducing the HK detachment and promoting apoptotic pathway (Pastorino JG and Hoek JB, J Bioenerg Biomembr 2008). The detachment of HK from mitochondria can be induced also by several chemical compounds such as clotrimazole (Chiara F *et al.*, Plos One 2008), methyl-jasmonate and STS (Shoshan-Barmatz V and Mizrachi D, Front Oncol 2012).

3.4.3 The Mitochondrial Carrier System

A specific transport system, called Mitochondrial Carrier System (MCS), localized in the IMM is essential for substrate/metabolites entry in the mitochondrial matrix. The MCS transports small molecules, such as intermediates of the TCA cycle, amino acids, vitamins, metals and nucleotides, from the intermembrane space to the mitochondrial matrix and *viceversa*, thus playing an important role in the regulation of cytosolic and mitochondrial functions. Due to the large number of substrates and metabolites that are carried by this system, several

transporters have not been identified yet or the transport mechanism used has not been well characterized. However, some of them have been discovered and studied in details, and mutations or alterations in the expression levels of 14 carriers (such as ANT, phosphate carrier and citrate carrier) are responsible for many diseases (Eric B Taylor, Trends cell Biol 2017).

In the following paragraphs, some of the well described mitochondrial carriers will be presented, particularly the recently described Mitochondrial Pyruvate Carrier.

Mitochondrial Pyruvate Carrier

Since 1970, it has been revealed the existence of a specific pyruvate transporter located in the IMM; however, the molecular and genetic identity of the mitochondrial pyruvate carrier (MPC) have been described only recently when, in 2012, two different groups identified the two genes coding for the two obligatory, interdependent subunits, MPC1 and MPC2 (15kDa each), which form a multimeric complex that constitutes the functional MPC (Bricker DK *et al.*, Science 2012; Herzig S *et al.*, Science 2012).

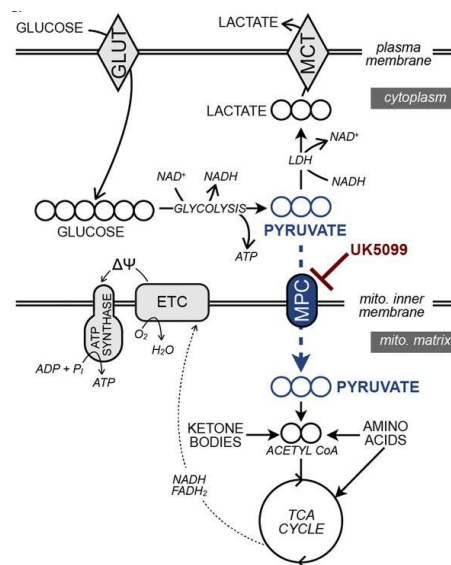


Figure 20 The Mitochondrial Pyruvate Carrier (MPC, blue) sits at the central hub of cellular energetics, facilitating the transport of cytosolic pyruvate into mitochondria. Divakaruni AS *et al.*, J Cell Biol 2017

Recent studies showed that the whole body MPC1 or MPC2 KO mice results in embryonic lethality (Vanderperre B *et al.*, Plos Genet 2016; Vigueira PA *et al.*, Cell Rep 2014). Mouse embryonic fibroblasts (MEFs), from MPC1-KO embryos, showed a reduced mitochondrial activity. In particular, no differences have been observed in basal oxygen consumption rate between WT and MPC-KO MEFs, while a strong reduction in this parameter has been

measured upon FCCP addition, measuring the maximal OCR, meaning that pyruvate is essential to sustain the respiratory chain correct activity and, thus, mitochondrial functionality. The defect was completely rescued by the addition of methyl-pyruvate, able to freely diffuse in mitochondrial matrix. The same authors demonstrated also that both lethality and metabolism defects, observed in MPC-KO MEFs, were prevented when the pregnant dam was maintained on a ketogenic diet (Vanderperre B *et al.*, Plos Genet 2016). Similar results have been obtained when the mitochondrial pyruvate carrier was pharmacologically blocked by UK5099 (Vanderperre B *et al.*, Plos Genet 2016; Divakaruni AS *et al.*, J Cell Biol 2017). Due to reduced mitochondrial activity (caused by reduced levels of MPC, or its blockage), both groups showed that cells undergo metabolism plasticity, in order to provide alternative substrates to mitochondria and sustain the TCA cycle. Indeed, the TCA cycle flux can be maintained through an increase in glutamine-glutamate pathway and fatty acid oxidation. In addition, to compensate for the reduced pyruvate import, some pyruvate is synthesized in the mitochondrial matrix, starting from alanine (Vanderperre B *et al.*, Plos Genet 2016; Divakaruni AS *et al.*, J Cell Biol 2017; Taylor E, Trends cell biol 2017).

Other transporters of the Mitochondrial Carrier System

A high number of transporters, localized in the IMM, have been studied and well characterized; they mainly transport substrates between cytosol and mitochondria in order to maintain the metabolism of both compartments. Between them, four glutamate transporters have been identified (Figure 21): aspartate-glutamate carrier 1 and 2 (AGC1 and AGC2) are two proteins that import glutamate in the mitochondrial matrix while exporting an aspartate in the cytosol (Amoedo ND *et al.*, Biochim Biophys Acta 2016). AGC1 and AGC2 are Ca^{2+} -binding Mitochondrial Carriers (CAMCs), regulated by Ca^{2+} concentration in the mitochondrial intermembrane space (Del Arco A *et al.*, J Biol Chem 2004; as described above); they are also part of the Malate-Aspartate shuttle system (see below). Glutamate carrier 1 and 2 (GC1 and GC2) regulate a glutamate/ H^+ symport inside the matrix. They are differently distributed in different tissues and cell types; AGC1 and GC1 are the isoforms mainly present in the brain: deficiency in one of the two proteins causes hypomyelination and infantile epilepsy (Wilbom R *et al.*, N Engl J Med 2009).

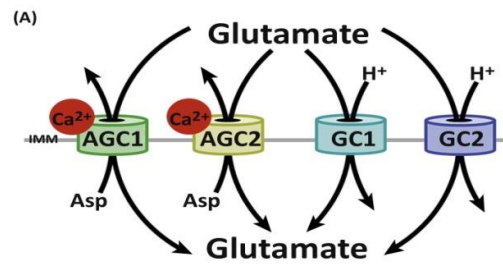


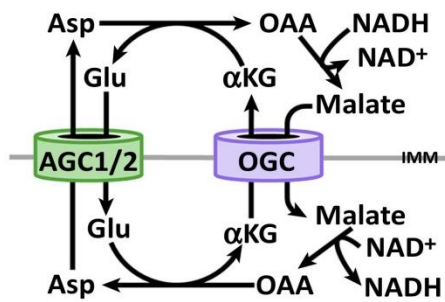
Figure 21: Aspartate-glutamate carrier 1-2 (AGC1 and AGC2) and glutamate carrier 1-2 (GC1 and GC2).
Taylor E, Trends Cell Biol 2017

Other transporters of the MCS are the oxoglutarate carrier (OGC) that exchanges α -ketoglutarate between cytosol and mitochondria; the dycarboxylate (DIC), citrate (CIC) and alanine carriers that transport malate, citrate and alanine, respectively.

Interestingly, each of the carriers just mentioned does not work alone but they almost always function together to maintain the correct equilibrium in the amount of substrates and in the redox state of both cytosol and mitochondrial matrix. Hence, in the IMM we can find different groups of transporters (the most important are here described):

- Malate-Aspartate shuttle: it exchanges malate, glutamate, aspartate and α -ketoglutarate between cytosol and mitochondria, allowing the transfer in the mitochondrial matrix of NADH equivalents. OGC works exporting in the cytosol α -ketoglutarate and importing malate in mitochondria; this exchange is coupled with the entrance in mitochondria of glutamate and the exit of aspartate, mediated by AGC (Figure 22A). The final outcome of this transport system is the entrance in mitochondria of one molecule of NADH used by the TCA cycle.
- MPC and mitochondrial alanine carrier coupling. When the mitochondrial transport of pyruvate by MPC is impaired, pyruvate can be converted into alanine by an alanine transaminase (Atl1) in the cytosol; alanine can then be imported in the mitochondrial matrix through its specific carrier. Here, it is re-converted into pyruvate by Atl2, thus contributing to pyruvate production in mitochondria when its transport is impaired (Figure 22B; McCommis KS *et al.*, Cell Met 2015).

A



B

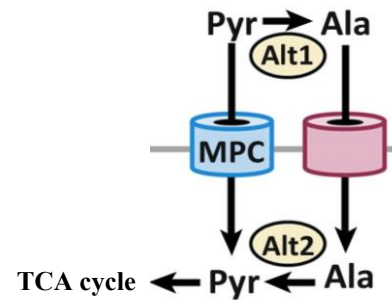


Figure 22: Transporters of the MCS. (A) Malate-Aspartate shuttle; (B) Pyruvate-Alanine exchanger. Taylor E. Trends Cell Biol 2017

- Pyruvate cycling. It is regulated by the activity of three different transporters: DIC, CIC and MPC. MPC mediates the entry in the mitochondrial matrix of pyruvate that can be converted into malate, oxoacetate and citrate. This latter can enter the TCA cycle sustaining mitochondria energetics; however, malate and citrate can also return in the cytosol through CIC and DIC. Citrate can be converted into malate that, in turn, can be transformed again into pyruvate, by malic enzyme1, producing a molecule of NADPH equivalent (figure 23 A; Taylor E, Trend Cell Biol 2017).
- Citrate cycling. It is regulated by the activity of two different transporters: CIC and OGC. α -ketoglutarate, produced in the mitochondria matrix by the TCA cycle or from glutamine, is transported in the cytosol by OGC. Here, it is converted in citrate and isocitrate that can be again transferred by CIC in the mitochondrial matrix, thus contributing to the TCA cycle. Moreover, their re-conversion in α -ketoglutarate allows the production of reducing equivalents (NADPH) in the mitochondrial matrix, used to augment the mitochondrial ROS defence (Figure 23B; Taylor E, Trend Cell Biol 2017).

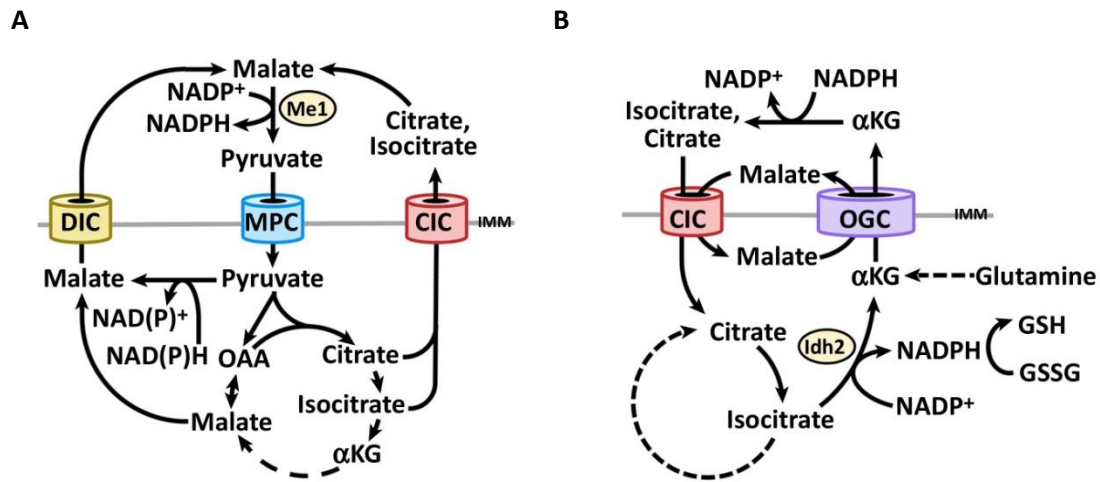


Figure 23: (A) Pyruvate Cycling scheme; (B) Citrate Cycling scheme.
Taylor E, Trends Cell Biol 2017

3.5 AMPK

All the pathways and the mechanisms described in this chapter are involved in the maintenance and in the production of the right amount of energy that cells need to function properly. Alterations, mutations or defects on these systems can cause a reduction in the amount of ATP, thus providing insufficient energy to the whole cell. The most important protein that senses low ATP levels and is responsible for restoring of energy homeostasis is the AMP-activated protein kinase (AMPK). AMPK, the energy sensor of the cell, is activated in response to energy stress; in particular, it senses the increase in AMP:ATP or ADP:ATP ratios; when activated, in order to restore the energy homeostasis, it inhibits anabolic processes, that consume ATP, and stimulates catabolic processes that, on the contrary, generate ATP (Hardie DG *et al.*, Nat Rev Mol Cell Biol 2012). Interestingly, AMPK, being involved in metabolic pathways and regulating the amount of energy in the cell, becomes essential for many processes that occur in the cell; indeed, it can stimulate or inhibit the activity of proteins involved in key processes, such as autophagy, mitophagy, mitochondrial fusion and fission, protein synthesis, glycogen and lipids synthesis and lysis (Garcia D and Reuben JS, Mol Cell Rev 2017). Structurally, it is a trimeric complex composed by a catalytic subunit (α subunit) and two regulatory subunits (β and γ subunits); in mammals, two isoforms of the α and β subunits, while three of the γ subunits, exist; they are differently expressed in different tissues, even if AMPK α 1, AMPK β 1 and AMPK γ 1 are ubiquitously expressed. The N-terminus of the α subunit

contains the kinase domain (KD). AMPK is totally activated when it is phosphorylated on Thr172, residue localized in the activation loop of the KD (Hawley SA *et al.*, J Biol Chem 1996); the C-terminus, instead, binds the β and γ subunits. The β subunit presents a domain that senses glycogen and a C-terminal domain that binds α and γ subunits. γ subunit is the one that makes AMPK the energy sensor of the cell since it presents four sites that can bind competitively AMP, ADP and ATP (Garcia D, Mol Cell Rev 2017).

AMPK can be activated by two distinct mechanisms: (1) AMP or ADP binding to the γ subunit promotes the phosphorylation of Thr172 on the activation loop in the KD of the α subunit; the phosphorylation is mediated by upstream kinases; one of them is the serine/threonine kinase LKB1 (Liver kinase B1), which responds to a decreased energy levels activating AMPK (Woods A *et al.*, Nat Cell Biol 2003); (2) AMP, or ADP, binding to the γ subunit induces a conformational change that prevents the de-phosphorylation of Thr172 by phosphatase (Suter M *et al.*, J Biol Chem 2006). The binding of ATP prevents both mechanisms. Moreover, the AMPK phosphorylation on Thr172 can be promoted also by another upstream kinase, the calcium/calmodulin-dependent kinase kinase 2 (CAMKK2; Hawley SA *et al.*, Cell Met 2005). This latter does not sense changes in the energy levels but it is stimulated by increases in intracellular Ca^{2+} (Garcia D Mol Cell Rev 2017).

AMPK can be inhibited by the phosphorylation in other serine or threonine residues. Indeed, during gluconeogenesis, a process inhibited by activated AMPK, Ser485 in AMPK α 1 or Ser491 in AMPK α 2 can be phosphorylated by PKA, in order to inhibit the activity of AMPK (Hurley RL *et al.*, J Biol Chem 2006). Moreover, a recent study demonstrated that AMPK α can be phosphorylated in Thr479 by phospho-GSK3 (glycogen synthase 3; Suzuki T *et al.*, Mol Cell 2013).

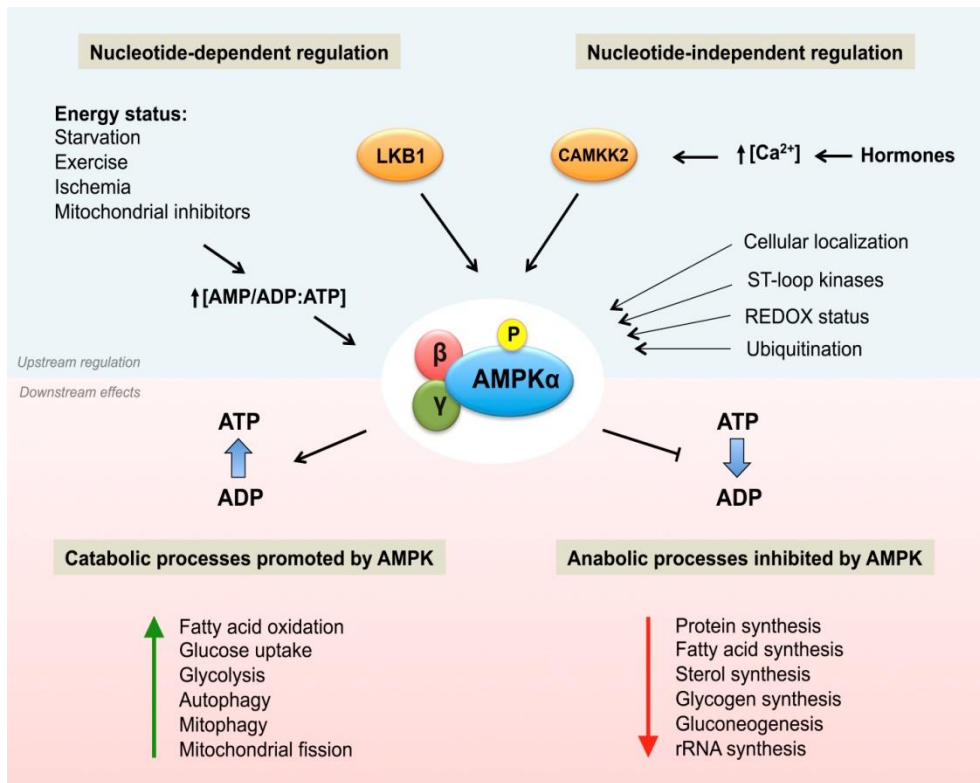


Figure 24: AMPK signalling pathway. Garcia D and Sahw RJ, Mol Cell Rev 2017

3.6 Mitochondrial dysfunctions and Alzheimer's Disease

Mitochondrial dysfunctions have been proposed to be early events in the development of AD (Du H *et al.*, PNAS 2010; Yao J *et al.*, PNAS 2009), due to the pivotal role played by mitochondria in neuronal health.

Mitochondria can be compromised in three main aspects:

- **Mitochondrial Dynamics:** Mitochondria are highly dynamic organelles that continuously undergo fusion and fission processes; two pathways highly connected that control mitochondrial health, morphology and functionality. Drp1 and Fis1 mainly modulate the fission process while Opa1, Mfn1 and 2 control mitochondrial fusion (review Mishra P and Chan DC, J Cell Biol 2016). Altered mitochondrial morphology has been observed in different AD models. In particular, changes in mitochondrial morphology, from elongated and thin to fragmented mitochondria, have been detected both in brain samples from AD patients and in neuroblastoma cells overexpressing mutated APP (Wang X *et al.*,

PNAS 2008; Trimmer PA et al., Antiox Red Signal 2005). Other studies reveal that hippocampal neurons treated with A β (1-42) present shorter mitochondria compared to untreated controls, and that the density of mitochondria in neurites is reduced upon treatment (Heng D *et al.*, PNAS 2010). The precise molecular mechanisms involved in the observed mitochondrial morphology changes is still unknown; however, an alteration in the expression levels and localization of fusion/fission proteins have been found. Different groups reported an increase in the expression levels of fission proteins (Drp1 and Fis1) and in their mitochondrial localization, while they found a decrease in the levels of fusion proteins (Opa1, Mfn1 and 2). They also observed that A β peptides associate with synaptic mitochondria and interact with Drp1 (Wang X *et al.*, J Neurosci 2009; Manczak M *et al.*, Hum Mol Genet 2011).

- Mitochondria Bioenergetics. One of the most important functions of these organelles is ATP production, essential to sustain neuronal activity and prevent cell injury. Over the last years, several studies demonstrated that this essential mitochondrial function is impaired in AD models; indeed, reduced ATP production, respiratory chain activity and TCA cycle functionality coupled with an increase in ROS production have been observed (review Cabezas-Opazo FA *et al.*, Oxid Med Cell Longev 2015). Different groups observed changes in mitochondria morphology, loss of synaptic mitochondria integrity and reduced ATP production in FAD-PS1/APP mouse models; they found also a decrease activity of the respiratory chain and a reduced function and levels of some enzymes of the TCA cycle, such as PDH, thus altering mitochondrial functionality (Yao J *et al.*, PNAS 2009; Trushina E *et al.*, Plos One 2012). It has been also suggested that the observed mitochondrial injury in AD models is due to A β peptides: the treatment of isolated mitochondria with different concentrations of A β , dramatically reduces respiratory chain activity and increases ROS production, contributing to mitochondrial damage (Casley CS *et al.*, J Neurochem 2002).
- Mitochondria transport. Mitochondria can move from the soma to the nerve terminals through an anterograde transport, or from the terminal to the soma by a retrograde transport. These processes are mainly mediated by microtubules that, interacting with several proteins, allow the organelles transport around the cell. The movement of mitochondria to the cell periphery plays a pivotal role in neuronal health: impairment in the anterograde transport of these organelles can

contribute to synaptic dysfunction and memory loss that characterized AD. Reduced mitochondria transport has been observed in AD mouse models by different groups (Iijma-Ando K *et al.*, Plos Genet 2012). Also in this case, A β peptides seem to have a role in determining the defect. Calkins and co-authors showed that the increase in A β oligomers affects mitochondrial morphology and reduces their anterograde transport, thus negatively regulating synaptic activity (Calkins JM *et al.*, Hum Mol Genet 2011).

Aim of the work

Alzheimer's Disease (AD) is the most common form of dementia. It is mainly sporadic, however, autosomal dominant mutations on three different genes, coding for Amyloid Precursor Protein (APP), Presenilin 1 (PS1) and Presenilin 2 (PS2), are responsible for a little percentage of inherited cases (Familial AD, FAD). Presenilins (PS1 and PS2) are mainly localized at Endoplasmic Reticulum (ER) membranes; PSs form, alternately, the catalytic core of the γ -secretase complex, the enzyme that cleaves APP to produce $A\beta$ peptides. Beyond being part of this complex, PSs have also several γ -secretase-independent activities, such as those involved in the modulation of neurites outgrowth, apoptosis, autophagy, synaptic functions and Ca^{2+} homeostasis.

Ca^{2+} , a key intracellular second messenger, is involved in multiple cellular functionalities. Importantly, it has been reported that alterations in Ca^{2+} homeostasis is an early event of AD and FAD-PSs mutants have been shown to be directly involved in these dysregulations. In our lab, it has been previously demonstrated that PS2 expression, both WT and, more efficiently, FAD mutants (such as PS2-T122R), but not PS1, decreases the ER Ca^{2+} content, mainly by inhibiting SERCA pump activity. Moreover, PS2 increases ER-mitochondria physical and functional coupling, favouring the process of ER to mitochondria Ca^{2+} transfer upon similar ER Ca^{2+} release; however, due to its effect on ER $[Ca^{2+}]$, which results in a lower amount, its expression dampens mitochondrial Ca^{2+} rises upon cell stimulation.

Based on the well-established role of Ca^{2+} on mitochondrial metabolism, the aim of this study is to investigate the possible effects on mitochondrial functionalities of the complex balance between alterations in ER Ca^{2+} content and increased ER-mitochondria coupling induced by FAD-PS2 mutants expression. To address this issue, we mainly used a neuroblastoma cell line (SH-SY5Y), grown in a medium containing galactose, as a substitute of glucose, to enhance mitochondrial metabolism and underline possible mitochondrial defects. We also used FAD-PS2-N141I patient-derived fibroblasts and primary cortical neurons from FAD-PS2-N141I transgenic (Tg) mice, to confirm the results obtained in cell lines. On these models, by several techniques, we evaluated mitochondrial functionality, in particular basal ATP levels, mitochondrial ATP production and respiratory chain activity. We then investigated the mechanisms through which FAD-PS2 affects mitochondrial metabolism.

Results

1. FAD-linked PS2 mutants, but not PS1, affect mitochondrial ATP production

In the last years, we have demonstrated that PS2 (and more potently FAD-PS2 mutants), but not PS1, modulates ER Ca^{2+} content, mitochondrial Ca^{2+} uptake and ER-mitochondria contact sites. In details, we have showed that PS2 decreases the ER [Ca^{2+}], thus reducing the amount of Ca^{2+} taken up by mitochondria upon release of the cation from the ER; moreover, we have also showed that PS2 increases ER-mitochondria tethering, a feature that favours mitochondrial Ca^{2+} uptake, upon similar ER Ca^{2+} release (Zampese E. *et al.*, PNAS 2011; Kipanyula *et al.*, Aging Cell 2012). Though, on the one hand, PS2 favors the process of ER to mitochondria Ca^{2+} transfer, due to its capability to increase ER-mitochondria physical and functional coupling, on the other hand, its effects on the amount of available Ca^{2+} within the ER reduce mitochondrial Ca^{2+} rises. Based on the well-established role of Ca^{2+} on mitochondrial metabolism (Jouaville LS *et al.*, PNAS 1999, McCormack *et al.*, Physiol Rev 1990), we decided to critically evaluate the possible effects on mitochondrial functionalities of the complex balance between alterations of ER Ca^{2+} content and increased ER-mitochondria coupling, induced by FAD-PS2 mutants expression.

To address this aim, we firstly used a neuroblastoma cell line (SH-SY5Y) grown in a medium containing galactose instead of glucose; cells grown in galactose are not able to produce enough ATP through glycolysis and thus they mainly rely on mitochondrial oxidative phosphorylation to synthesize ATP. Therefore, to grow cells in galactose medium, enhancing mitochondrial metabolism, is an useful strategy to reveal possible mitochondrial defects (W. Dott *et al.*, Redox Biology 2014).

Total cellular ATP levels were measured in SH-SY5Y cells expressing the FAD-PS2-T122R mutant, compared to controls; this particular PS2 mutant form was chosen because it is one of the most effective in modulating Ca^{2+} homeostasis and ER-mitochondria tethering (Zampese E. *et al.*, PNAS 2011). Lower total ATP levels were measured in PS2-T122R expressing cells, grown either in glucose or galactose medium, with a more evident effect in the latter condition (FIG25A). Hence, these data suggest possible mitochondrial defects induced by PS2 expression. Indeed, cells grown in galactose medium produced ATP mainly through the mitochondrial oxidative phosphorylation, as demonstrated by the oligomycin-induced drop in ATP levels specifically observed in cells fuelled with galactose (FIG 25B).

Figure25

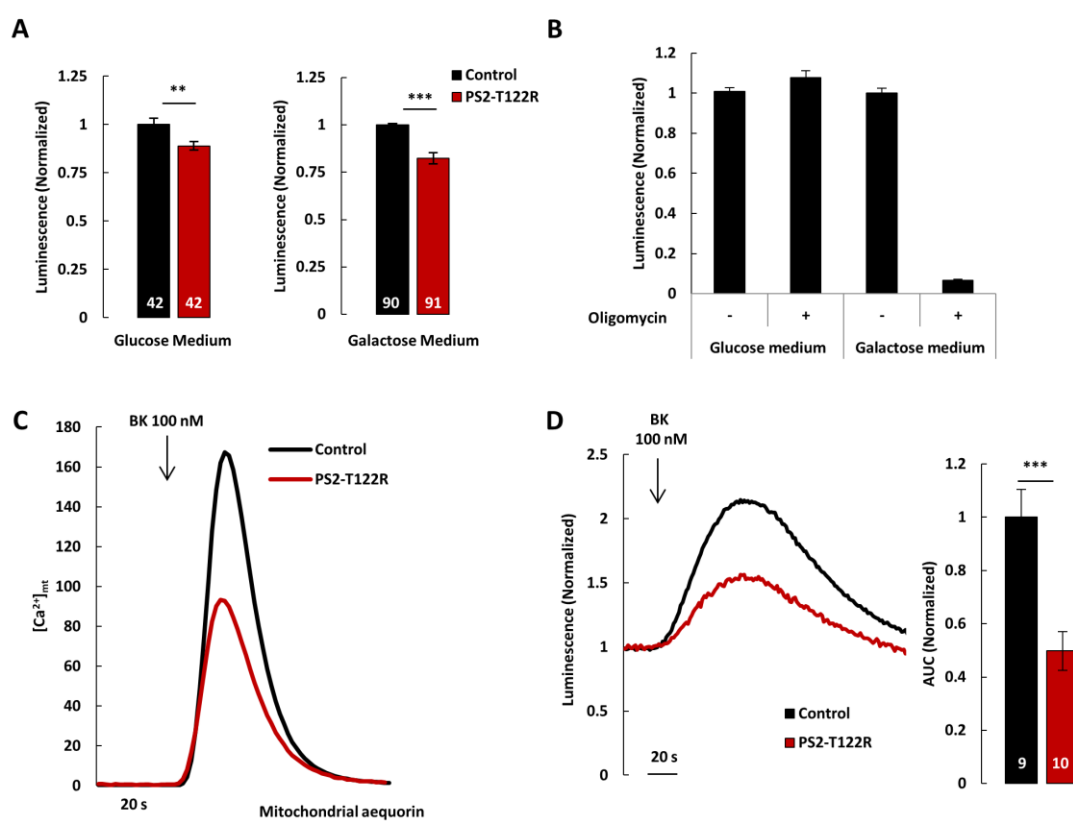


Figure 25. The FAD-PS2-T122R mutant decreases total cellular ATP levels and mitochondrial ATP production upon maximal IP3R stimulation. **(A)** Total cellular ATP levels were measured in SH-SY5Y cells, grown either in galactose- or glucose-containing medium, and transfected either with pcDNA3 (Control, black) or PS2-T122R (red) cDNA; luciferin/luciferase assay ATPlite 1 step (PerkinElmer) was used. **(B)** Total cellular ATP levels measured (as in panel A) in SH-SY5Y cells, grown either in galactose or glucose medium, and treated or not with oligomycin (2 μM) for 10 minutes. N ≥ 5. (A) and (B) Bars show mean luminescence values, normalized to controls. N = number of wells. **(C)** Mitochondrial Ca²⁺ uptake measured in SH-SY5Y cells grown in galactose medium and transfected with a mitochondrial matrix aequorin together with either pcDNA3 (Control, black) or PS2-T122R (red) cDNA; mitochondrial Ca²⁺ uptake was induced by acute exposure to bradykinin (BK, 100 nM). Representative traces of mitochondrial Ca²⁺ uptake induced by BK. **(D)** Mitochondrial ATP production was measured in SH-SY5Y cells, grown in galactose medium and transfected with a mitochondrial matrix luciferase together with either pcDNA3 (controls, black) or PS2-T122R (red) cDNA. Glycolysis was inhibited by 5 mM 2-deoxyglucose and the mitochondrial ATP production was stimulated by BK-induced ER-mitochondria Ca²⁺ transfer. Luminescence values were normalized to baseline. Representative luminescence traces (left) and mean values (right) of the Area Under the Curve (AUC). (C) and (D) N = number of coverslips. (** p < 0.01; *** p < 0.001). Data are presented as mean ± SEM.

Since Ca²⁺ plays a pivotal role in mitochondrial metabolism (Jouaville LS *et al.*, PNAS 1999), and considering the profound alterations in intracellular Ca²⁺ homeostasis induced by FAD-PS2 expression, we decided to investigate how Ca²⁺ dysregulation induced by FAD-PS2 expression could influence mitochondrial functionality. Employing a mitochondrial-targeted aequorin (see Materials and Methods for details on the different Ca²⁺ affinity of the aequorin variants used

in this study), we measured mitochondrial Ca^{2+} uptake in control and PS2-T122R expressing cells upon ER Ca^{2+} release induced by bradykinin (BK, 100nM) addition, a maximal IP3R stimulus; as expected, a reduced mitochondrial Ca^{2+} uptake has been measured upon FAD-PS2 expression (Zampese E *et al.*, PNAS 2011; FIG 25C). One of the main consequences of the reduced mitochondrial Ca^{2+} uptake observed in PS2-T122R expressing cells could be an alteration in mitochondrial ATP production. A luciferase-based ATP probe targeted to mitochondrial matrix was used; cells were grown in galactose medium and the Ca^{2+} -induced mitochondrial ATP production was stimulated by the ER-mitochondria Ca^{2+} transfer induced by BK. A reduced mitochondria ATP production induced by BK was measured in FAD-PS2 expressing cells compared to control (FIG 25D).

The stimulus (BK) used in the experiment just described represents a maximal IP3R stimulation; to study, in a more physiological way, the effect of Ca^{2+} homeostasis alterations on mitochondrial metabolism, we decided to apply an alternative protocol. In 2010, Foskett and co-authors showed that a constitutive, FCS (Fetal Calf Serum)-promoted, IP3-mediated ER to mitochondria Ca^{2+} transfer is essential for the maintenance of cellular bioenergetics; in particular, they demonstrated that peptides and growth factors contained in FCS can modulate the constitutive ER-mitochondria Ca^{2+} transfer (Cardenas C *et al.*, Cell 2010). Using a mitochondrial-targeted aequorin, we firstly evaluated whether acute application of FCS as stimulus (Cardenas C *et al.*, Cell 2010) is able to induce mitochondrial $[\text{Ca}^{2+}]$ rises. FIG. 26A shows that acute FCS stimulations trigger mitochondrial Ca^{2+} uptake. Importantly, FCS-induced mitochondrial Ca^{2+} -rises were observed even when the stimulus was applied in a Ca^{2+} -free, EGTA-containing medium (FIG. 26A, grey trace), suggesting that Ca^{2+} release from intracellular stores is involved in this phenomenon. Again, when we compared the FCS-induced mitochondrial Ca^{2+} uptake of control or PS2-T122R expressing cells, we observed a dampened mitochondrial Ca^{2+} uptake in the latter cells, as expected because of the decreased ER $[\text{Ca}^{2+}]$ caused by FAD-PS2 expression (FIG26A). In these conditions, we measured again mitochondrial ATP production employing a luciferase-based ATP probe targeted to the mitochondrial matrix; cells were grown in galactose medium and the physiological, Ca^{2+} -induced mitochondrial ATP production was evaluated by using FCS as stimulus, due to its ability of inducing ER-mitochondria Ca^{2+} transfer. We found that PS2 (both WT and FAD-PS2-T122R) expression causes a decrease in mitochondria ATP production upon FCS stimulation; on the contrary, PS1 expression (both WT and FAD-PS1-A246E), that does not cause Ca^{2+} dysregulation as PS2 (Zatti G *et al.*, Cell Calcium 2006), does not significantly reduce mitochondrial ATP production as PS2 (FIG 26 B).

Figure26

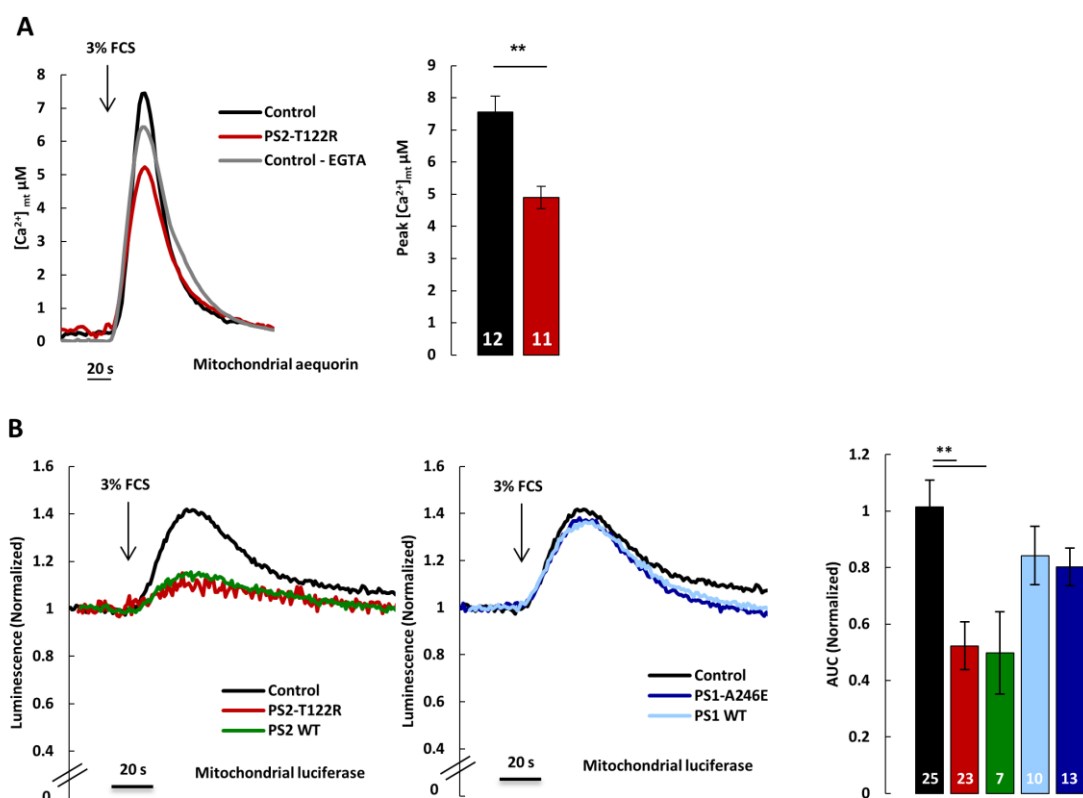


Figure 26. The FAD-PS2-T122R mutant, but not FAD-PS1, decreases mitochondria ATP production upon physiological IP₃-mediated ER-mitochondria Ca²⁺ transfer. **(A)** Mitochondrial Ca²⁺ uptake measured in SH-SY5Y cells grown in galactose medium, and transfected with a mitochondrial matrix aequorin together with either pcDNA3 (Control, black or grey) or PS2-T122R (red) cDNA. Mitochondrial Ca²⁺ uptake was induced by acute exposure to Fetal Calf Serum (FCS, 3 %) in either mKRB or Ca²⁺-free mKRB containing EGTA (500 μM). Representative traces (left) and mean [Ca²⁺]_{mt} peaks (right) induced by FCS. **(B)** Mitochondrial ATP production was measured in SH-SY5Y cells grown in galactose and transfected with a mitochondrial matrix luciferase together with either pcDNA3 (controls, black), PS2-T122R (red), PS2 WT (green), PS1 WT (light blue) or PS1-A246E (blue) cDNA. Glycolysis was inhibited by 5 mM 2-deoxyglucose and the mitochondrial ATP production was stimulated by FCS-induced ER-mitochondria Ca²⁺ transfer. Luminescence values were normalized to baseline. Representative luminescence traces (left) and mean AUC values (right). N = number of coverslips (** p<0.01). Data are presented as mean ± SEM.

Since, by luciferase probe, it is not possible to measure basal ATP levels in single cell, but only changes in [ATP] upon stimulation in the overall cell population, we co-expressed a nuclear and a mitochondrial matrix targeted FRET-based ATP probe, Ateam1.03 (Imamura H *et al.*, PNAS 2009); by this tool, we were able to measure, at the same time and in the same cell, ATP basal levels in the nucleus and within mitochondria. The nucleus has been used as a surrogate of the cytosol, since it has been shown that ATP in the nuclear compartment is in equilibrium with the ATP in the cytosol (Imamura H *et al* PNAS 2009). Using this approach, we measured lower ATP basal levels both in the nucleus and in the mitochondria of SH-SY5Y (FIG27A) and MEFs (FIG 27B) cells expressing PS2-T122R, compared to controls.

Considering the defects in mitochondrial metabolism found in cells expressing PS2-T122R, we checked the phosphorylation status of the energy sensor of the cell, AMPK. AMPK, AMP-activated protein kinase, is a protein that can be activated under energy stress conditions: it can sense the increase in AMP:ATP or ADP:ATP ratio. The activation of AMPK occurs through its phosphorylation at Threonine 172, located in the catalytic subunit of the protein; once activated, the enzyme can promote catabolic processes and block anabolic processes in order to re-establish the energy homeostasis of the cell (GarciaD and Shaw RJ, Mol Cell Rev 2017). Checking by western blot the status of this protein, we found, in accordance with ATP measurements, an increase in the AMPK phosphorylation in PS2-T122R expressing cells, compared to controls (FIG27C).

Figure 27

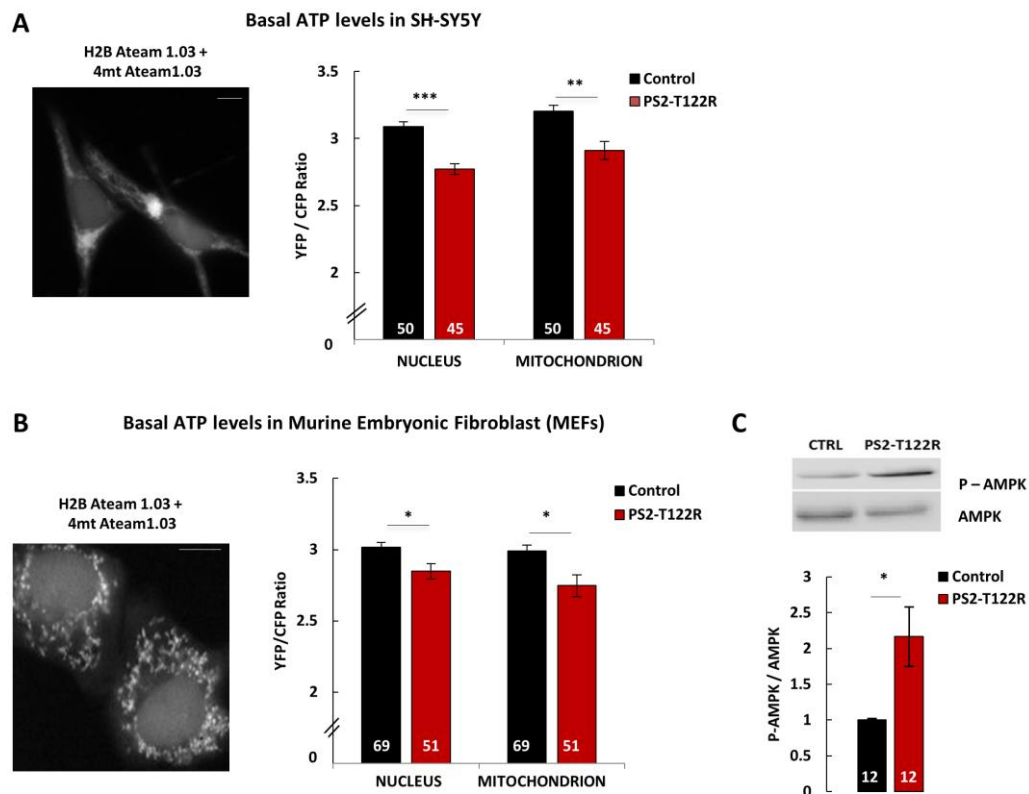


Figure 27. The FAD-PS2-T122R mutant decreases basal ATP levels both in SH-SY5Y and MEFs cells. Basal ATP was measured in SH-SY5Y (A) and in MEFs cells (B). Cells were grown in galactose medium and transfected with both H2B-Ateam1.03 (nuclear) and 4mt-Ateam1.03 (mitochondrial matrix) together with either pcDNA3 (control, black) or PS2-T122R (red) cDNA. Mean values of YFP/CFP ratios and representative picture of cells expressing the two probes (YFP channel). N = number of cells. (C) SH-SY5Y cells grown in galactose medium expressing or not PS2-T122R. 24h after transfection total proteins were extracted and subjected to western blot with antibodies anti-AMPK and anti-P-AMPK. On the left: representative western blot; on the right: P-AMPK/AMPK quantification (normalized to control). N = number of independent experiments (* p<0.05; ** p<0.01; *** p<0.001). Data are presented as mean \pm SEM.

The ATeam1.03 probes were also used to measure the ATP basal levels in primary cortical neurons from WT and PS2-N141I transgenic mice (PS2.30H, Tg). Neurons were bathed in mKRB containing pyruvate, in order to force mitochondrial metabolism. Surprisingly, we did not observe any significant difference neither in the nuclear nor in the mitochondrial ATP basal levels, but only a tendency to reduced basal ATP levels in Tg neurons (FIG 28A-B). Since primary neurons in culture are particularly inactive and quiescent, considering also the fact that they are used relatively shortly after plating (6-7 DIV) when they are not well connected between each other, we decided to challenge them to consume ATP. Neurons were treated with low doses of gramicidin, to force ATP consumption and observe if FAD-PS2 neurons can supply ATP demand as WT cells. Gramicidin is an ionophore able to insert in the PM and collapse its K^+/Na^+ gradient; in this way, it induces the activity of the Na^+/K^+ ATPase and, as consequence, ATP consumption (Brand MD and Nicholls, Biochem J 2011). We observed that, after gramicidin addition, nuclear ATP, and in particular mitochondrial ATP, levels decreased more rapidly in FAD-PS2 neurons than in WT neurons (FIG 28A-C). These results indicate that mitochondrial activity of FAD Tg neurons is impaired, since they are not able to supply enough cell energy demand.

Figure 28

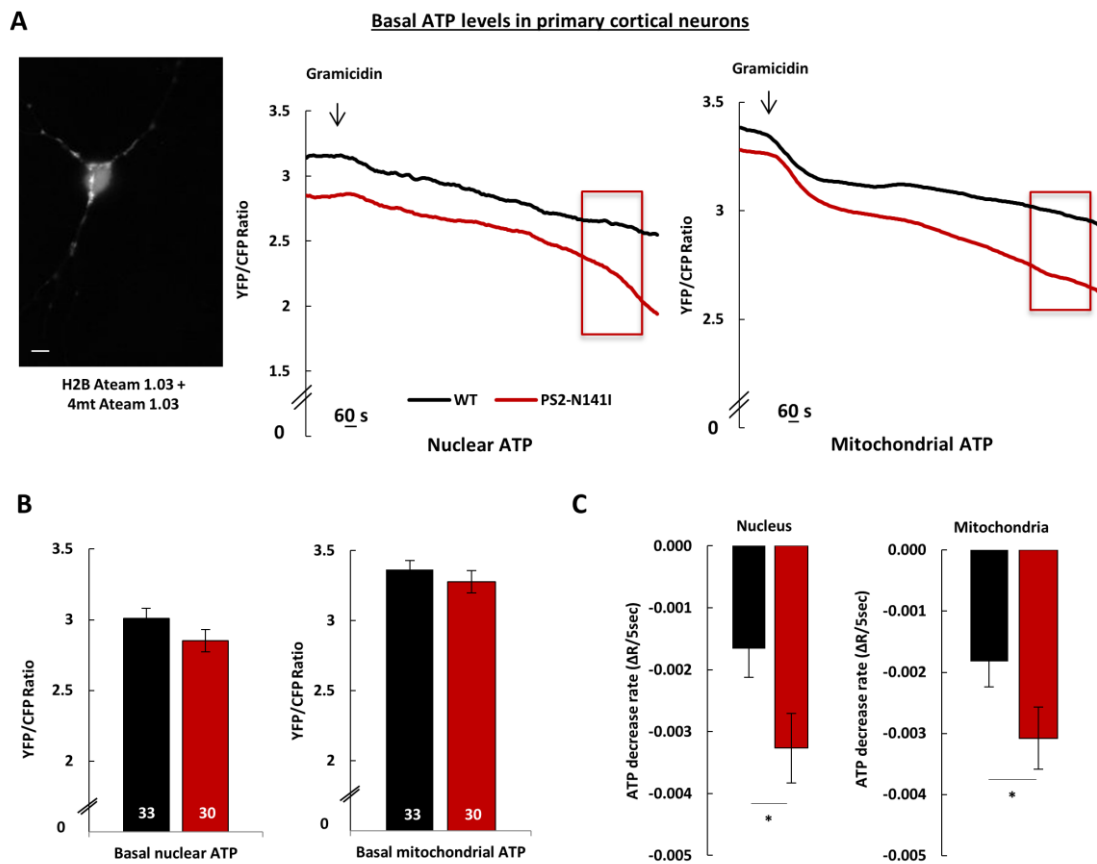


Figure 28. Mitochondrial functionality is impaired in primary cortical neurons from PS2-N141I Tg mice. **(A)** Nuclear and mitochondrial ATP basal levels were measured in primary cortical neurons from WT and Tg mice transfected at 5-6 DIV with both nuclear and mitochondrial ATeam1.03 probes. 24 h after transfection, ATP measurements were performed. On the left: representative image of a neuron transfected with the two probes (YFP channel); on the right: nuclear and mitochondrial representative traces. The experiment was performed in Ca^{2+} -free mKRB and, where indicated, gramicidin (0.3 μM) was applied; **(B)** and **(C)** Analysis of the experiments described in panel A. **(B)** Bars represent nuclear and mitochondrial ATP basal levels (YFP/CFP ratio); **(C)** mean decrease rate of nuclear and mitochondrial ratios; after 15 minutes from gramicidin addition, the rate of ratio decrease was followed for 3 min. Data are presented as $\Delta R/\text{frame}$. N = number of cells; (* $p < 0.05$). Data are presented as mean \pm SEM.

2. The FAD-linked PS2-T122R mutant does not impair glycolysis

In order to confirm that FAD-PS2 expression causes metabolic defects mainly by altering mitochondrial activity, we checked the glycolytic flux by two different approaches. First, using a cytosolic luciferase, we measured the ATP produced through glycolysis in the cytosol; cells were grown in galactose medium, the mitochondrial ATP-synthesis was blocked with oligomycin and glycolysis was induced exposing cells to glucose. In cell expressing FAD-PS2-

T122R, no defective ATP production by glycolysis was detected, compared to controls (FIG 29A). Moreover, we did not observe any defect also measuring the extracellular acidification (ECAR) by Seahorse platform, performing a typical experiment for ECAR evaluation (FIG 29B): we measured glycolysis at different glucose concentrations (basal glycolysis, measured at 2 mM glucose; glycolysis measured upon 8 mM glucose addition; glycolytic capacity, upon oligomycin addition, as described in panel B) and no difference has been found between control and mutated FAD-PS2 expressing cells (FIG 29C). Taken together these data suggest that FAD-PS2 expression in SH-SY5Y cells causes mainly mitochondrial metabolism defects.

Figure 29

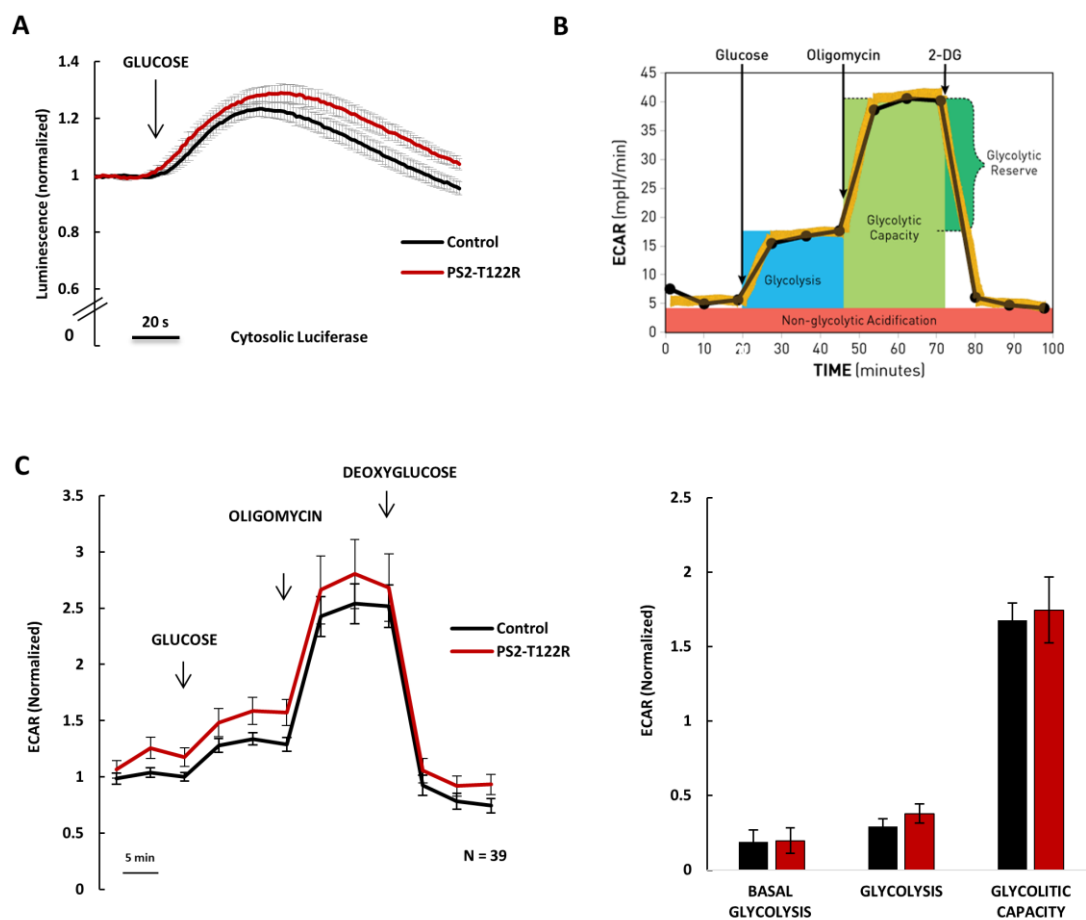


Figure 29. The FAD-PS2-T122R mutant does not affect glycolysis. **(A)** ATP produced by glycolysis in SH-SY5Y cells, grown in galactose medium and transfected with cytosolic-luciferase together with pcDNA3 (control, black) or PS2-T122R (red) cDNA. Cells were incubated for 2 minutes with oligomycin (2 μ M) and, where indicated, glucose (15 mM) was applied to stimulate glycolysis. Mean luminescence traces of control (black) and PS2-T122R (red). N= number of coverslips; **(B)** Scheme of a typical Seahorse experiment to measure extracellular acidification (ECAR). **(C)** ECAR was measured in SH-SY5Y cells grown in glucose medium and transfected with either pcDNA3 (control, black) or PS2-T122R (red) cDNA. After ECAR baseline measurements (2 mM glucose), glucose (8 mM), oligomycin (1 μ g/ml) and 5-deoxy-glucose (20 mM) were applied, as indicated. On the left: ECAR mean traces. Data were normalized for cells number and to controls baseline-ECAR. On the right: basal glycolysis (at 2 mM glucose), glycolysis

(upon 8 mM glucose addition) and glycolytic capacity (upon oligomycin addition) mean values analysed as showed in panel B. N = number of the wells. Data are presented as mean \pm SEM.

3. Mitochondrial defects caused by FAD-linked PS2 mutants are partly due to Ca²⁺ dysregulation

Given the marked Ca²⁺ dysregulation induced by FAD-PS2 expression, consistently with the observed mitochondrial impairment in intact cells, to investigate the mechanisms by which FAD-PS2 causes the defect, we decided to modulate Ca²⁺ homeostasis in control cells, to mimic ER Ca²⁺ depletion caused by PS2 expression.

Control cells were incubated for short periods of time with a SERCA pump inhibitor, cyclopiazonic acid (CPA), to reduce their ER Ca²⁺ content to levels similar to those retrieved in FAD-PS2 expressing cells. ER Ca²⁺ content reduction was induced perfusing cells with Ca²⁺-free extracellular saline containing CPA (20 μ M) for 4 minutes; ER Ca²⁺ release and mitochondrial Ca²⁺ uptake were induced by FCS and monitored with a cytosolic (FIG 30A) and a mitochondrial matrix (FIG 30B) targeted aequorin, respectively. In these conditions, for similar mitochondrial Ca²⁺ rises (FIG 30B), induced by FCS, in control and PS2-T122R expressing cells, we still observed a reduction in mitochondrial ATP production in PS2-expressing cells, compared to CPA-treated controls, though CPA treatment was able to strongly reduce the capacity of control cells to produce ATP (FIG 30C).

Similar results were obtained modulating the activity of the Mitochondrial Ca²⁺ Uniporter (MCU) complex. In this complex, MICU1, together with MICU2, are two components that modulate the channel (Mammucari C. *et al.*, Biochim Biophys Acta 2016). Moreover, MICU1 presents EF-hand domains that are essential for the MCU activity regulation. Hence, we overexpressed a form of MICU1 that is mutated on its EF-hand domains (MICU1^{EFmut}) (Patron M *et al.*, Mol Cell 2014), and we measured both mitochondrial Ca²⁺ uptake and ATP production, by a mitochondrial aequorin and mitochondrial luciferase, respectively. Upon MICU1^{EFmut} overexpression in control cells, a reduction in mitochondrial Ca²⁺ rises, similar to that caused by mutated PS2 expression, was measured (FIG 30D); nevertheless, mitochondrial ATP production in MICU1^{EFmut} expressing cells was reduced compared to control cells, but again PS2-expressing cells produce less ATP (FIG 30E).

Taken together these results suggest that FAD-PS2 expression causes mitochondrial metabolism impairments by reducing the ER Ca²⁺ content and mitochondrial Ca²⁺ uptake, thus negatively regulating Ca²⁺-dependent mitochondrial metabolism. However, additional and additive mechanisms are likely involved in mitochondrial dysfunctions.

Figure 30

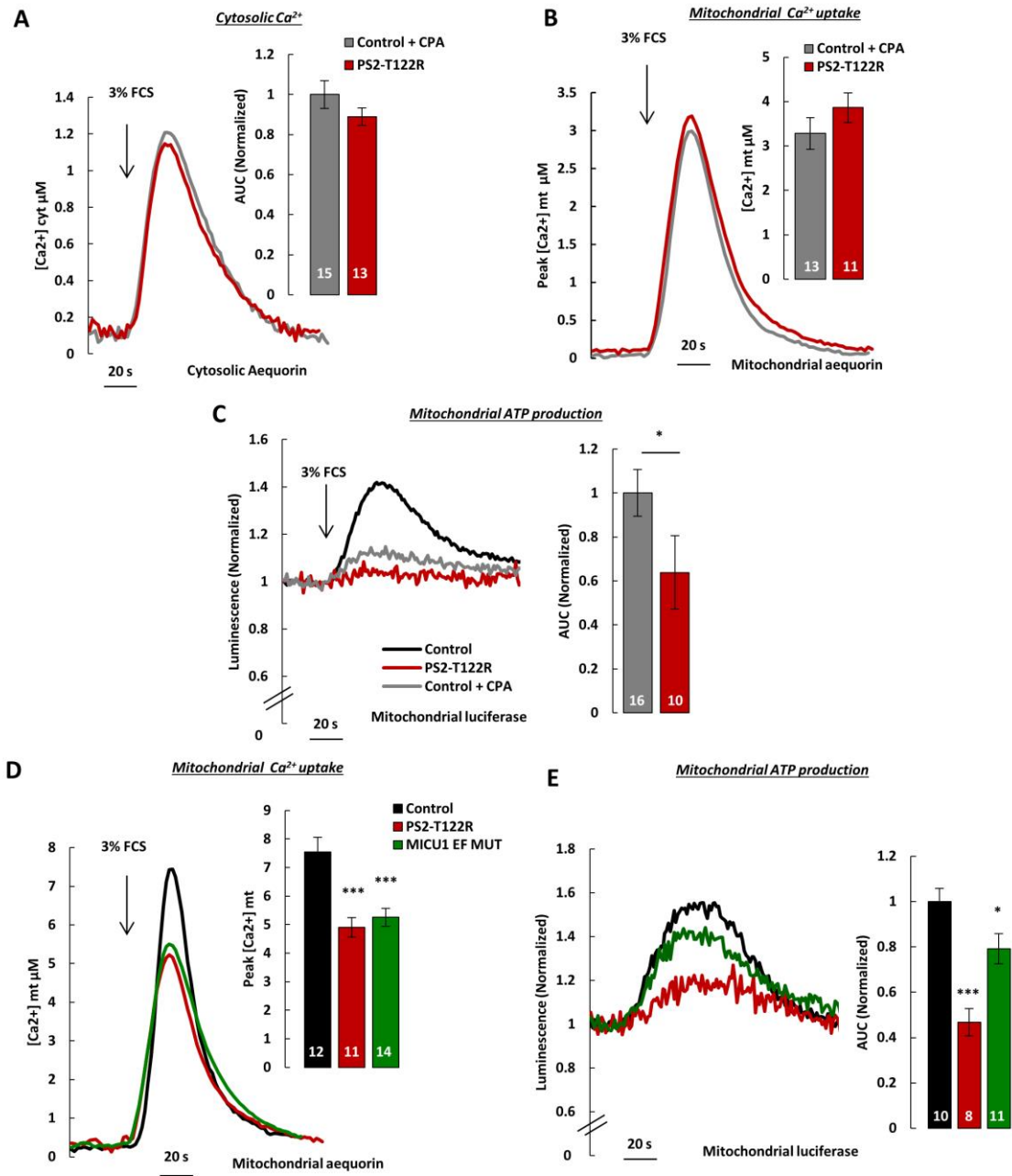


Figure 30. Mitochondrial dysfunction caused by the FAD-PS2-T122R mutant is partially due to Ca²⁺ dysregulation. Cytosolic Ca²⁺ rises (A) and mitochondrial Ca²⁺ uptake (B), upon ER Ca²⁺ release induced by FCS (3 %), were measured in SH-SY5Y cells grown in galactose medium and transfected with cytosolic (A) or mitochondrial matrix targeted aequorin (B), together with either pcDNA3 (Control, grey) or PS2-T122R (red) cDNA. To reduce the ER Ca²⁺ content, control cells were perfused with Ca²⁺-free medium containing the SERCA pump inhibitor, cyclopiazonic acid (CPA, 20 μM for 4 minutes). Representative [Ca²⁺]_{cyt} (A), mitochondrial Ca²⁺ uptake (B) traces, mean AUC values (A, right) and mean [Ca²⁺]_{mt} peaks (B, right). (C) Mitochondrial ATP production measured in SH-SY5Y cells transfected with a mitochondrial luciferase, together with either pcDNA3 or PS2-T122R cDNA. The experiment was performed as in panels A and B, and glycolysis was blocked with 5 mM 2-deoxy-glucose. Luminescence values were normalized to baseline. Representative luminescence traces (left) and mean AUC values (right).

Mitochondrial Ca^{2+} uptake (**D**) and mitochondrial ATP production (**E**) measured in SH-SY5Y cells grown in galactose medium and transfected with mitochondrial matrix aequorin (D) or mitochondrial matrix luciferase (E), together with either pcDNA3 (control, black) or PS2-T122R (red) or MICU1^{EF-mut} (green) cDNAs; ER Ca^{2+} release and thus mitochondrial Ca^{2+} uptake (D) and mitochondrial ATP production (E) were induced by FCS (3 %); (E) luminescence values were normalized to baseline. Representative traces (D and E, left), mean $[\text{Ca}^{2+}]_{\text{mt}}$ peaks (D, right) and mean AUC values (E, right). N = number of coverslips (* $p < 0.05$; *** $p < 0.001$). Data are presented as mean \pm SEM.

4 FAD-linked PS2 mutants, but not PS1, affect mitochondrial functionalities

To better evaluate the mitochondrial defect caused by FAD-PS2 and reveal the additional mechanism, beyond Ca^{2+} dysregulation, through which PS2 contributes to this impairment, we analysed different aspects of the activity of these organelles. Using the Seahorse assay, we firstly evaluated the Oxygen Consumption Rate (OCR), as described in panel A (FIG 31A); in our cell model, it is not possible to perform the experiment exactly as showed in panel A since, after oligomycin addition, we observed that the OCR does not increase beyond the basal level upon FCCP application. For this reason, two different experiments were performed to evaluate the OCR upon oligomycin or FCCP addition and parameters indicated in figure 31 (panels B, C and D) were analysed as described in panel A. We found that both basal and maximal OCR (induced by the mitochondrial uncoupler, FCCP) were reduced in PS2 (both FAD-linked mutants and WT, FIG 31B), but not in PS1 (PS1-A246E and WT, FIG 31D), expressing SH-SY5Y cells. Moreover, upon either PS2-T122R or PS2 WT expression, a reduced mitochondrial ATP-linked respiration was measured (FIG 31C), but no impairments have been detected in the proton leak (FIG 31C). Preliminary results showed no differences in the last two parameters in cells expressing either a FAD-PS1 mutant or PS1 WT (FIG 31D). The data obtained in PS2-expressing cells suggest possible defects in the respiratory chain, in particular in the functionality/expression level of the respiratory chain complexes and ATP synthase. These proteins expression levels were thus evaluated, by western blot, using an antibody-mix (anti-OXPHOS MitoProfile; see MM) that recognizes the main subunits of the complexes. We did not observe any significant difference between control and PS2-T122R expressing SH-SY5Y cells (FIG 32A). Given that the expression levels of ATP synthase and of the four respiratory chain complexes are unaffected by FAD-PS2 expression, and that functional experiments, previously performed in our lab on isolated mitochondria from WT and PS2-N141I Tg mice brains, did not reveal substantial differences between the two genotypes (Kipanjula M *et al.*, Cell Aging 2012), we reasoned that the mitochondrial defect observed in intact cells may depend on the cellular environment, rather than on defective mitochondria

per se.

Figure 31

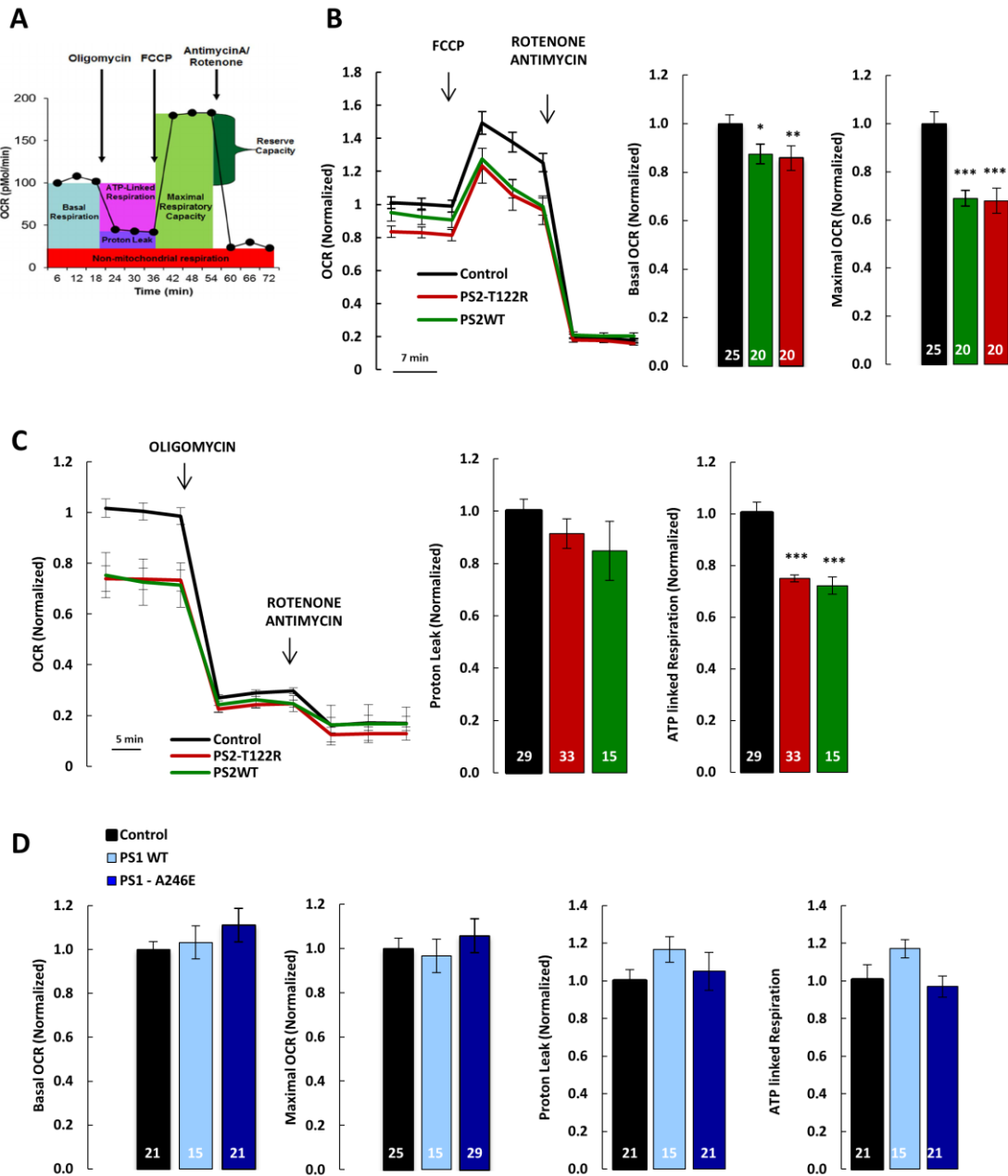


Figure 31. FAD-PS2 mutants, but not FAD-PS1, affect mitochondrial functionality. **(A)** Scheme of a typical Seahorse experiment to measure mitochondrial respiration. **(B), (C) and (D)** Oxygen Consumption Rate (OCR) measurements in SH-SY5Y cells grown in galactose medium and transfected either pcDNA3 (control, black), PS2-T122R (red), PS2 WT (green), PS1 WT (light blue) or PS1-A246E (blue) cDNAs. After OCR baseline measurements, either FCCP (0.5 μ M) (B) or oligomycin (1 μ g/ml) (C) were applied. Rotenone (1 μ M) and antimycin (0.1 μ M) were added at the end of the experiments to obtain minimum OCR. Basal and maximal OCR (B and D), proton leak and ATP-linked respiration (C and D), were calculated as reported in panel A and normalized to control. (B) and (C), on the left: OCR mean traces; data were normalized for cells number and to controls baseline-OCR. On the right: histograms show basal and maximal OCR (B), proton leak and ATP-linked respiration (C) mean values, calculated as showed in panel A and normalized to control. (D) Histograms show basal, maximal OCR, proton leak and ATP-linked respiration mean values calculated as showed in panel A and normalized to control. N =

number of wells. Data are presented as mean \pm SEM (** $p < 0.01$; *** $p < 0.001$).

Figure 32

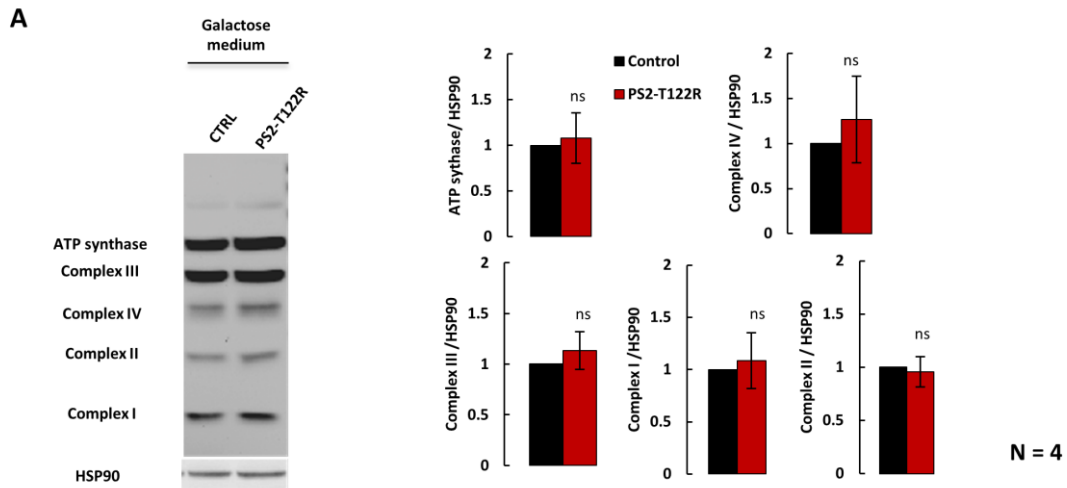


Figure 32. The FAD-PS2-T122R mutant does not affect ATP synthase and respiratory chain complexes expression levels. **(A)** SH-SY5Y, grown in galactose medium, were transfected with pcDNA3 or PS2-T122R cDNA. 24h after transfection, total proteins were extracted and subjected to western blot with antibodies anti-OXPHOS MitoProfile and anti-HSP90 (as a housekeeping protein). Representative blot and quantification (normalized to control) are shown. N = number of independent experiments. Data are presented as mean \pm SEM.

The observed reduced OCR could be due to Ca^{2+} dysregulation caused by PS2 expression; in fact, Ca^{2+} plays a pivotal role in mitochondrial functionality since, as already described, it can modulate the activity of several substrate carriers, TCA cycle enzymes and respiratory chain complexes inside mitochondria. Moreover, mitochondrial functionality relies also on the amount of substrates, coming from the cytosol, that enter mitochondria and fuel the TCA cycle and, consequently, the respiratory chain activity.

5 FAD-linked PS2 mutants induce the detachment of Hexokinase1 from mitochondria

As described above, Ca^{2+} dysregulation induced by FAD-PS2 is likely not the only mechanism that causes mitochondrial impairment, since, upon similar ER Ca^{2+} release and mitochondrial Ca^{2+} uptake, the mitochondria of FAD-PS2 expressing cells still produced significantly less ATP induced by FCS stimulation, compared to controls.

In order to work properly, mitochondria have to receive the right amount of substrates,

produced by glycolysis in the cytosol, to support TCA cycle and respiratory chain activity (Vanderperre B *et al*, Plos Genetics 2016; Li X *et al*, Oncotarget 2017). VDAC, localized in the OMM, is responsible for the exchange of substrates, metabolites and ions between cytosol and mitochondria (see Introduction). Its activity is believed to be modulated by the dynamic interaction with Hexokinase1 (HK1), the enzyme that catalyses the first step of glycolysis, converting glucose to glucose 6-phosphate. It seems that HK1 interaction/detachment from mitochondria, and in particular from VDAC, can modulate its open/close state, allowing or inhibiting mitochondrial substrates import. Thus, HK1-mitochondria interaction is essential to couple cytosolic and mitochondrial metabolism, allowing proper mitochondria activity. Interestingly, it has been recently demonstrated that PS2 interacts with VDAC (Wakabayashi T *et al.*, Nature Cell Biology 2009). We, thus, wondered whether PS2 could, in some way, modulate the HK1-VDAC interaction.

Firstly, we evaluated HK1-mitochondria co-localization in SH-SY5Y cells; cells were co-transfected with FAD-PS2-T122R and a mitochondrial Red Fluorescent Protein (mt-RFP) encoding cDNAs. After fixation, endogenous HK1 was visualized by a specific immuno-staining and HK1-mitochondria (mt-RFP) co-localization was analysed by confocal microscopy. Significant reduction in HK1-mitochondria co-localization was measured in FAD-PS2 expressing cells compared to controls (FIG 33A). Similar results were obtained also analysing HK1-mitochondria (immune-stained for cytochrome C) co-localization in FAD-PS2-N141I patient-derived fibroblasts, compared to cells from three different healthy controls (FIG 33B). The same experiment was performed also in cortical neurons from PS2-N141I Tg mice compared to WT: a significant reduction in HK1-mitochondria (cytochrome C) co-localization was measured in PS2-N141I cortical neurons compared to WT neurons (FIG 34A). The total HK1 expression levels were checked by western blot in both SH-SY5Y cells expressing FAD-PS2 (FIG 34B) and in cortical neurons from WT and PS2-N141I Tg mice and no significant differences have been detected between the two genotypes (FIG 34C). Moreover, we have already reported that PS2 expression does not influence VDAC1 expression levels (Filadi R *et al.*, Cell Report 2016), thus excluding that the differences in HK-mitochondria association could be due to diverse levels of VDAC protein.

Figure 33

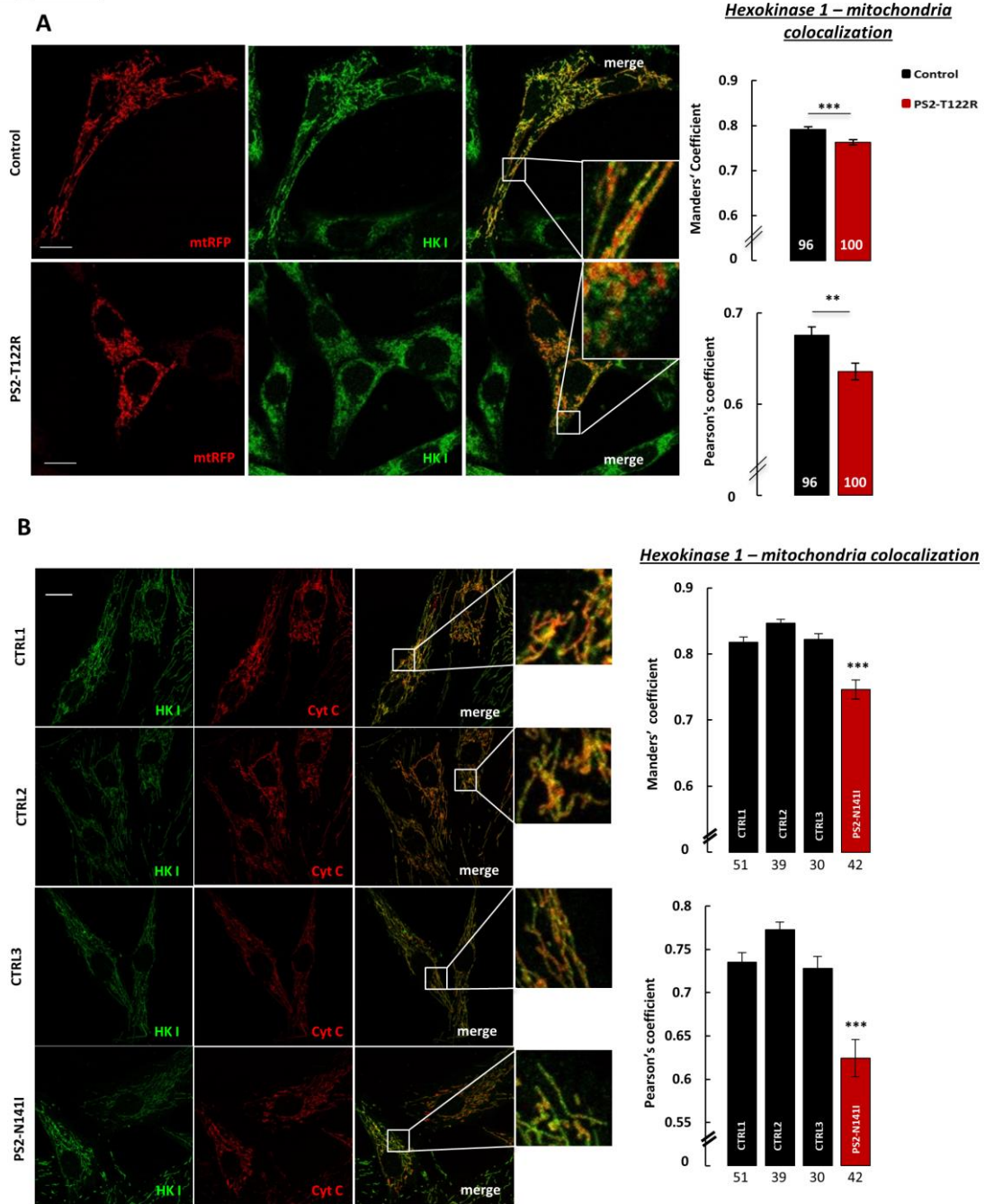


Figure 33. FAD-PS2 mutants expression decreases HK1-mitochondria co-localization. **(A)** Hexokinase 1 (HK1)-mitochondria co-localization in SH-SY5Y cells grown in galactose medium and transfected with a mitochondrial RFP (mtRFP) together with either pcDNA3 (control, black) or PS2-T122R (red) cDNA. **(B)** HK1-mitochondria co-localization in fibroblasts from three healthy controls (CTRL 1, 2, 3) and a FAD-PS2-N141I patient. mtRFP (A) or cytochrome C (B) were used to visualize mitochondria while for endogenous HK1 an antibody α -HK1 was used. (A) and (B), on the left: representative confocal images of mt-RFP (A) or cytochrome C (B), HK1 and HK1-mitochondria co-localization of control and PS2-T122R expressing cells (A) or FAD-PS2 patient-derived fibroblasts (B); on the right: (A and B) mean values of Mander's and Pearson's co-localization coefficients calculated using ImageJ plugins. Scale bar 10 μ m. N = number of cells (** $p < 0.01$; *** $p < 0.001$). Data are presented as mean \pm SEM.

Figure 34

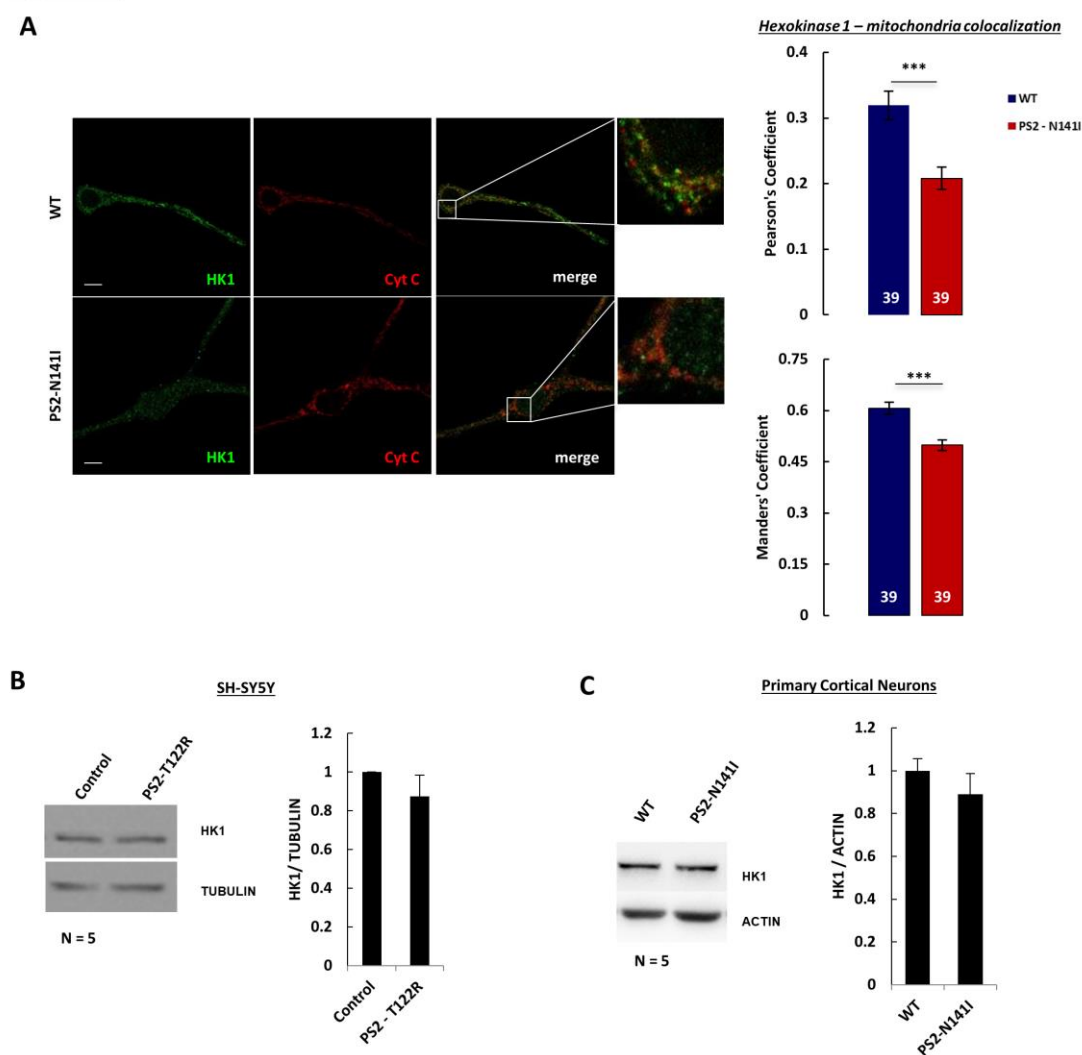


Figure 34. HK1-mitochondria co-localization is decreased in cortical neurons from FAD-PS2 Tg mice. **(A)** HK1-mitochondria co-localization in primary cortical neurons from WT and PS2-N141I Tg mice fixed at 10-12 DIV. Antibodies against cytochrome C and HK1 were used to visualize mitochondria and endogenous HK1, respectively. On the left: representative confocal images of cytochrome C, HK1 and HK1-mitochondria co-localization of WT and FAD-PS2 Tg neurons; on the right: mean values of Manders' and Pearson's co-localization coefficients measured using ImageJ plugins. Scale bar, 10 μ m. N = number of cells. **(B)** and **(C)** Expression levels of endogenous HK1 in SH-SY5Y cells grown in galactose medium expressing or not PS2-T122R (B), or in primary cortical neurons from WT and FAD-PS2 Tg mice (C). 24h after transfection (for SH-SY5Y cells) or at 10-12 DIV (for neurons), total proteins were extracted and subjected to western blot with antibodies anti-HK1 and anti-tubulin or actin. On the left: representative western blot; on the right: HK1/Tubulin or HK1/actin ratios are presented (normalized to control). N = number of independent experiments (***) $p < 0.001$). Data are presented as mean \pm SEM.

6 FAD-PS2-induced Hexokinase1 detachment from mitochondria contributes to mitochondrial impairment

In order to verify whether the impairment in mitochondrial ATP production caused by FAD-PS2 expression might be linked, at least in part, to HK1 detachment from mitochondria, we

tried to mimic the PS2-mediated effect on mitochondrial metabolism altering HK1-mitochondria interaction by both pharmacological and genetic approaches. Firstly, clotrimazole (CTM), an antifungal drug that has been reported to induce the detachment of HK from mitochondria (Chiara F *et al.*, Plos One 2008) has been used to obtain, in control cells, the degree of HK-mitochondria interaction observed in FAD-PS2-expressing cells. CTM, however, could have also several side effects within the cells (Crowley PD *et al.*, J Appl Microbiol 2014); among them, it causes mitochondrial defects, such as reduced mitochondrial Ca^{2+} uptake and altered mitochondrial membrane potential, triggering cell death (Kadavakollu S *et al.*, Med Chem 2014). Thus, we firstly checked at which concentration and time of treatment the drug does not induce mitochondrial impairments, while maintaining its effects on HK1-mitochondria interaction. Mitochondrial membrane potential ($\Delta\Psi$) was evaluated loading cells with the tetra-methyl rhodamine methyl-ester (TMRM) fluorescent dye; after 10 minutes of treatment with 5 μM CMT, no mitochondrial depolarization was observed (FIG 35A). Then, FCS-induced mitochondrial Ca^{2+} rises were evaluated in cells treated, or not, with 5 μM CMT for 10 minutes and, again, no differences were observed (FIG 35B). In parallel experiments, HK1-mitochondria co-localization was evaluated upon clotrimazole (5 μM , 10 minutes) treatment in both living and fixed cells. For live imaging experiments, cells expressing a mtRFP and a HK1-YFP were analysed at confocal microscope and CMT-induced HK1 detachment from mitochondria was evaluated during time. Instead, for experiments with fixed cells, SH-SY5Y were transfected with a mt-RFP and an immune-staining was performed to visualize endogenous HK1. In both cases, a reduction in HK1-mitochondria co-localization was measured in cells treated with CMT compared to control (FIG 35C); importantly, the degree of HK1-mitochondria colocalization upon CTM treatment is similar to that observed upon PS2 expression (see FIG 33A; HK1-mitochondria colocalization coefficients decrease about of 5 % upon PS2-T122R expression and about of 8 % upon CTM treatment).

Established the conditions in which CMT detaches HK1 from mitochondria, without affecting mitochondrial membrane potential and Ca^{2+} uptake, we measured mitochondria ATP production, induced by FCS, in control cells treated with CMT, by employing the mitochondrial luciferase probe. CMT-treated cells showed a reduction in mitochondrial ATP production compared to controls; however, the effect of CMT on ATP production was less pronounced than the impairment caused by FAD-PS2 expression (FIG 35D). This is consistent with a model in which FAD-PS2 expression causes mitochondrial defects by modulating HK1-mitochondria interaction, on the one hand, and by causing Ca^{2+} dysregulation, on the other.

Figure 35

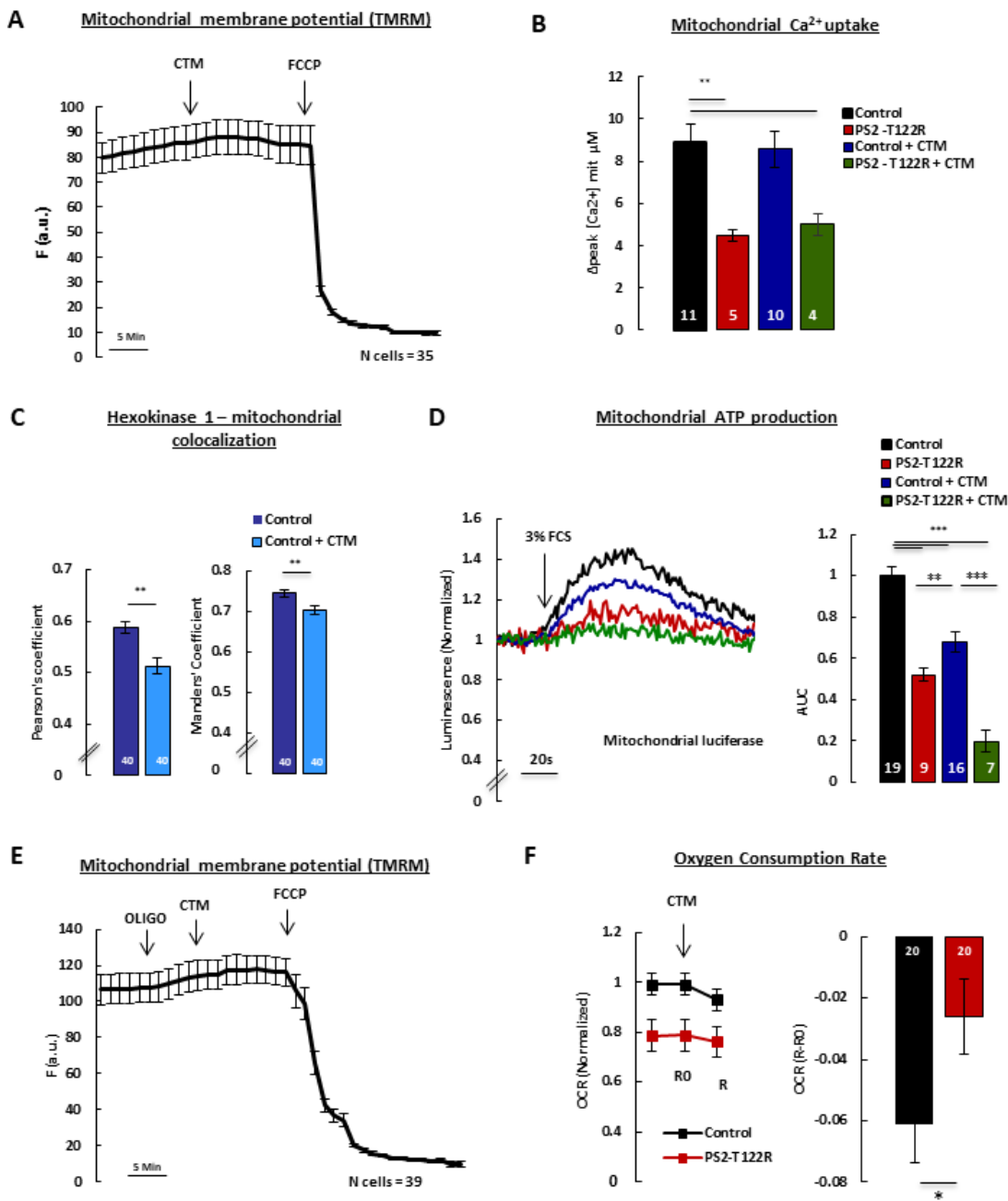


Figure 35. Clotrimazole (CMT) mimics mitochondrial ATP production defect caused by FAD-PS2 expression. **(A)** Mitochondrial membrane potential was measured in SH-SY5Y cells loaded with TMRM for 45 minutes at RT. The mean trace of TMRM fluorescence is shown; where indicated CTM (5 μ M) or FCCP (10 μ M) have been applied. N = number of cells. **(B)** Mitochondrial Ca²⁺ uptake was measured in SH-SY5Y cells transfected with mitochondrial-aequorin together with either pcDNA3 or PS2-T122R cDNA, treated or not with CTM (5 μ M) for 10 minutes. ER Ca²⁺ release and thus mitochondrial Ca²⁺ uptake were induced by FCS (3 %). Mean [Ca²⁺]_{mit} peaks induced by FCS. N = number of coverslips. **(C)** HK1-mitochondria co-localization in SH-SY5Y cells treated or not with CTM (5 μ M) for 10 minutes. Antibodies against cytochrome C and HK1 were used to visualize mitochondria and endogenous HK1, respectively. Mean values of Manders' and Pearson's co-localization coefficients, measured using ImageJ plugins, are shown. Scale bar 10 μ m. N = number of cells. **(D)** Mitochondrial ATP production measured in SH-SY5Y cells grown in galactose medium and transfected with mitochondrial-luciferase together with either pcDNA3 or PS2-T122R cDNA treated or not with CTM (5 μ M) for 10 minutes. Mitochondrial ATP production was stimulated by FCS (3 %) and glycolysis was blocked with 5 mM 2-

deoxy-glucose. Luminescence values were normalized to baseline. Representative luminescence traces and histograms of mean AUC values, normalized to control, are showed. N = number of coverslips. **(E)** Mitochondrial membrane potential measured as described in panel A. Mean trace of TMRM fluorescence is shown and where indicated oligomycin (1 $\mu\text{g/ml}$), CTM (5 μM) and FCCP (10 μM) were applied. N = number of cells. **(F)** Oxygen Consumption Rate (OCR) measured in SH-SY5Y cells grown in galactose medium and transfected with either pcDNA3 (control, black) or PS2-T122R (red) cDNA. After OCR baseline measurements, CTM (5 μM) was applied. On the left: OCR mean traces. Data were normalized for cells number and to controls baseline-OCR. On the right: histograms show OCR (R-R0) mean values, where R is the first OCR value after CTM addition (10 minutes treatment) and R0 is the last OCR value before CMT addition. N = number of wells, from 3 independent experiments (* $p < 0.05$; ** $p < 0.01$; *** $p < 0.001$). Data are presented as mean \pm SEM.

CMT could have several side effects in the cell; among them, it can depolarize mitochondria. We have showed that the CMT treatment applied (5 μM , 10 minutes) does not depolarized mitochondria but it detaches HK1 from mitochondria, reducing mitochondrial ATP production. The reduced ATP production observed, could, however, be due to the ATP synthase reverse activity that consumes ATP to maintain the mitochondrial membrane potential. To check this possibility, we measured again mitochondrial membrane potential by TMRM in cells treated or not with CMT blocking the ATP synthase activity with oligomycin, before drug addition (FIG 35E). By this experiment, we confirmed that 5 μM CMT for 10 minutes does not depolarized mitochondria and the mitochondrial membrane potential is not kept by the reverse activity of the ATP synthase. These data further suggest that the decreased mitochondrial ATP production observed in CMT-treated cells is likely due to HK1 detachment from mitochondria. To further check to what extent the reduction in OCR induced by PS2 expression (see above) was specifically due to HK1 detachment from mitochondria, we measured OCR in both control and PS2 expressing cells before and after CMT addition. Upon CMT-treatment, a higher decrease in OCR was observed in control cells compared to treated, FAD-PS2-expressing cells (FIG 35F), likely because, in the latter cell type, a substantial amount of HK1 is already detached from mitochondria due to FAD-PS2 expression.

The pharmacological approach described above suggests that HK1 detachment from mitochondria is likely involved in mitochondrial impairments caused by FAD-PS2 expression. To validate further these results a genetic approach was applied. A mouse hippocampal cell line (HT22 cells) was used to both downregulate (by siRNA) endogenous HK1 (mouse sequence) and overexpress siRNA-resistant HK1 constructs (rat or human sequence). Firstly, we confirmed, in these cells, the effect of FAD-PS2 expression on mitochondrial ATP production upon FCS stimulation (FIG 36A).

Figure 36

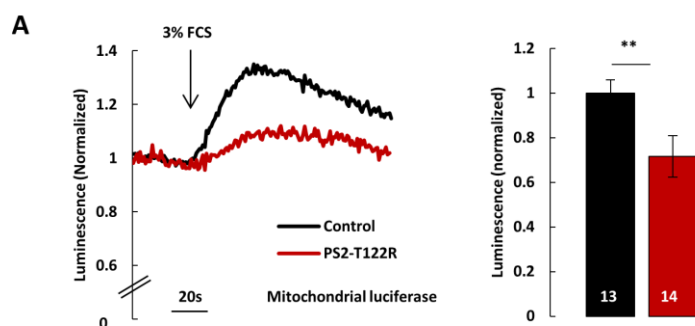


Figure 36. The FAD-PS2-T122R mutant decreases mitochondria ATP production in HT22 cells. **(A)** Mitochondrial ATP production was measured in HT22 cells grown in galactose medium and transfected with a mitochondrial matrix luciferase together with either pcDNA3 (controls, black) or PS2-T122R (red) cDNA. Glycolysis was inhibited by 5 mM 2-deoxyglucose and mitochondrial ATP production was stimulated by FCS-induced ER-mitochondria Ca^{2+} transfer. Luminescence values were normalized to baseline. Representative luminescence traces (left) and mean AUC values (right). N = number of coverslips (** $p < 0.01$). Data are presented as mean \pm SEM.

The downregulation of endogenous HK1 and the re-expression of a rat Full Length-HK1 (FL-HK1/FL-HK1-YFP, rat sequence, Scott J *et al.*, Plos One 2011) in these cells were checked by western blot (FIG 37A). In parallel, the subcellular distribution of the rat FL-HK1 was evaluated. The rat FL-HK1 was only partially resistant to siRNA-mediated downregulation of the mouse endogenous protein, as revealed by the faint band retrieved at the correct molecular weight (FIG 37A). Similarly, low expression levels of rat FL-HK1 were observed, in HT-22 cells in the same conditions, by confocal microscopy, with an almost complete localization of the protein on the OMM (FIG 37B). Mitochondrial ATP production was measured by mitochondrial luciferase upon FCS-induced ER to mitochondria Ca^{2+} transfer. We found that, in HK1 depleted cells, FCS-stimulated mitochondrial ATP production was strongly reduced. Importantly, the re-expression of rat FL-HK1 on HK1-silenced cells was able to completely rescue ATP production (FIG 37C).

To further evaluate whether the physical interaction of HK1 with mitochondria and/or its enzymatic activity is important to sustain mitochondrial functionality, the following experiments were performed. In HK1-silenced HT22 cells, a truncated version of human HK1 (Tr-HK1, Tr-HK1-GFP; Sun L *et al.*, Mol and Cell Biology 2008), that conserves the catalytic activity but lacks the mitochondrial binding domain, was expressed. In parallel, human FL-HK1 was also expressed, as control (FL-HK1/FL-HK1-GFP, human sequence, Sun L *et al.*, Mol and Cell Biology 2008). Both Tr-HK1 and FL-HK1 were fully resistant to siRNA-mediated protein downregulation (FIG 38A-B). Confocal microscopy evaluation of the subcellular distribution of

these two proteins revealed, as expected, a cytosolic distribution of the former (FIG 38C) and a mitochondrial localization of the latter (FIG 38D). When mitochondrial ATP production was measured, as described above, Tr-HK1 was not able to rescue the drop in ATP synthesis induced by endogenous HK1 downregulation (FIG 38E). Surprisingly, however, neither human FL-HK1 expression was able to do it (FIG 38F). These results suggest that likely subtle differences in the sequence of human and rat HK1 are important for the proper activity of these proteins in murine HT22 cells. Further experiments will be necessary to better investigate and clarify the experiments described above.

Overall, these data indicate that the dynamic interaction of HK1 with mitochondria, and possible additional partners, is likely important for the modulation of mitochondrial functionality.

Figure 37

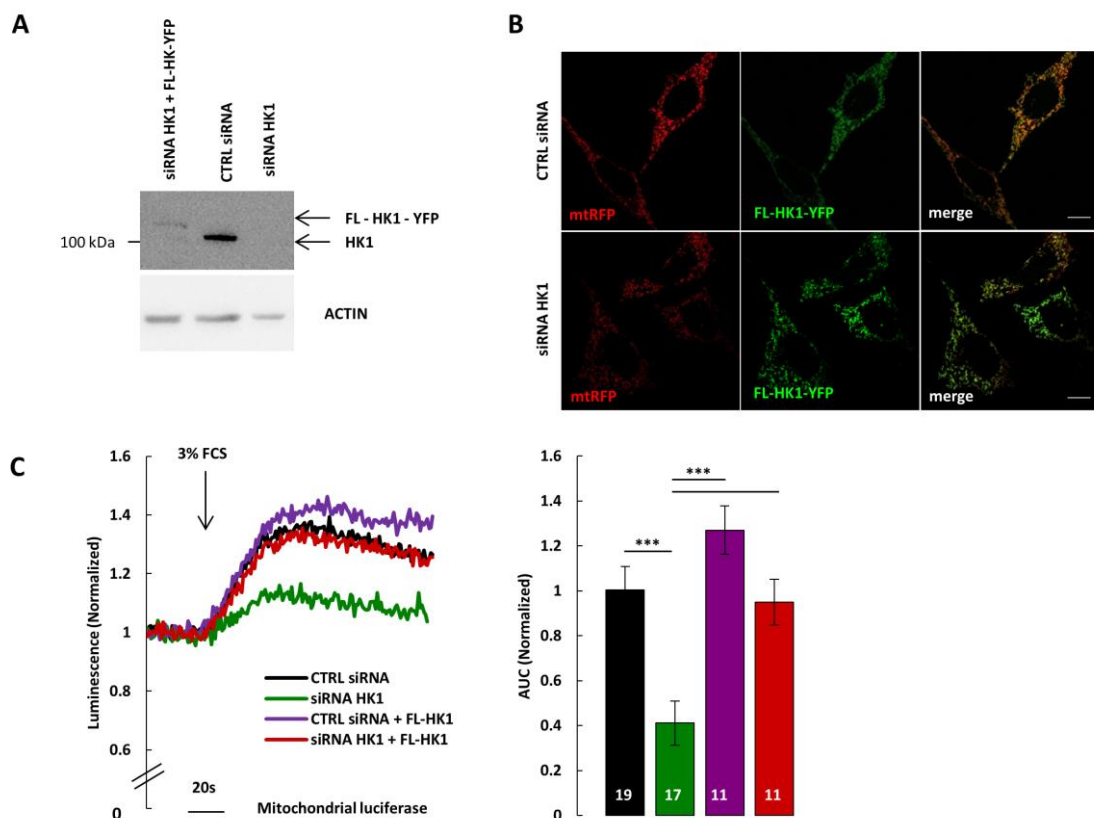


Figure 37 HK1 detachment from mitochondria, induced by FAD-PS2, causes mitochondrial ATP production defects. **(A)** HT22 cells, grown in galactose medium, were transfected with Full-Length (FL-HK1-YFP, rat sequence) and with either control- or HK1-specific siRNA. After 48h, total proteins were extracted and subjected to western blot with antibodies anti-HK1 and anti-actin. Representative western blot; **(B)** HT22 cells, grown in galactose medium, were transfected with a mtRFP together with Full-Length (FL-HK1-YFP, rat sequence) and with either control- or HK1-specific siRNA. Representative confocal images of mtRFP, HK1 and FL-HK1-YFP/mitochondria co-localization of control- or HK1-specific

siRNA HT22 cells are showed. Scale bar 10 μm . **(C)** Mitochondrial ATP production measured in HT22 cells transfected with a mitochondrial-luciferase together with either pcDNA3 or Full-Length HK1 (FL-HK1) cDNA and with either control- or HK1-specific siRNA. After 48h, mitochondrial ATP production was measured; glycolysis was blocked by 5mM 2-deoxyglucose and the mitochondrial ATP production was stimulated by ER-mitochondria Ca^{2+} transfer induced by FCS. Representative luminescence traces (left) and mean AUC value (right), normalized to controls. N = number of the coverslips (***) $p < 0.001$). Data are presented as mean \pm SEM.

Figure 38

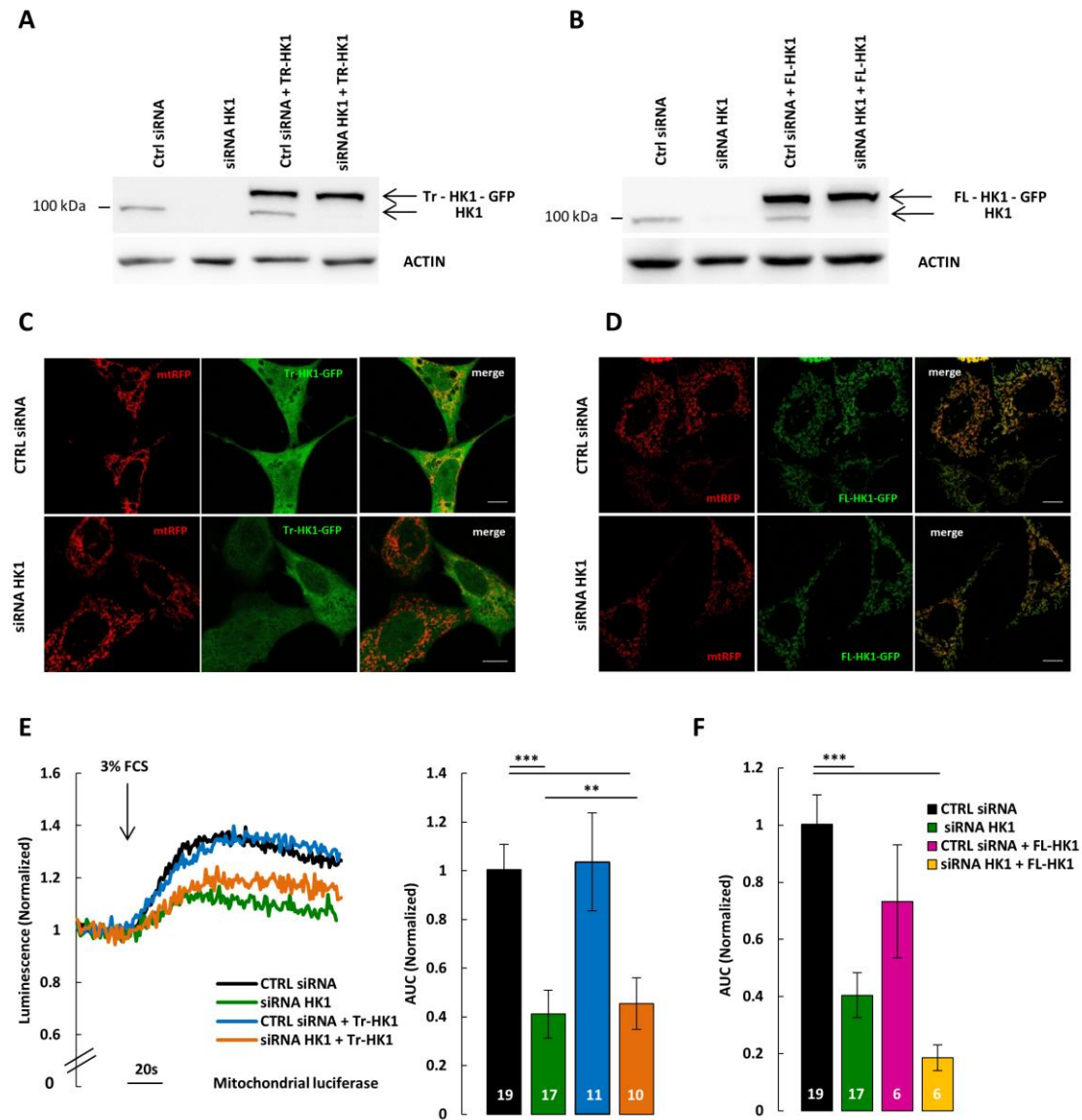


Figure 38 HK1 detachment from mitochondria is involved in the mitochondrial defect caused by FAD-PS2. **(A)** and **(B)** HT22 cells, grown in galactose medium, were transfected with either truncated-HK1 (Tr-HK1-GFP, human sequence) (A) or Full-Length-HK1 (FL-HK1-GFP, human sequence) (B) and with either control- or HK1-specific siRNA. After 48h, total proteins homogenate was extracted and subjected to western blot with antibodies anti-HK1 and anti-actin. Representative western blot; **(C)** and **(D)** HT22 cells, grown in galactose medium, were transfected with a mtRFP together with either truncated HK1 (Tr-HK1-GFP, human sequence) (C) or Full-Length-HK1 (FL-HK1-GFP, human sequence) (D) and with either control- or HK1-specific siRNA. Representative confocal images of mtRFP, HK1 and Tr-HK1-GFP-mitochondria (C) or FL-HK1-YFP-mitochondria (D) co-localization of control- or HK1-specific

siRNA HT22 cells are showed. Scale bar 10 μm . **(E)** and **(F)** Mitochondrial ATP production measured in HT22 cells transfected with a mitochondrial luciferase together with either pcDNA3 or Tr-HK1 (E) or FL-HK (F) and with either control- or HK1-specific siRNA. After 48h, mitochondrial ATP production was measured; glycolysis was blocked by 5 mM 2-deoxyglucose and mitochondrial ATP production was stimulated by ER-mitochondria Ca^{2+} transfer induced by FCS (3 %). Representative luminescence traces (E, left) and mean AUC value (E right and F), normalized to controls. N = number of coverslips (** $p < 0.01$; *** $p < 0.001$). Data are presented as mean \pm SEM.

7 The FAD-PS2-T122R mutant causes mitochondrial pyruvate import defect and cytosolic pyruvate accumulation

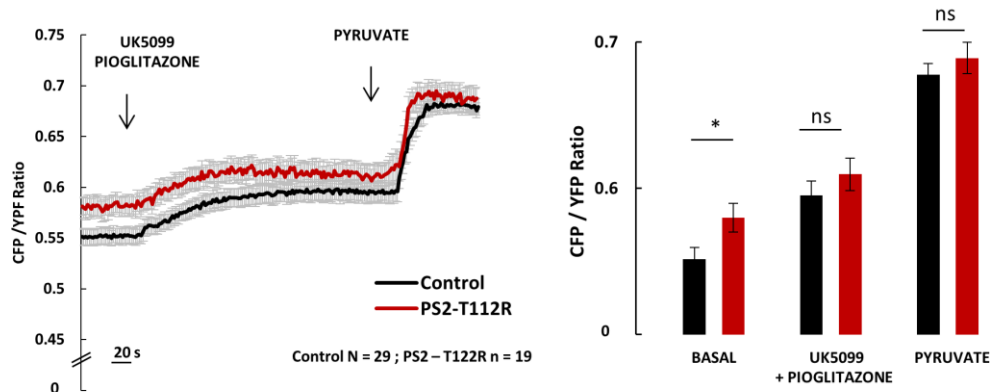
A reduction in the HK1-mitochondria interaction could result in a decrease in mitochondrial (via VDAC1) substrates and metabolites permeability. A substrate that is essential for the functionality of the TCA cycle is pyruvate, the last product of glycolysis that can be imported within mitochondria, fuelling the TCA cycle and thus the oxidative phosphorylation. In order to understand if HK1 detachment from mitochondria, induced by FAD-PS2, could impair mitochondrial substrates import, pyruvate accumulation in the cytosol was evaluated. Unfortunately, the direct measurement of mitochondrial matrix pyruvate levels was not possible, because the targeting of a previously described FRET-based pyruvate probe to the mitochondrial matrix resulted in severe mitochondrial toxicity and profound morphological alterations (not shown). We thus measured pyruvate accumulation in the cytosol, in order to verify, by an indirect approach, if FAD-PS2 expression impairs mitochondrial substrates import; indeed, a cytosolic accumulation of pyruvate can be linked to a defect in its import within mitochondria. Thus, we used a cytosolic FRET-based pyruvate probe, Pyronic (San Martin A *et al.*, Plos One 2013) to measure pyruvate levels: an increase in the cytosolic amount of the substrate was measured in FAD-PS2-expressing cells, compared to controls (FIG 39A). Interestingly, blocking the mitochondrial pyruvate carrier (MPC), the IMM-located protein responsible for the final step of mitochondrial pyruvate uptake, with two different drugs, UK5099 (Hildyard JC *et al.*, BBA 2004) and Pioglitazone (Divakaruni AS *et al.*, PNAS 2013), no more differences between FAD-PS2-expressing cells and controls were detected (FIG39A), suggesting that FAD-PS2 expression impairs mitochondrial pyruvate import. The expression levels of MPC was checked by western blot and no significative differences have been observed between control and PS2-T122R-expressing cells (FIG 39B), suggesting that, in these latter cells, the impairment in mitochondrial pyruvate import is likely upstream of MPC.

To evaluate the effect of the impaired mitochondrial pyruvate import on reduced OCR, we measured OCR in both control and FAD-PS2-expressing cells before and after MPC inhibition; a higher decrease in OCR was observed in control cells treated with the two MPC inhibitors,

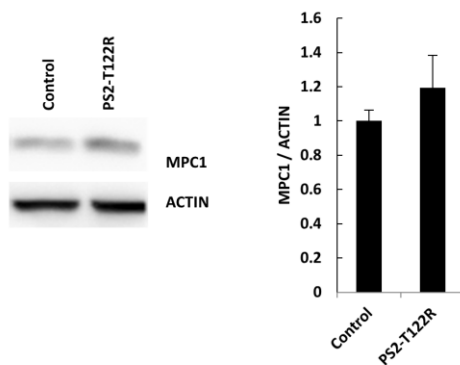
compared to treated FAD-PS2-expressing cells (FIG 39C). These results suggest that PS2 induces cytosolic pyruvate accumulation likely by triggering HK1 detachment from mitochondria, thus altering mitochondrial substrates permeability.

Figure 39

A Cytosolic pyruvate levels : FRET based pyruvate probe, Pyronic



B



C

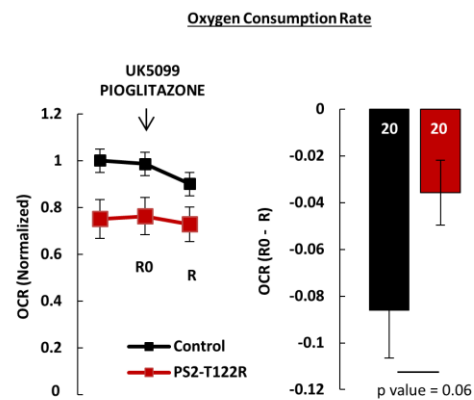


Figure 39. The FAD-PS2-T122R mutant increases cytosolic pyruvate levels. **(A)** Cytosolic pyruvate levels measured in SH-SY5Y cells grown in glucose medium and transfected with Pyronic together with either pcDNA3 (control, black) or PS2-T122R (red) cDNA. On the left: mean traces of the CFP/YFP ratio; where indicated UK5099 (4 μM), Pioglitazone (20 μM) and Pyruvate (1 mM) were applied. On the right: mean of 5 CFP/YFP ratio values before and upon UK5099+pioglitazone or pyruvate addition. N = number of cells. **(B)** and **(C)** SH-SY5Y cells grown in galactose medium and transfected with either pcDNA3 (control, black) or PS2-T122R (red) cDNA. **(B)** Western blot analysis. 24h after transfection, total proteins were extracted and subjected to western blot with antibodies anti-MPC1 and anti-actin. On the left: representative western blot; on the right: P-MPC1/actin quantification (normalized to control). N = number of independent experiments. **(C)** Oxygen Consumption Rate (OCR). After OCR baseline measurements, UK5099 (4 μM) and Pioglitazone (20 μM) were applied. On the left: OCR mean traces. Data were normalized for cells number and to controls baseline-OCR. On the right: histograms show OCR (R-R0) mean values, where R is the first OCR value after drugs addition (10 minutes treatment) and R0 is the last OCR value before drugs addition. N = number of wells, from 3 independent experiments. Data are presented as mean ± SEM (* p < 0.05).

Discussion

The development of AD is characterized by amyloid plaques deposition in the extracellular space and intracellular neurofibrillary tangles formation. However, it is well established that these are relatively late events in the advancement of the pathology. Indeed, cells from AD models show alterations in several processes; among them, dysregulated Ca^{2+} homeostasis (Ito E. *et al.*, PNAS 1994; Etcheberrigaray R. *et al.*, Neurobiol Dis 1998), lipids metabolism dysfunctions and impairments in mitochondrial functionalities, including reduced respiratory chain activity and ATP production and increased oxidative stress, have been reported to be early events in the progression of the disease (Du H *et al.*, PNAS 2010; Yao J *et al.*, PNAS 2009).

Mitochondria are essential organelles for brain healthy and functionality, especially for neurons. These cells need a high amount of energy to sustain their functions, in particular their synaptic activity and, differently from astrocytes that produce ATP mainly through glycolysis, they mainly rely on mitochondria metabolism to synthesize ATP. Alterations of several mitochondrial functions (such as dynamics, bioenergetics and movements) have been reported to be features of several neurodegenerative disorders, including AD. It is however unknown if these alterations represent a primary defect in the pathogenesis, or simply a consequence of causal upstream events, such as $\text{A}\beta$ plaques deposition or tau neurofibrillary tangles formation. On the same line, the impact of these mitochondrial defects on AD onset/progression is unclear.

Mitochondria are responsible to provide the amount of energy required for the neuronal activity. Under stress conditions, when neurons are highly activated, a large quantity of ATP is requested; if mitochondria are damaged, and thus not able to provide the amount of energy required by neurons, neuronal activities can be impaired, leading to damages accumulation and/or cell death, causing, over long term, neurodegeneration.

In our lab, we have recently demonstrated that PS2 expression, both wt but more efficiently FAD-PS2 mutants, reduces the ER Ca^{2+} content; moreover, PS2 increases ER-mitochondria physical and functional coupling, favouring the process of ER to mitochondria Ca^{2+} transfer. However, due to its effect on ER Ca^{2+} concentration, which results in a lower amount of available Ca^{2+} within the ER, overall its expression dampens mitochondrial Ca^{2+} rises upon cell stimulation (Zampese E *et al.*, PNAS 2011).

It is also well known the role of ER-mitochondria Ca^{2+} cross-talk in the modulation of several cell functions involved in cell survival and death. In particular, the amount of Ca^{2+} within

mitochondria, both at resting conditions and upon cell stimulation, plays a pivotal role in the regulation of mitochondrial metabolism, due to the high number of mitochondrial reactions, involved in energy production, regulated by Ca^{2+} (Jouaville LS *et al.*, PNAS 1999). In the study here described, I have evaluated how FAD-PS2 expression influences mitochondrial metabolism. In different cell models, FAD-PS2 expression damages mitochondrial functionality by impairing the capability of mitochondria to produce ATP. FAD-PS2 reduces mitochondrial ATP production and the respiratory chain activity through two main mechanisms: (1) it reduces the amount of Ca^{2+} available for mitochondrial uptake, thus negatively regulating Ca^{2+} -dependent mitochondrial metabolism; (2) it impairs substrates import by mitochondria, by likely affecting their permeability within mitochondria.

In particular, I have firstly showed that FAD-PS2 expression reduces total cellular ATP levels. To investigate how FAD-PS2 can affect mitochondrial metabolism, I have directly measured ATP produced by mitochondria upon Ca^{2+} stimulation. ER Ca^{2+} release, and the resulting mitochondrial Ca^{2+} uptake, that stimulates mitochondrial metabolism, was induced by either using a maximal IP3R stimulus, bradykinin, or fetal calf serum (FCS), as a more physiological IP3-mediated ER-mitochondria Ca^{2+} transfer stimulus (Cardenas C *et al.*, Cell 2010). The use of FCS as a stimulus, to promote ER-mitochondria Ca^{2+} transfer and to study mitochondrial metabolism, mimicking more physiological conditions, reveals that the ATP produced by mitochondria in cell expressing FAD-PS2 was lower. Similar results were obtained measuring ATP basal levels by a single cell approach (FRET-based ATP probe, ATeam 1.03), not only in two cell lines overexpressing FAD-PS2, but also in primary cortical neurons from PS2-N141I tg mice, compared to wt. The reduced ATP levels measured in cortical neurons from tg mice suggest a possible pathogenic mechanism in AD progression. Indeed, injured mitochondria, not able to supply the neurons energy demand, are potentially able to contribute to the final damage of neuronal cells, triggering their inability to properly respond to stress and stimuli. Considering the neurodegeneration observed in AD, these mitochondrial alterations may be causally linked and/or able to modulate the progression of the disease. Further investigations however will be necessary to address this point.

Because of the importance of healthy mitochondria to sustain neuronal functions, we decided to investigate how FAD-PS2 mutants induce the bioenergetics defects described in this thesis. I found that these defects are partially linked to the already described FAD-PS2-induced Ca^{2+} alterations (Zampese E *et al.*, PNAS 2011); however, additional mechanisms contribute to a

reduced ATP production. Indeed, modulating (*i.e.*, reducing), by different means, both ER Ca²⁺ content and mitochondria Ca²⁺ uptake in control cells, in order to mimic the defects on Ca²⁺ handling induced by FAD-PS2 expression, we observed, as expected, that mitochondrial ATP production was reduced; however, in FAD-PS2 expressing cells the defect was more pronounced. This suggests that, beyond Ca²⁺ dysregulation, FAD-PS2 negatively regulates the amount of ATP produced by mitochondria by an additional mechanism.

A reduced activity of the respiratory chain in cell expressing FAD-PS2 was also observed. However, no difference in the expression levels of the respiratory chain complexes and ATP synthase, between control and FAD-PS2 expressing cells, has been found. Moreover, published data (Kipanjula M *et al.*, Aging Cell 2012), recently confirmed in our lab by a different approach, demonstrated that there are no differences in the activity of the respiratory chain in brain-isolated mitochondria from WT and FAD-PS2N141I tg mice. Thus, these data suggest that the defects in mitochondrial functionality, observed in intact cells, are not due to an impaired mitochondrial activity *per se*, but likely link to the cellular environment. For instance, the reduced OCR could be, at least in part, due to a lower amount of Ca²⁺ entering mitochondria in FAD-PS2-expressing cells (see above), a feature that is lost in isolated mitochondria.

Essential for mitochondrial activity, however, is also the correct amount of substrates that cross both the OMM and the IMM, reaching the mitochondrial matrix and here sustaining mitochondrial metabolism. One of the substrates that plays a crucial role in the modulation of the TCA cycle is pyruvate, the final product of glycolysis; once produced in the cytosol, it crossed the OMM, probably through VDAC, and the IMM, thanks to the activity of the mitochondrial pyruvate carrier (MPC). Importantly, it has been recently showed that the complete KO of MPC is lethal and that MPC-KO MEF cells show impaired mitochondrial metabolism, displaying reduced basal and maximal OCR (Vanderperre B *et al.*, Plos Genet 2016; Divakaruni AS *et al.*, J Cell Biol 2017). Considering the role of pyruvate, as well as of other substrates, in mitochondrial metabolism, a defective substrates import could be an additional mechanism responsible for the impaired mitochondrial metabolism observed in FAD-PS2-expressing cells, beyond, or in addition to, Ca²⁺ homeostasis dysregulation. The co-localization between HK and mitochondria was thus evaluated because this latter enzyme, binding to OMM probably through VDAC, has been hypothesized to modulate mitochondrial substrates permeability (Robey RB and Hay N, Oncogene 2006). A reduction in HK-

mitochondria co-localization was found in SH-SY5Y cells expressing FAD-PS2, FAD-PS2 patients derived fibroblasts and cortical neurons from FAD-PS2N141I tg mice .

Interestingly, by reducing the HK binding to mitochondria, both pharmacologically and genetically, in order to mimic the FAD-PS2 effect, we observed similar mitochondrial metabolism defects in control and FAD-PS2 expressing cells. Thus, HK, and in particular its interaction with mitochondria, is essential to sustain mitochondrial activity, since preliminary results show that the down-regulation of endogenous HK protein induced a strong reduction in mitochondria ATP production; moreover, the re-expression of a Tr-HK, that conserves the enzymatic activity but lacks the capacity to interact with mitochondria, was not able to rescue the ATP production defect. The N-terminal part of HK seems to be essential for both the binding of the protein to mitochondria, as already demonstrated (Pastorino *et al.*, J Biol Chem 2002), and to sustain mitochondrial metabolism. A difference, however, is probably present in this domain between the rat and human form of FL-HK1. Indeed, while expression of the former was able to fully recover ATP production in murine cells knocked-down for endogenous HK, the expression of the latter was effectless. Further experiments will be necessary to better evaluate/explain this point.

In accordance with a role of FAD-PS2 in modulating cytosol-mitochondria metabolic communication, higher cytosolic levels of pyruvate were found in cells expressing FAD-PS2. Future experiments will be aimed at understanding the molecular mechanism through which FAD-PS2 induces the detachment of HK from mitochondria, thus negatively contributing to mitochondrial metabolism. Up to now, our data suggest two possible molecular mechanisms, still to investigate, that can mediate this HK-dependent effect: (1) PS2 is a TM protein mainly located in ER membranes, which presents a big loop that lies in the cytosol. Moreover, it has been showed that PS2 and VDAC-1 can directly interact (Wakabayashi T. *et al.*, Nature Cell Biology 2009). We can thus suppose that PS2, located in the ER, and particularly enriched at sites of contacts between ER and mitochondria, is able to bind VDAC, located in the OMM, and induce the detachment of HK from mitochondria, thus impairing mitochondrial metabolism. (2) The involvement of other proteins can be also considered; indeed, HK detachment from mitochondria can also occur upon VDAC phosphorylation. It is reported that an increase in GSK3 β phosphorylation can induce a cascade of signals ending on VDAC phosphorylation in its Threonine 51; this event leads to the detachment of HK from mitochondria. FAD-PS2 could modulate this signalling cascade, since GSK3 β phosphorylation has been reported to be enhanced by FAD-PS2 mutants (Leroy K *et al.*, Neuropath Appl Neurobiol 2007; Qin W *et al.*, Mol Psich 2006).

In conclusion, FAD-PS2 expression likely induces mitochondrial dysfunctions by two distinct mechanisms: (1) by altering (reducing) the amount of Ca^{2+} within the ER, and thus the amount of Ca^{2+} that can be taken up by mitochondria upon cell stimulation; (2) by favouring the detachment of HK from mitochondria, thus inhibiting substrates import and availability inside mitochondria.

In agreement with our results, recently, two different studies reported mitochondrial damage in AD models. Contino and coauthors showed that PSs ablated MEF cells present strongly damaged mitochondria with affected cristae structure, impaired respiratory chain activity and decreased NAD⁺/NADH ratio. The authors demonstrated that the observed defects were mainly due to a reduced expression level and activity of respiratory chain complexes (Contino S *et al.*, *Front Physiol* 2017). In parallel, the Area-Gomez's group described mitochondria defects in cells from FAD patients. They observed a reduction in the oxygen consumption rate due to a defect in the respiratory chain complexes activity. The authors suggested that the observed damage was due to an accumulation of the APP-derived C99 fragment, generated by β -secretase, in MAM. The presence of C99 in sites of contact between ER and mitochondria altered lipid metabolism increasing the production of ceramide that eventually accumulated in organelle membranes, and in particular in that of mitochondria, leading to respiratory chain defects (Pera M *et al.*, *EMBO J* 2017)

Alterations in mitochondrial metabolism have already been described in different AD models, but the molecular mechanisms responsible for these defects, as well as their link with the onset/progression of AD, are still debated. The effects here described are limited to the expression of FAD-PS2, while no significant impairment in the capacity of mitochondria to produce ATP was found in transiently FAD-PS1-expressing cells, though a tendency to a small reduction was observed.

In the present study, it has been shown that over-expression of WT PS2 mimics the effects of the FAD-PS2-T122R mutant on mitochondrial functionalities. Similar observations have been previously done by our group, showing that the over-expression of both FAD-PS2-T122R and WT PS2 similarly altered Ca^{2+} handling, reducing ER Ca^{2+} content and increasing ER-mitochondria tethering (Zatti G *et al.*, *Neurobiol Dis*, 2004; Zampese E. *et al.*, *PNAS* 2011). However, when the transient expression of the two forms of the protein (WT and FAD-mutant) was modulated by a tetracycline-inducible system (Giacomello M *et al.*, *Neurobiol. Dis.*, 2005), higher levels of WT PS2 were required to mimic the action of the FAD mutant form on Ca^{2+} handling, indicating a more potent action of the latter protein in Ca^{2+} signalling

pathways. Moreover, the effects of FAD-PS2 on Ca^{2+} handling, as well as those on mitochondrial functionality (here reported), have been observed not only in different cell lines, where PS2 was over-expressed, but also in primary cortical neurons from FAD-PS2-N141I tg mice, where the protein is expressed only two-fold compared to controls, and in FAD-PS2 patient-derived fibroblasts, which express normal level of the mutated protein (Zatti G *et al.*, *Neurobiol dis* 2004; Kipanjula M *et al.*, *Aging cell* 2012; Zampese E *et al.*, *PNAS* 2011). Altogether, these data indicate that FAD-PS2 is able to induce the described effects on mitochondria, independently from its expression level, and high levels of WT PS2 are able to mimic them. On this aspect, it has been observed that, in several sporadic AD forms, there are alterations in the expression level of REST (Repressor Element 1-Silencing Transcription factor) (Lu T *et al.*, *Nature* 2014). Interestingly, REST modulates the transcription of different genes, including PSEN2. REST has been proposed to be a neuroprotective modulator that represses genes involved in cell death and AD pathology; accordingly, high levels of REST are correlated to increase longevity and preservation of cognitive functions. In AD samples, a loss of nuclear REST, associated with changes in the expression of pathogenic genes, has been observed. Among them, an increase in PS2 expression has been detected (Lu T *et al.*, *Nature* 2014). Hence, an upregulation of PS2 transcript/protein could mimic the effect of the expression of a FAD-PS2 mutant in the sporadic forms of the disease.

To conclude, the data described in my thesis suggest that mitochondrial damage (defects in ATP production and in respiratory chain activity) is an early event in the FAD-PS2-linked AD pathology, directly caused by the expression of the mutated protein. The inability of mitochondria to produce the sufficient amount of energy to supply the neurons demand can impair their functionality, potentially leading to neuronal death and thus contributing to the neurodegeneration responsible for cognitive and memorial impairments typical of AD.

We did not observe appreciable mitochondrial impairments upon acute FAD-PS1 expression, suggesting a distinct functionality of PS1 and PS2. However, in the literature, similar mitochondrial defects have been reported in different FAD-models and also in sporadic AD cases (Yao J *et al.*, *PNAS* 2009; Du H *et al.*, *PNAS* 2010), suggesting the intriguing possibility that, over time, different pathological mechanisms may converge on the same mitochondrial pathway. For instance, while we here showed that FAD-PS2 expression directly (or more quickly) impinge on mitochondrial functionality, it is tempting to speculate that a slower, chronic $\text{A}\beta$ -oligomers accumulation (such as that induced by FAD-PS1 or FAD-APP expression, but also observed in sporadic AD) may trigger, over longer periods, the same defects. Clearly,

the mechanisms responsible for this convergence need to be investigated, but, as an example, the recent finding that A β is generated at MAM (Area-Gomez E *et al.*, Am J Pathol 2009; Pavlov PF *et al.*, J Cell Mol Med 2009), a subcellular domain critically involved in the fine tuning of mitochondrial activity, appears appealing on this regard.

The understanding of the molecular mechanisms through which these mitochondrial defects could modulate the onset/progression of the pathology is extremely urgent. The exact comprehension of the cascade of events that drives AD progression, and in particular the events that occur during the early phases, such as Ca²⁺ dysregulation and mitochondrial impairment, is crucial for developing effective new therapeutic strategies. The mitochondrial damage, described by us in this work, but also by others in different AD models, is an early event in AD. Thus, its recovering, as well as neuronal bioenergetics restoration, appears a potentially promising target for developing an early pharmacological intervention, capable to prevent or slow down AD neurodegeneration.

Materials and methods

Cell Culture and Transfection

Human fibroblasts (from Coriell Institute for medical research: FAD-PS2-N141I (AG09908); control fibroblasts (AG08525, AG08269, AG09173) were grown in DMEM (DMEM 5671, Sigma) containing 15% FCS, supplemented with L-glutamine (2mM), penicillin (100 U/ml) and streptomycin (100µg/ml), in a humidified atmosphere containing 5% CO₂.

Glucose medium: DMEM (DMEM 5671, Sigma), supplemented with 10% FCS, L-glutamine (2 mM), penicillin (100 µg /ml) and streptomycin (100 µg/ml).

Galactose medium: DMEM no glucose (Gibco, 11966025), supplemented with 10mM galactose, 5% FCS, L-glutamine (2 mM), penicillin (100 U/ml) and streptomycin (100 µg/ml).

SH-SY5Y, HT22 and MEFs cells were grown in glucose medium, in a humidified atmosphere containing 5% CO₂. Cells were seeded onto glass coverslips (13, 18 or 24-mm diameter) in glucose or galactose medium.

The transfection was performed at 60% confluence using Lipofectamine™ 2000 Transfection Reagent (Life Technologies). Cells were transfected with 1.5 µg of DNA (0.5 µg of either Aequorin or Pyronin or ATeam1.03 probes together with 1 µg of either pcDNA3 or PSs or HK1 codifying cDNAs). Aequorin and FRET measurements were usually performed 24 or 48 h after transfection.

siRNAs (mouse HK1,SASI_Mm01_00022875; Universal Negative Control, siC-001; Sigma Aldrich) were added to the transfection mixes to a final concentration of 50 nM.

Animals

The transgenic mouse lines PS2.30H (TG) were kindly provided by Dr. L. Ozmen (F. Hoffmann-La Roche Ltd, Basel, Switzerland) (Ozmen, *et al.* 2009; Rhein, *et al.* 2009; Richards, *et al.* 2003). The line has the background strain of C57BL/6 mice, which was used as Wild-Type controls and acquired from Charles River (Lecco, Italy). All procedures were carried out in strict adherence to the Italian regulations on animal protection and care with the explicit approval of the local veterinary authority (CEASA Nr 56880).

Mouse line features:

(1) The PS2.30H is a homozygous single transgenic line expressing the FAD-linked mutant human PS2-N141I under the mouse prion protein promoter. These mice display 2-3-fold increase of PS2 levels, both in cortices and hippocampi, compared to WT.

(2) The C57BL/6J WT mice share > 90% genetic background of the other line.

Primary neuronal cultures

Primary neuronal cultures were obtained from cortices, dissected from 0 to 1 day new-born mice as previously described (Kipanyula *et al.*, Aging Cell 2012a). Cells were seeded on poly-L-lysine (100 µg/mL) coated coverslips (3x10⁵ cells/well, for co-localization experiments; or 8x10⁵ cells/well for FRET experiments) in MEM (Gibco, 32360026) containing glucose (20 mM), L-glutamine (0.5 mM), B27 supplement (0.5%), N2 supplement (1%), pyruvic acid (1mM), biotin (3.6µM), penicillin (25 µg/mL), streptomycin (25 µg/mL), neomycin (50 µg/mL) and horse serum (10%). 24 h after plating, the complete MEM was replaced with serum- and antibiotic-free Neurobasal (Gibco, 10888022) medium containing B27 (2%) and L-glutamine (2 mM) or with BME (Gibco, 41010026) supplemented with B27 (2%), L-glutamine (2 mM) and Sodium Pyruvate (0,23 mM). Fresh medium was added (1/5 of total volume) every 4 days.

Co-localization experiments were performed between 10-12 days in vitro (DIV); for FRET ATP measurements, the neurons were transfected at 5-6 DIV with 1.2 µg of DNA (0.6 µg H2B ATeam1.03 + 0.6 µg 4mtATeam1.03) and the experiments were performed 24h after transfection.

Total cellular ATP measurements

SH-SY5Y cells (2x10⁵ cells/well) were seeded in 6 well plate in glucose or galactose medium (see Cell culture and transfection); after 24 h the cells were transfected with either pcDNA3 or PS2-T122R codifying cDNAs. 24 hours later the cells were washed once with PBS and detached using trypsin; cells (1.5x10⁴ cells/well) were re-seeded in a 96-well plate in 100µl of glucose- or galactose-containing fresh medium. 5h later, total ATP content in each well was measured with the luciferin/luciferase assay ATPlite 1 step (PerkinElmer), following the manufacturer's instructions. Luminescence was measured through a Fluoroskan Ascent FL Microplate Fluorometer and Luminometer (Thermo Scientific).

Aequorin Ca²⁺ Measurements

SH-SY5Y cells (0.5×10^5 cells/well) were plated on coverslips (13 mm diameter) in galactose medium (see Cell culture and transfection); after 24h, cells were transfected with either cytosolic or mitochondrial Aequorin (either wt for experiments performed with FCS-stimulation or mutated for BK-stimulation) together with either pcDNA3 or PS2-T122R codifying DNAs; they were used for Ca^{2+} measurements the day after transfection. Cells were incubated at 37°C with coelenterazine (5 μM) for 1 h in the grown medium and then transferred to the perfusion chamber. All the luminescence measurements were performed in a modified Krebs–Ringer buffer (mKRB, in mM: 135 NaCl, 5 KCl, 0.4 KH_2PO_4 , 1 MgCl_2 , 1 CaCl_2 , 20 HEPES, pH 7.4 at 37°C).

After aequorin reconstitution, cells were transferred to the perfusion chamber and perfused with different buffers (in the order and for the time indicated) depending on the different protocols.

To evaluate cytosolic Ca^{2+} rise and mitochondrial Ca^{2+} uptake in parallel to ATP measurements performed with luciferase, the cells were perfused with the following saline: (1) mKRB (30s); (2) mKRB supplemented with 0.1mM pyruvate and 1mM lactate (1.5 min); (3) mKRB supplemented with 0.1mM pyruvate, 1mM lactate and 3%FCS (Fetal Calf Serum) or Bradykinin (100nM) to stimulate the ER Ca^{2+} release.

To partially deplete the ER Ca^{2+} content, the following depleting protocol was applied: (1) mKRB (30s); (2) Ca^{2+} - free mKRB containing 500 μM EGTA, 0.1mM pyruvate and 1mM lactate (30 s); (3) Ca^{2+} - free mKRB containing 500 μM EGTA, 0.1mM pyruvate, 1mM lactate and a SERCA pump inhibitor (CPA, cyclopiazonic acid; 15-20 μM , 4 min); (4) Ca^{2+} - free mKRB containing 500 μM EGTA, 0.1mM pyruvate and 1mM lactate (100 s); (5) mKRB supplemented with 0.1 mM pyruvate, 1mM lactate and 3%FCS .

All the experiments ended permeabilizing cells with digitonin (100 μM) in a hypotonic Ca^{2+} -rich solution (10 mM CaCl_2 in H_2O) to discharge the remaining unused aequorin pool. The light signal was collected and analyzed as previously described (Brini M. *et al.*, 1995).

Luciferase ATP Measurements

SH-SY5Y cells (0.5×10^5 cells/well) were plated on coverslips (13 mm diameter) in galactose medium (see Cell culture and transfection); after 24 h cells were transfected with cytosolic or

mitochondrial Luciferase together with either pcDNA3 or indicated codifying DNAs and used for ATP measurements the day after transfection.

HT22 cells (0.5×10^5 cells/well) were plated on coverslips (13 mm diameter) in glucose medium (see Cell culture and transfection); after 24 h, before the transfection, the glucose medium was replaced with fresh galactose medium. Cells were transfected with a mitochondrial Luciferase together with either pcDNA3 or Truncated HK1 or Full-length HK1 and with either control-siRNA or a HK1-specific siRNA; cells were then used for ATP measurements 48 h after transfection.

All the luminescence measurements were performed in a mKRB (see above the *Aequorin Ca²⁺ measurements* paragraph).

Cells were transferred to the perfusion chamber and perfused with different buffers (in the order and for the time indicated) depending on the different protocols.

To measure the mitochondrial ATP production upon ER-mitochondrial Ca²⁺ transfer stimulation, the following protocol has been used: (1) mKRB containing 5mM D-deoxy-glucose, in order to block glycolysis (30s); (2) mKRB supplemented with 5mM D-deoxy-glucose; 0.1mM pyruvate, 1mM lactate, 0.1mM glucose and 15 μ M luciferin (1.5 min); (3) mKRB supplemented with 5mM D-deoxy-glucose, 0.1mM pyruvate, 1mM lactate, 15 μ M luciferin and 3% FCS, as Ca²⁺ transfer stimulus.

To measure the cytosolic ATP produced through the glycolysis the following protocol has been applied: cells were first incubated in mKRB containing 2 μ M oligomycin (2 minutes), to block the ATP synthase; then the cells were moved to the perfusion chamber and perfused with the following buffers: (1) mKRB (30s); (2) mKRB supplemented with 15 μ M luciferin (1.5 min); (3) mKRB supplemented with 15 μ M luciferin and 15mM glucose as glycolysis stimulus.

To measure the mitochondrial ATP production upon partially depletion of the ER Ca²⁺ content, the following depleting protocol was applied: (1) mKRB supplemented with 5mM D-deoxy-glucose (30s); (2) free Ca²⁺ - mKRB containing 500 μ M EGTA, 5mM D-deoxy-glucose, 0.1mM pyruvate, 1mM lactate, 15 μ M luciferin (30 s); (3) free Ca²⁺ - mKRB containing 500 μ M EGTA, 5mM D-deoxy-glucose, 0.1mM pyruvate, 1mM lactate, 15 μ M luciferin and a SERCA pump inhibitor (CPA, cyclopiazonic acid; 15-20 μ M, 4 min); (4) free Ca²⁺ - mKRB containing 500 μ M

EGTA, 5mM D-deoxy-glucose, 0.1mM pyruvate and 1mM lactate, 15 μ M luciferin (100s); (5)) free Ca^{2+} - mKRB containing 500 μ M EGTA, 5mM D-deoxy-glucose, 0.1mM pyruvate and 1mM lactate, 15 μ M luciferin and 3% FCS.

Off-line analysis was performed normalizing the luminescence values of the traces on the average of the 25 frames before the stimulus; then the Area Under the Curve (AUC) was analysed using Origin 7.5 SR5 (OriginLab Corporation).

FRET experiments

Cells or neurons expressing FRET probes were studied using a DM6000 inverted microscope (Leica, Wetzlar, Germany) and a 40X oil objective (HCX Plan Apo, NA 1.25) was used. Excitation light produced by a 410nm LED (Led Engin #LZ1-00UA00 LED) was filtered at the appropriate wavelength (425 nm) through a band pass filter, and the emitted light was collected through a beam splitter (OES s.r.l., Padua, Italy) (emission filters HQ 480/40M (for CFP) and HQ 535/30M (for YFP); dichroic mirror 515 DCXR). The beam splitter permits the collection of the two emitted wavelengths at the same time, thus preventing artefact due to movement of the organelles. All filters and dichroics were from Chroma Technologies (Bellow Falls, VT, USA). Images were acquired using an IM 1.4C cool camera (Jenoptik Optical Systems) attached to a 12-bit frame grabber. Synchronization of the excitation source and the cool camera was performed through a control unit run by a custom-made software package, Roboscope (developed by Catalin Dacian Ciubotaru at VIMM, Padua, Italy).

Exposure time was 200ms. Images were acquired every 5 seconds for ATeam1.03 probes or 2 seconds for Pyronic probe. During the experiment, cells were mounted into an open-topped chamber and maintained in the proper medium.

Basal ATP levels measurements with FRET-based ATP probe (ATeam1.03, Imamura *et al* PNAS 2009): SH-SY5Y or MEFs cells (8×10^5 cells/well) were seeded on 18mm coverslips in galactose medium (see Cell culture and transfection) and after 24h they were transfected with either pcDNA3 or PS2-T122R together with both H2B ATeam1.03 (nuclear) and 4mt ATeam1.03 (mitochondrial) codifying DNAs.

The experiments were performed in Krebs-Ringer Buffer, mKRB; in mM: 135 NaCl, 5 KCl, 0.4 KH_2PO_4 , 1 MgCl_2 , 1 CaCl_2 , 20 HEPES, 10mM galactose pH 7.4 at RT.

Primary cortical neurons were grown in BME supplemented with B27 (2%), L-glutamine (2 mM) and Sodium Pyruvate (0.23 mM). At 5-6 DIV neurons were transfected with both

H2BATEam1.03 (nuclear) and 4mtATEam1.03 (mitochondrial) probes and the day after transfection ATP measurements were performed. Experiments were carried out in mKRB, in mM: 140 NaCl, 2.8 KCl, 2 MgCl₂, 10 Hepes and 1 Sodium Pyruvate. After 17 frames of recording, EGTA (50 μM) and Gramicidin (0.3μM) were added and the YFP/CFP ratio was monitored for 250 frames.

Basal cytosolic pyruvate levels measurements with FRET-based pyruvate probe (Pyronic, San Martin *et al.* Plos One 2013): SH-SY5Y (8x10⁴ cells/well) were seeded on 18mm coverslips in glucose medium (see Cell culture and transfection) and after 24h they were transfected with either pcDNA3 or PS2-T122R together with Pyronic codifying DNAs.

The experiments were performed in Krebs-Ringer Buffer, mKRB, in mM: 135 NaCl, 5 KCl, 0.4 KH₂PO₄, 1 MgCl₂, 1 CaCl₂, 20 HEPES, 10 glucose pH 7.4 at RT. After basal pyruvate measurements (60 seconds), UK5099 (4μM) and pioglitazone (20μM), two blockers of the mitochondrial pyruvate carrier, were added; at the end of the experiment 1mM pyruvate was applied.

Off-line analysis of FRET experiments was performed with ImageJ (Wayne Rasband, Bethesda, USA). YFP and CFP images were subtracted of background signals and distinctly analysed after selecting proper regions of interest (ROIs) on each cell; subsequently, a ratio between YFP and CFP emissions was calculated ($R = F530/F480$). Data are presented as YFP/CFP ratio or as a $\Delta R/R_0$ values (where ΔR is the change of the YFP/CFP emission intensity ratio at any time, R_0 is the average of values (10 frames) before drug addition).

Preparation of protein extracts and Western Blot analysis

SH-SY5Y cells (2.5x10⁵) were seeded in glucose or galactose medium (see Cell culture and transfection); after 24 h the cells were transfected with pcDNA3 or PS2-T122R codifying cDNAs. 24 h after transfection the cells were collected.

HT22 cells (2.5x10⁵) were seeded in glucose medium (see Cell culture and transfection); after 24 h, before the transfection, the glucose medium was replaced with fresh galactose medium. Cells were transfected with either pcDNA3 or Truncated HK1 or Full-length HK1 and with either control-siRNA or a HK1 specific siRNA. 48 h after transfection the cells were collected.

Briefly, the medium was removed and the cells were washed once with PBS1x; the cells were then collected, using a cells scraper, in RIPA buffer (50 mM Tris, 150 mM NaCl, 1% Triton X-100, 0.5% deoxycholic acid, 0,1% SDS, protease inhibitor cocktail, phosphatase inhibitors, pH

7.5) and incubated on ice for 30 min. The not solubilized material was spun down at 13000 x g for 15 min at 4°C. The supernatant was collected and the proteins concentration was measured by BCA assay kit (EuroClone). 50 µg of proteins were loaded onto polyacrylamide gels (8-12-15%) and immunoblotted.

Western blot analysis was carried out with: α-PS2 C-term (1987-1 Epitomics); α-actin (A4700; Sigma-Aldrich); α-AMPK (Cell Signalling, 2532S); α-Phospho - AMPK (Thr172, Cell Signalling, 2531S); α-HK1 (Thermo Scientific Pierce, #MA5-14789); α-OXPHOS MitoProfile (MitoSciences); α-MPC1 (Sigma, HPA045119); α-tubulin (Santa Cruz Biotech, sc-53646).

The proteins were visualized by the chemiluminescent reagent ECL (Amersham, GEHealthcare, U.K. Ltd) or LiteAbloT TURBO (EuroClone) on an Uvitec Mini HD9 (Eppendorf) apparatus. The intensity of the bands was analysed using ImageJ software program.

Oxygen Consumption measurements

SH-SY5Y cells (1×10^4 cells/well) were seeded in 250 µl of galactose medium (see Cell culture and transfection) in XF24 cell culture microplates (Seahorse Bioscience) and transfected after 24 h with either pcDNA3 or indicated codifying DNAs. 24 h after transfection, the medium was replaced with 670 µl of mKRB. Cells were incubated at 37 °C for 30 min, and then oxygen consumption rate (OCR) was measured with an XF24 Extracellular Flux Analyzer (Seahorse Bioscience). After OCR baseline measurement, either oligomycin-A (1 µg/ml) or carbonyl cyanide-4-(trifluoromethoxy) phenylhydrazone (FCCP, 0.5 µM) or Pioglitazone (20 µM) and UK5099 (4µM) or Clotrimazole (5 µM) were added. The minimum OCR was measured applying rotenone (1 µM) and antimycin A (1 µM). After the experiments, cells were counted and data were normalized for cells number and further normalized to controls baseline-OCR.

Extracellular acidification measurements

SH-SY5Y cells (1×10^4 cells/well) were seeded in 250 µl of glucose medium (see Cell culture and transfection) in XF24 cell culture microplates (Seahorse Bioscience) and transfected after 24 h with either pcDNA3 or PS2-T122R. 24 h after transfection, the medium was replaced with 670 µl of mKRB, in mM: 135 NaCl, 5 KCl, 0.4 KH₂PO₄, 1 MgCl₂, 1 CaCl₂, 20 HEPES, 2 glucose pH 7.4 at 37 °C. Cells were incubated at 37 °C for 30 min, and then extracellular acidification (ECAR) was measured with an XF24 Extracellular Flux Analyser (Seahorse Bioscience). After ECAR baseline measurement, glucose (8 mM), oligomycin (1 µg/ml) and 2-deoxy-glucose (20 mM)

were added in the described order. After the experiments, cells were counted and data were normalized for cells number and further normalized to controls baseline-ECAR.

Mitochondrial Transmembrane Potential Measurements

Mitochondrial membrane potential ($\Delta\Psi$) was detected by tetramethyl rhodamine methyl ester (TMRM) fluorescent dye. SH-SY5Y (2×10^5 cells/well) were seeded on 24mm coverslips in galactose medium (see Cell culture and transfection); after 24 h the cells were loaded for 45 min at RT with 10 nM TMRM, in mKRB in mM: 135 NaCl, 5 KCl, 0.4 KH₂PO₄, 1 MgCl₂, 1 CaCl₂, 20 HEPES, 10 galactose pH 7.4 at RT. TMRM fluorescence was recorded using an inverted microscope (Zeiss Axiovert 100) with a 40X oil objective (Fluar, NA 1.30). Excitation light at 540 ± 7.5 nm was produced by a monochromator (polychrome V; TILL Photonics) and passed through a Zeiss TRITC filter (Emission 573-613 nm) and a dichroic mirror (565 DCXR). Images were acquired by a cooled CCD camera (SensicamQE PCO). Filters and dichroics were from Chroma Technologies. Images were acquired every 60 s. Where indicated, oligomycin-A (1 μ M), clotrimazole (5 μ M) and FCCP (10 μ M) was added. Images were exported as TIFF, background subtracted and analysed with ImageJ.

Immunofluorescence (IF) and confocal analysis

SH-SY5Y cells (2.5×10^4 cells/well) were seeded on 13mm coverslip in glucose or galactose medium (see Cell culture and transfection); 24h h later cells were transfected with a mitochondrial -RFP together with either pcDNA3 or PS2-T122R encoding DNAs. Primary cortical neurons (3×10^5 cells /well) were seeded on 13 mm coverslips and grown in neurobasal medium; Fibroblasts from patients were seeded on 13mm coverslip in DMEM (see Cell culture and transfection).

SH-SY5Y cells (24 h after transfection), cortical neurons (at 11-12 DIV) and fibroblasts (24h after seeding), were first washed once with PBS and then fixed in 4% PFA. After 15 minutes in PFA, cells were washed three times (5 minutes each) in PBS and then quenched 20 minutes with NH₄Cl (50 mM in PBS). Cells were then permeabilized for 3 min with 0.1% Triton X-100 in PBS and blocked with a PBS solution containing 2% BSA, 10% goat serum and 0.2% gelatin for 30 min.

Cells were incubated with primary antibodies diluted in blocking solution (dilution 1:200 for HK1 Thermo Scientific Pierce MA5-14789, 1:200 Cytocrome C Cell Signaling #12963S) for 1h30' at RT and washed three times (5 minutes each) with the blocking solution.

Cells were then incubated for 45 min at RT with AlexaFluor488/555-conjugated secondary antibodies (Life Technologies; 1:300 dilution in blocking solution). Coverslips were washed three times (5 minutes each) with the blocking solution and then with PBS (10 minutes); they were in the end mounted with Mowiol.

Endogenous HK1 – mitochondria colocalization was analyzed in SH-SY5Y cells, cortical neurons and fibroblasts at a Leica SP5 confocal system (DM IRE2) using the WLL white laser line. For co-localization analysis, red and green channel images were acquired independently, and photomultiplier gain for each channel was adjusted and maintained among different experiments to minimize background noise and saturated pixels. Once acquired, images were not modified anymore. Analysis was performed using ImageJ plugins. In details, a background ROI was selected and the corresponding backgrounds were subtracted. Then, ROIs were designed following the cells profiles, as defined by the external perimeter of the investigated marker (HK) and applied as such to the mitochondrial channel. The overlap Manders' R and Pearson's coefficients were calculated applying the ImageJ co-localization analysis plug-in.

Materials

Most of the materials were purchased from Sigma-Aldrich.

All other materials were analytical or of the highest available grade.

Statistical analysis

All data are representative of at least three different experiments. Data were analysed using Origin 7.5 SR5 (OriginLab Corporation) and ImageJ (National Institutes of Health,).

Unless otherwise stated, numerical values presented throughout the text refer to mean \pm SEM (n=number of independent experiments or cells; * = $p < 0.05$, ** = $p < 0.01$, *** = $p < 0.001$, unpaired Wilcoxon-Mann-Whitney Test).

References

- Abu-Hamad, S., Sivan, S., and Shoshan-Barmatz, V. (2006). The expression level of the voltage-dependent anion channel controls life and death of the cell. *Proc. Natl. Acad. Sci. U. S. A.* *103*, 5787-5792.
- Abu-Hamad, S., Zaid, H., Israelson, A., Nahon, E., and Shoshan-Barmatz, V. (2008). Hexokinase-I protection against apoptotic cell death is mediated via interaction with the voltage-dependent anion channel-1: mapping the site of binding. *J. Biol. Chem.* *283*, 13482-13490.
- Amigo, I., Traba, J., Gonzalez-Barroso, M.M., Rueda, C.B., Fernandez, M., Rial, E., Sanchez, A., Satrustegui, J., and Del Arco, A. (2013). Glucagon regulation of oxidative phosphorylation requires an increase in matrix adenine nucleotide content through Ca²⁺ activation of the mitochondrial ATP-Mg/Pi carrier SCA₃. *J. Biol. Chem.* *288*, 7791-7802.
- Amoedo, N.D., Punzi, G., Obre, E., Lacombe, D., De Grassi, A., Pierri, C.L., and Rossignol, R. (2016). AGC1/2, the mitochondrial aspartate-glutamate carriers. *Biochim. Biophys. Acta* *1863*, 2394-2412.
- Anflous-Pharayra, K., Lee, N., Armstrong, D.L., and Craigen, W.J. (2011). VDAC3 has differing mitochondrial functions in two types of striated muscles. *Biochim. Biophys. Acta* *1807*, 150-156.
- Anunciado-Koza, R.P., Zhang, J., Ukropec, J., Bajpeyi, S., Koza, R.A., Rogers, R.C., Cefalu, W.T., Mynatt, R.L., and Kozak, L.P. (2011). Inactivation of the mitochondrial carrier SLC25A25 (ATP-Mg²⁺/Pi transporter) reduces physical endurance and metabolic efficiency in mice. *J. Biol. Chem.* *286*, 11659-11671.
- Area-Gomez, E., de Groof, A.J., Boldogh, I., Bird, T.D., Gibson, G.E., Koehler, C.M., Yu, W.H., Duff, K.E., Yaffe, M.P., Pon, L.A., and Schon, E.A. (2009). Presenilins are enriched in endoplasmic reticulum membranes associated with mitochondria. *Am. J. Pathol.* *175*, 1810-1816.
- Area-Gomez, E., Del Carmen Lara Castillo, M., Tambini, M.D., Guardia-Laguarta, C., de Groof, A.J., Madra, M., Ikenouchi, J., Umeda, M., Bird, T.D., Sturley, S.L., and Schon, E.A. (2012). Upregulated function of mitochondria-associated ER membranes in Alzheimer disease. *Embo j.* *31*, 4106-4123.
- Arzoine, L., Zilberberg, N., Ben-Romano, R., and Shoshan-Barmatz, V. (2009). Voltage-dependent anion channel 1-based peptides interact with hexokinase to prevent its anti-apoptotic activity. *J. Biol. Chem.* *284*, 3946-3955.
- Baughman, J.M., Perocchi, F., Girgis, H.S., Plovanich, M., Belcher-Timme, C.A., Sancak, Y., Bao, X.R., Strittmatter, L., Goldberger, O., Bogorad, R.L., Koteliansky, V., and Mootha, V.K. (2011). Integrative genomics identifies MCU as an essential component of the mitochondrial calcium uniporter. *Nature* *476*, 341-345.
- Belanger, M., Allaman, I., and Magistretti, P.J. (2011). Brain energy metabolism: focus on astrocyte-neuron metabolic cooperation. *Cell. Metab.* *14*, 724-738.

- Berg, J., Tymoczko, J., and Stryer L. (2002). *Biochemistry* Berg JM, Tymoczko JL, Stryer L.).
- Berman, D.E., Dall'Armi, C., Voronov, S.V., McIntire, L.B., Zhang, H., Moore, A.Z., Staniszewski, A., Arancio, O., Kim, T.W., and Di Paolo, G. (2008). Oligomeric amyloid-beta peptide disrupts phosphatidylinositol-4,5-bisphosphate metabolism. *Nat. Neurosci.* *11*, 547-554.
- Bernardi, P. (1999). Mitochondrial transport of cations: channels, exchangers, and permeability transition. *Physiol. Rev.* *79*, 1127-1155.
- Berridge, M.J. (2012). Calcium signalling remodelling and disease. *Biochem. Soc. Trans.* *40*, 297-309.
- Berridge, M.J., Bootman, M.D., and Roderick, H.L. (2003). Calcium signalling: dynamics, homeostasis and remodelling. *Nat. Rev. Mol. Cell Biol.* *4*, 517-529.
- Bojarski, L., Pomorski, P., Szybinska, A., Drab, M., Skibinska-Kijek, A., Gruszczynska-Biegala, J., and Kuznicki, J. (2009). Presenilin-dependent expression of STIM proteins and dysregulation of capacitative Ca²⁺ entry in familial Alzheimer's disease. *Biochim. Biophys. Acta* *1793*, 1050-1057.
- Bolanos, J.P., Almeida, A., and Moncada, S. (2010). Glycolysis: a bioenergetic or a survival pathway? *Trends Biochem. Sci.* *35*, 145-149.
- Bondarenko, A.I., Jean-Quartier, C., Parichatikanond, W., Alam, M.R., Waldeck-Weiermair, M., Malli, R., and Graier, W.F. (2014). Mitochondrial Ca(2+) uniporter (MCU)-dependent and MCU-independent Ca(2+) channels coexist in the inner mitochondrial membrane. *Pflugers Arch.* *466*, 1411-1420.
- Bootman, M.D., Chehab, T., Bultynck, G., Parys, J.B., and Rietdorf, K. (2017). The regulation of autophagy by calcium signals: Do we have a consensus? *Cell Calcium*
- Bragadin, M., Pozzan, T., and Azzone, G.F. (1979). Activation energies and enthalpies during Ca²⁺ transport in rat liver mitochondria. *FEBS Lett.* *104*, 347-351.
- Brand, M.D., and Nicholls, D.G. (2011). Assessing mitochondrial dysfunction in cells. *Biochem. J.* *435*, 297-312.
- Bravo, R., Vicencio, J.M., Parra, V., Troncoso, R., Munoz, J.P., Bui, M., Quiroga, C., Rodriguez, A.E., Verdejo, H.E., Ferreira, J., *et al.* (2011). Increased ER-mitochondrial coupling promotes mitochondrial respiration and bioenergetics during early phases of ER stress. *J. Cell. Sci.* *124*, 2143-2152.
- Brdiczka, D.G., Zorov, D.B., and Sheu, S.S. (2006). Mitochondrial contact sites: their role in energy metabolism and apoptosis. *Biochim. Biophys. Acta* *1762*, 148-163.
- Bricker, D.K., Taylor, E.B., Schell, J.C., Orsak, T., Boutron, A., Chen, Y.C., Cox, J.E., Cardon, C.M., Van Vranken, J.G., Dephoure, N., *et al.* (2012). A mitochondrial pyruvate carrier required for pyruvate uptake in yeast, *Drosophila*, and humans. *Science* *337*, 96-100.
- Brookes, P.S., Parker, N., Buckingham, J.A., Vidal-Puig, A., Halestrap, A.P., Gunter, T.E., Nicholls, D.G., Bernardi, P., Lemasters, J.J., and Brand, M.D. (2008). UCPS--unlikely calcium porters. *Nat. Cell Biol.* *10*, 1235-7; author reply 1237-40.
- Brunello, L., Zampese, E., Florean, C., Pozzan, T., Pizzo, P., and Fasolato, C. (2009). Presenilin-2 dampens intracellular Ca²⁺ stores by increasing Ca²⁺ leakage and reducing Ca²⁺ uptake. *J. Cell. Mol. Med.* *13*, 3358-3369.

- Brunkan, A.L., and Goate, A.M. (2005). Presenilin function and gamma-secretase activity. *J. Neurochem.* *93*, 769-792.
- Cabezas-Opazo, F.A., Vergara-Pulgar, K., Perez, M.J., Jara, C., Osorio-Fuentealba, C., and Quintanilla, R.A. (2015). Mitochondrial Dysfunction Contributes to the Pathogenesis of Alzheimer's Disease. *2015*, 509654.
- Cali, T., Ottolini, D., and Brini, M. (2011). Mitochondria, calcium, and endoplasmic reticulum stress in Parkinson's disease. *Biofactors* *37*, 228-240.
- Cali, T., Ottolini, D., Negro, A., and Brini, M. (2013). Enhanced parkin levels favor ER-mitochondria crosstalk and guarantee Ca(2+) transfer to sustain cell bioenergetics. *Biochim. Biophys. Acta* *1832*, 495-508.
- Cali, T., Ottolini, D., Negro, A., and Brini, M. (2012). alpha-Synuclein controls mitochondrial calcium homeostasis by enhancing endoplasmic reticulum-mitochondria interactions. *J. Biol. Chem.* *287*, 17914-17929.
- Cali, T., Ottolini, D., Soriano, M.E., and Brini, M. (2015). A new split-GFP-based probe reveals DJ-1 translocation into the mitochondrial matrix to sustain ATP synthesis upon nutrient deprivation. *Hum. Mol. Genet.* *24*, 1045-1060.
- Calkins, M.J., and Reddy, P.H. (2011). Amyloid beta impairs mitochondrial anterograde transport and degenerates synapses in Alzheimer's disease neurons. *Biochim. Biophys. Acta* *1812*, 507-513.
- Carafoli, E. (2005). Calcium--a universal carrier of biological signals. Delivered on 3 July 2003 at the Special FEBS Meeting in Brussels. *Febs j.* *272*, 1073-1089.
- Cardenas, C., Miller, R.A., Smith, I., Bui, T., Molgo, J., Muller, M., Vais, H., Cheung, K.H., Yang, J., Parker, I., *et al.* (2010). Essential regulation of cell bioenergetics by constitutive InsP3 receptor Ca2+ transfer to mitochondria. *Cell* *142*, 270-283.
- Cardenas, M.L., Cornish-Bowden, A., and Ureta, T. (1998). Evolution and regulatory Oxid Med. Cell. Longev role of the hexokinases. *Biochim. Biophys. Acta* *1401*, 242-264.
- Casley, C.S., Canevari, L., Land, J.M., Clark, J.B., and Sharpe, M.A. (2002). Beta-amyloid inhibits integrated mitochondrial respiration and key enzyme activities. *J. Neurochem.* *80*, 91-100.
- Catterall, W.A. (2011). Voltage-gated calcium channels. *Cold Spring Harb Perspect. Biol.* *3*, a003947.
- Chan, S.L., Mayne, M., Holden, C.P., Geiger, J.D., and Mattson, M.P. (2000). Presenilin-1 mutations increase levels of ryanodine receptors and calcium release in PC12 cells and cortical neurons. *J. Biol. Chem.* *275*, 18195-18200.
- Chen, Y.R., and Glabe, C.G. (2006). Distinct early folding and aggregation properties of Alzheimer amyloid-beta peptides Abeta40 and Abeta42: stable trimer or tetramer formation by Abeta42. *J. Biol. Chem.* *281*, 24414-24422.
- Chiara, F., Castellaro, D., Marin, O., Petronilli, V., Brusilow, W.S., Juhaszova, M., Sollott, S.J., Forte, M., Bernardi, P., and Rasola, A. (2008). Hexokinase II detachment from mitochondria triggers apoptosis through the permeability transition pore independent of voltage-dependent anion channels. *PLoS One* *3*, e1852.
- Chow, J., Rahman, J., Achermann, J.C., Dattani, M.T., and Rahman, S. (2017). Mitochondrial disease and endocrine dysfunction. *Nat. Rev. Endocrinol.* *13*, 92-104.

- Chow, J., Rahman, J., Achermann, J.C., Dattani, M.T., and Rahman, S. (2017). Mitochondrial disease and endocrine dysfunction. *Nat. Rev. Endocrinol.* *13*, 92-104.
- Chung, S.H. (2009). Aberrant phosphorylation in the pathogenesis of Alzheimer's disease. *BMB Rep.* *42*, 467-474.
- Chyung, J.H., Raper, D.M., and Selkoe, D.J. (2005). Gamma-secretase exists on the plasma membrane as an intact complex that accepts substrates and effects intramembrane cleavage. *J. Biol. Chem.* *280*, 4383-4392.
- Cieri, D., Vicario, M., Giacomello, M., Vallese, F., Filadi, R., Wagner, T., Pozzan, T., Pizzo, P., Scorrano, L., Brini, M., and Cali, T. (2017). SPLICS: a split green fluorescent protein-based contact site sensor for narrow and wide heterotypic organelle juxtaposition. *Cell Death Differ.*
- Citron, M., Westaway, D., Xia, W., Carlson, G., Diehl, T., Levesque, G., Johnson-Wood, K., Lee, M., Seubert, P., Davis, A., *et al.* (1997). Mutant presenilins of Alzheimer's disease increase production of 42-residue amyloid beta-protein in both transfected cells and transgenic mice. *Nat. Med.* *3*, 67-72.
- Clapham, D.E. (2007). Calcium signaling. *Cell* *131*, 1047-1058.
- Clarke, D., and Sokoloff, L. (1999). Intermediary metabolism. In *Basic Neurochemistry: molecular, cellular and medical aspects*, Siegel GJ, Agranoff BW, Albers RW, *et al.*)
- Colombini, M. (1979). A candidate for the permeability pathway of the outer mitochondrial membrane. *Nature* *279*, 643-645.
- Contino, S., Porporato, P.E., Bird, M., Marinangeli, C., Opsomer, R., Sonveaux, P., Bontemps, F., Dewachter, I., Octave, J.N., Bertrand, L., Stanga, S., and Kienlen-Campard, P. (2017). Presenilin 2-Dependent Maintenance of Mitochondrial Oxidative Capacity and Morphology. *Front. Physiol.* *8*, 796.
- Contreras, L., Drago, I., Zampese, E., and Pozzan, T. (2010). Mitochondria: the calcium connection. *Biochim. Biophys. Acta* *1797*, 607-618.
- Cooper, G. (2000). *The Cell: A Molecular Approach*
- Cosson, P., Marchetti, A., Ravazzola, M., and Orci, L. (2012). Mitofusin-2 independent juxtaposition of endoplasmic reticulum and mitochondria: an ultrastructural study. *PLoS One* *7*, e46293.
- Cribbs, J.T., and Strack, S. (2007). Reversible phosphorylation of Drp1 by cyclic AMP-dependent protein kinase and calcineurin regulates mitochondrial fission and cell death. *EMBO Rep.* *8*, 939-944.
- Crowley, P.D., and Gallagher, H.C. (2014). Clotrimazole as a pharmaceutical: past, present and future. *J. Appl. Microbiol.* *117*, 611-617.
- Csordas, G., Golenar, T., Seifert, E.L., Kamer, K.J., Sancak, Y., Perocchi, F., Moffat, C., Weaver, D., de la Fuente Perez, S., Bogorad, R., *et al.* (2013). MICU1 controls both the threshold and cooperative activation of the mitochondrial Ca²⁺(+) uniporter. *Cell. Metab.* *17*, 976-987.
- Csordas, G., Renken, C., Varnai, P., Walter, L., Weaver, D., Buttle, K.F., Balla, T., Mannella, C.A., and Hajnoczky, G. (2006). Structural and functional features and significance of the physical linkage between ER and mitochondria. *J. Cell Biol.* *174*, 915-921.

- Csordas, G., Thomas, A.P., and Hajnoczky, G. (1999). Quasi-synaptic calcium signal transmission between endoplasmic reticulum and mitochondria. *Embo j.* 18, 96-108.
- de Brito, O.M., and Scorrano, L. (2008). Mitofusin 2 tethers endoplasmic reticulum to mitochondria. *Nature* 456, 605-610.
- de la Fuente, S., Fonteriz, R.I., Montero, M., and Alvarez, J. (2013). Ca²⁺ homeostasis in the endoplasmic reticulum measured with a new low-Ca²⁺-affinity targeted aequorin. *Cell Calcium* 54, 37-45.
- De Marchi, E., Bonora, M., Giorgi, C., and Pinton, P. (2014). The mitochondrial permeability transition pore is a dispensable element for mitochondrial calcium efflux. *Cell Calcium* 56, 1-13.
- De Stefani, D., Bononi, A., Romagnoli, A., Messina, A., De Pinto, V., Pinton, P., and Rizzuto, R. (2012). VDAC1 selectively transfers apoptotic Ca²⁺ signals to mitochondria. *Cell Death Differ.* 19, 267-273.
- De Stefani, D., Raffaello, A., Teardo, E., Szabo, I., and Rizzuto, R. (2011). A forty-kilodalton protein of the inner membrane is the mitochondrial calcium uniporter. *Nature* 476, 336-340.
- De Strooper, B., and Annaert, W. (2010). Novel research horizons for presenilins and gamma-secretases in cell biology and disease. *Annu. Rev. Cell Dev. Biol.* 26, 235-260.
- De Strooper, B., Iwatsubo, T., and Wolfe, M.S. (2012). Presenilins and gamma-secretase: structure, function, and role in Alzheimer Disease. *Cold Spring Harb Perspect. Med.* 2, a006304.
- De Vos, K.J., Morotz, G.M., Stoica, R., Tudor, E.L., Lau, K.F., Ackerley, S., Warley, A., Shaw, C.E., and Miller, C.C. (2012). VAPB interacts with the mitochondrial protein PTPIP51 to regulate calcium homeostasis. *Hum. Mol. Genet.* 21, 1299-1311.
- del Arco, A., and Satrustegui, J. (2004). Identification of a novel human subfamily of mitochondrial carriers with calcium-binding domains. *J. Biol. Chem.* 279, 24701-24713.
- DELUCA, H.F., and ENGSTROM, G.W. (1961). Calcium uptake by rat kidney mitochondria. *Proc. Natl. Acad. Sci. U. S. A.* 47, 1744-1750.
- Demuro, A., and Parker, I. (2013). Cytotoxicity of intracellular abeta42 amyloid oligomers involves Ca²⁺ release from the endoplasmic reticulum by stimulated production of inositol trisphosphate. *J. Neurosci.* 33, 3824-3833.
- Denton, R.M. (2009). Regulation of mitochondrial dehydrogenases by calcium ions. *Biochim. Biophys. Acta* 1787, 1309-1316.
- Denton, R.M., Richards, D.A., and Chin, J.G. (1978). Calcium ions and the regulation of NAD⁺-linked isocitrate dehydrogenase from the mitochondria of rat heart and other tissues. *Biochem. J.* 176, 899-906.
- Di Benedetto, G., Penden, D., Greotti, E., Pizzo, P., and Pozzan, T. (2014). Ca²⁺ and cAMP cross-talk in mitochondria. *J. Physiol.* 592, 305-312.
- Divakaruni, A.S., Wallace, M., Buren, C., Martyniuk, K., Andreyev, A.Y., Li, E., Fields, J.A., Cordes, T., Reynolds, I.J., Bloodgood, B.L., *et al.* (2017). Inhibition of the mitochondrial pyruvate carrier protects from excitotoxic neuronal death. *J. Cell Biol.* 216, 1091-1105.
- Divakaruni, A.S., Wiley, S.E., Rogers, G.W., Andreyev, A.Y., Petrosyan, S., Loviscach, M., Wall, E.A., Yadava, N., Heuck, A.P., Ferrick, D.A., *et al.* (2013). Thiazolidinediones are

acute, specific inhibitors of the mitochondrial pyruvate carrier. *Proc. Natl. Acad. Sci. U. S. A.* *110*, 5422-5427.

- Dott, W., Mistry, P., Wright, J., Cain, K., and Herbert, K.E. (2014). Modulation of mitochondrial bioenergetics in a skeletal muscle cell line model of mitochondrial toxicity. *Redox Biol.* *2*, 224-233.
- Drago, I., Giacomello, M., Pizzo, P., and Pozzan, T. (2008). Calcium dynamics in the peroxisomal lumen of living cells. *J. Biol. Chem.* *283*, 14384-14390.
- Du, H., Guo, L., Yan, S., Sosunov, A.A., McKhann, G.M., and Yan, S.S. (2010). Early deficits in synaptic mitochondria in an Alzheimer's disease mouse model. *Proc. Natl. Acad. Sci. U. S. A.* *107*, 18670-18675.
- Etcheberrigaray, R., Hirashima, N., Nee, L., Prince, J., Govoni, S., Racchi, M., Tanzi, R.E., and Alkon, D.L. (1998). Calcium responses in fibroblasts from asymptomatic members of Alzheimer's disease families. *Neurobiol. Dis.* *5*, 37-45.
- Falkowska, A., Gutowska, I., Goschorska, M., Nowacki, P., Chlubek, D., and Baranowska-Bosiacka, I. (2015). Energy Metabolism of the Brain, Including the Cooperation between Astrocytes and Neurons, Especially in the Context of Glycogen Metabolism. *Int. J. Mol. Sci.* *16*, 25959-25981.
- Fiala, J.C. (2007). Mechanisms of amyloid plaque pathogenesis. *Acta Neuropathol.* *114*, 551-571.
- Filadi, R., Greotti, E., Turacchio, G., Luini, A., Pozzan, T., and Pizzo, P. (2016). Presenilin 2 Modulates Endoplasmic Reticulum-Mitochondria Coupling by Tuning the Antagonistic Effect of Mitofusin 2. *Cell. Rep.* *15*, 2226-2238.
- Filadi, R., Greotti, E., Turacchio, G., Luini, A., Pozzan, T., and Pizzo, P. (2015). Mitofusin 2 ablation increases endoplasmic reticulum-mitochondria coupling. *Proc. Natl. Acad. Sci. U. S. A.* *112*, E2174-81.
- Filadi, R., Theurey, P., Rossi, A., Fedeli, C., and Pizzo, P. (2017). Mitochondrial Ca²⁺ handling and behind : the importance of being in contact with other organelles.
- Fill, M., and Copello, J.A. (2002). Ryanodine receptor calcium release channels. *Physiol. Rev.* *82*, 893-922.
- Florean, C., Zampese, E., Zanese, M., Brunello, L., Ichas, F., De Giorgi, F., and Pizzo, P. (2008). High content analysis of gamma-secretase activity reveals variable dominance of presenilin mutations linked to familial Alzheimer's disease. *Biochim. Biophys. Acta* *1783*, 1551-1560.
- Forner, S., Baglietto-Vargas, D., Martini, A.C., Trujillo-Estrada, L., and LaFerla, F.M. (2017). Synaptic Impairment in Alzheimer's Disease: A Dysregulated Symphony. *Trends Neurosci.* *40*, 347-357.
- Forstl, H., and Kurz, A. (1999). Clinical features of Alzheimer's disease. *Eur. Arch. Psychiatry Clin. Neurosci.* *249*, 288-290.
- Foskett, J.K., White, C., Cheung, K.H., and Mak, D.O. (2007). Inositol trisphosphate receptor Ca²⁺ release channels. *Physiol. Rev.* *87*, 593-658.
- Gandy, S. (2005). The role of cerebral amyloid beta accumulation in common forms of Alzheimer disease. *J. Clin. Invest.* *115*, 1121-1129.
- Garcia, D., and Shaw, R.J. (2017). AMPK: Mechanisms of Cellular Energy Sensing and Restoration of Metabolic Balance. *Mol. Cell* *66*, 789-800.

- Garrib, A., and McMurray, W.C. (1986). Purification and characterization of glycerol-3-phosphate dehydrogenase (flavin-linked) from rat liver mitochondria. *J. Biol. Chem.* *261*, 8042-8048.
- Giacomello, M., Barbiero, L., Zatti, G., Squitti, R., Binetti, G., Pozzan, T., Fasolato, C., Ghidoni, R., and Pizzo, P. (2005). Reduction of Ca²⁺ stores and capacitative Ca²⁺ entry is associated with the familial Alzheimer's disease presenilin-2 T122R mutation and anticipates the onset of dementia. *Neurobiol. Dis.* *18*, 638-648.
- Giacomello, M., Drago, I., Bortolozzi, M., Scorzeto, M., Gianelle, A., Pizzo, P., and Pozzan, T. (2010). Ca²⁺ hot spots on the mitochondrial surface are generated by Ca²⁺ mobilization from stores, but not by activation of store-operated Ca²⁺ channels. *Mol. Cell* *38*, 280-290.
- Giacomello, M., Drago, I., Pizzo, P., and Pozzan, T. (2007). Mitochondrial Ca²⁺ as a key regulator of cell life and death. *Cell Death Differ.* *14*, 1267-1274.
- Gilibert, J.A., and Parekh, A.B. (2000). Respiring mitochondria determine the pattern of activation and inactivation of the store-operated Ca²⁺ current I(CRAC). *Embo j.* *19*, 6401-6407.
- Glancy, B., Willis, W.T., Chess, D.J., and Balaban, R.S. (2013). Effect of calcium on the oxidative phosphorylation cascade in skeletal muscle mitochondria. *Biochemistry* *52*, 2793-2809.
- Green, K.N., Demuro, A., Akbari, Y., Hitt, B.D., Smith, I.F., Parker, I., and LaFerla, F.M. (2008). SERCA pump activity is physiologically regulated by presenilin and regulates amyloid beta production. *J. Gen. Physiol.* *132*, i1.
- Guo, Q., Furukawa, K., Sopher, B.L., Pham, D.G., Xie, J., Robinson, N., Martin, G.M., and Mattson, M.P. (1996). Alzheimer's PS-1 mutation perturbs calcium homeostasis and sensitizes PC12 cells to death induced by amyloid beta-peptide. *Neuroreport* *8*, 379-383.
- Haass, C., and Selkoe, D.J. (2007). Soluble protein oligomers in neurodegeneration: lessons from the Alzheimer's amyloid beta-peptide. *Nat. Rev. Mol. Cell Biol.* *8*, 101-112.
- Halim, N.D., Mcfate, T., Mohyeldin, A., Okagaki, P., Korotchkina, L.G., Patel, M.S., Jeoung, N.H., Harris, R.A., Schell, M.J., and Verma, A. (2010). Phosphorylation status of pyruvate dehydrogenase distinguishes metabolic phenotypes of cultured rat brain astrocytes and neurons. *Glia* *58*, 1168-1176.
- Hansford, R.G., and Chappell, J.B. (1967). The effect of Ca²⁺ on the oxidation of glycerol phosphate by blowfly flight-muscle mitochondria. *Biochem. Biophys. Res. Commun.* *27*, 686-692.
- Hardie, D.G., Ross, F.A., and Hawley, S.A. (2012). AMPK: a nutrient and energy sensor that maintains energy homeostasis. *Nat. Rev. Mol. Cell Biol.* *13*, 251-262.
- Hardy, J., and Selkoe, D.J. (2002). The amyloid hypothesis of Alzheimer's disease: progress and problems on the road to therapeutics. *Science* *297*, 353-356.
- Harris, J.J., Jolivet, R., and Attwell, D. (2012). Synaptic energy use and supply. *Neuron* *75*, 762-777.
- Hawley, S.A., Davison, M., Woods, A., Davies, S.P., Beri, R.K., Carling, D., and Hardie, D.G. (1996). Characterization of the AMP-activated protein kinase kinase from rat liver

and identification of threonine 172 as the major site at which it phosphorylates AMP-activated protein kinase. *J. Biol. Chem.* *271*, 27879-27887.

- Hawley, S.A., Pan, D.A., Mustard, K.J., Ross, L., Bain, J., Edelman, A.M., Frenguelli, B.G., and Hardie, D.G. (2005). Calmodulin-dependent protein kinase kinase-beta is an alternative upstream kinase for AMP-activated protein kinase. *Cell. Metab.* *2*, 9-19.
- Herms, J., Anliker, B., Heber, S., Ring, S., Fuhrmann, M., Kretzschmar, H., Sisodia, S., and Muller, U. (2004). Cortical dysplasia resembling human type 2 lissencephaly in mice lacking all three APP family members. *Embo j.* *23*, 4106-4115.
- Herreman, A., Serneels, L., Annaert, W., Collen, D., Schoonjans, L., and De Strooper, B. (2000). Total inactivation of gamma-secretase activity in presenilin-deficient embryonic stem cells. *Nat. Cell Biol.* *2*, 461-462.
- Herrero-Mendez, A., Almeida, A., Fernandez, E., Maestre, C., Moncada, S., and Bolanos, J.P. (2009). The bioenergetic and antioxidant status of neurons is controlled by continuous degradation of a key glycolytic enzyme by APC/C-Cdh1. *Nat. Cell Biol.* *11*, 747-752.
- Herzig, S., Raemy, E., Montessuit, S., Veuthey, J.L., Zamboni, N., Westermann, B., Kunji, E.R., and Martinou, J.C. (2012). Identification and functional expression of the mitochondrial pyruvate carrier. *Science* *337*, 93-96.
- Hildyard, J.C., Ammala, C., Dukes, I.D., Thomson, S.A., and Halestrap, A.P. (2005). Identification and characterisation of a new class of highly specific and potent inhibitors of the mitochondrial pyruvate carrier. *Biochim. Biophys. Acta* *1707*, 221-230.
- Hirabayashi, Y., Kwon, S.K., Paek, H., Pernice, W.M., Paul, M.A., Lee, J., Erfani, P., Raczkowski, A., Petrey, D.S., Pon, L.A., and Polleux, F. (2017). ER-mitochondria tethering by PDZD8 regulates Ca(2+) dynamics in mammalian neurons. *Science* *358*, 623-630.
- Holmuhamedov, E., and Lemasters, J.J. (2009). Ethanol exposure decreases mitochondrial outer membrane permeability in cultured rat hepatocytes. *Arch. Biochem. Biophys.* *481*, 226-233.
- Holtzman, D.M., Morris, J.C., and Goate, A.M. (2011). Alzheimer's disease: the challenge of the second century. *Sci. Transl. Med.* *3*, 77sr1.
- Honarnejad, K., and Herms, J. (2012). Presenilins: role in calcium homeostasis. *Int. J. Biochem. Cell Biol.* *44*, 1983-1986.
- Hoppe, U.C. (2010). Mitochondrial calcium channels. *FEBS Lett.* *584*, 1975-1981.
- Hung, A.Y., Koo, E.H., Haass, C., and Selkoe, D.J. (1992). Increased expression of beta-amyloid precursor protein during neuronal differentiation is not accompanied by secretory cleavage. *Proc. Natl. Acad. Sci. U. S. A.* *89*, 9439-9443.
- Hurley, R.L., Barre, L.K., Wood, S.D., Anderson, K.A., Kemp, B.E., Means, A.R., and Witters, L.A. (2006). Regulation of AMP-activated protein kinase by multisite phosphorylation in response to agents that elevate cellular cAMP. *J. Biol. Chem.* *281*, 36662-36672.
- Iijima-Ando, K., Sekiya, M., Maruko-Otake, A., Ohtake, Y., Suzuki, E., Lu, B., and Iijima, K.M. (2012). Loss of axonal mitochondria promotes tau-mediated neurodegeneration

and Alzheimer's disease-related tau phosphorylation via PAR-1. *PLoS Genet.* 8, e1002918.

- Imamura, H., Nhat, K.P., Togawa, H., Saito, K., Iino, R., Kato-Yamada, Y., Nagai, T., and Noji, H. (2009). Visualization of ATP levels inside single living cells with fluorescence resonance energy transfer-based genetically encoded indicators. *Proc. Natl. Acad. Sci. U. S. A.* 106, 15651-15656.
- Ito, E., Oka, K., Etcheberrigaray, R., Nelson, T.J., McPhie, D.L., Tofel-Grehl, B., Gibson, G.E., and Alkon, D.L. (1994). Internal Ca²⁺ mobilization is altered in fibroblasts from patients with Alzheimer disease. *Proc. Natl. Acad. Sci. U. S. A.* 91, 534-538.
- Jean-Quartier, C., Bondarenko, A.I., Alam, M.R., Trenker, M., Waldeck-Weiermair, M., Malli, R., and Graier, W.F. (2012). Studying mitochondrial Ca(2+) uptake - a revisit. *Mol. Cell. Endocrinol.* 353, 114-127.
- Jean-Quartier, C., Bondarenko, A.I., Alam, M.R., Trenker, M., Waldeck-Weiermair, M., Malli, R., and Graier, W.F. (2012). Studying mitochondrial Ca(2+) uptake - a revisit. *Mol. Cell. Endocrinol.* 353, 114-127.
- Jiang, D., Zhao, L., and Clapham, D.E. (2009). Genome-wide RNAi screen identifies Letm1 as a mitochondrial Ca²⁺/H⁺ antiporter. *Science* 326, 144-147.
- John, S., Weiss, J.N., and Ribalet, B. (2011). Subcellular localization of hexokinases I and II directs the metabolic fate of glucose. *PLoS One* 6, e17674.
- Jouaville, L.S., Pinton, P., Bastianutto, C., Rutter, G.A., and Rizzuto, R. (1999). Regulation of mitochondrial ATP synthesis by calcium: evidence for a long-term metabolic priming. *Proc. Natl. Acad. Sci. U. S. A.* 96, 13807-13812.
- Jung, D.H., Mo, S.H., and Kim, D.H. (2006). Calumenin, a multiple EF-hands Ca²⁺-binding protein, interacts with ryanodine receptor-1 in rabbit skeletal sarcoplasmic reticulum. *Biochem. Biophys. Res. Commun.* 343, 34-42.
- Kaether, C., Schmitt, S., Willem, M., and Haass, C. (2006). Amyloid precursor protein and Notch intracellular domains are generated after transport of their precursors to the cell surface. *Traffic* 7, 408-415.
- Kamal, A., Stokin, G.B., Yang, Z., Xia, C.H., and Goldstein, L.S. (2000). Axonal transport of amyloid precursor protein is mediated by direct binding to the kinesin light chain subunit of kinesin-I. *Neuron* 28, 449-459.
- Karabinos, A., Bhattacharya, D., Morys-Wortmann, C., Kroll, K., Hirschfeld, G., Kratzin, H.D., Barnikol-Watanabe, S., and Hilschmann, N. (1996). The divergent domains of the NEFA and nucleobindin proteins are derived from an EF-hand ancestor. *Mol. Biol. Evol.* 13, 990-998.
- Kasri, N.N., Kocks, S.L., Verbert, L., Hebert, S.S., Callewaert, G., Parys, J.B., Missiaen, L., and De Smedt, H. (2006). Up-regulation of inositol 1,4,5-trisphosphate receptor type 1 is responsible for a decreased endoplasmic-reticulum Ca²⁺ content in presenilin double knock-out cells. *Cell Calcium* 40, 41-51.
- Kim, J., Kleizen, B., Choy, R., Thinakaran, G., Sisodia, S.S., and Schekman, R.W. (2007). Biogenesis of gamma-secretase early in the secretory pathway. *J. Cell Biol.* 179, 951-963.

- Kim, T.W., Pettingell, W.H., Hallmark, O.G., Moir, R.D., Wasco, W., and Tanzi, R.E. (1997). Endoproteolytic cleavage and proteasomal degradation of presenilin 2 in transfected cells. *J. Biol. Chem.* 272, 11006-11010.
- Kimberly, W.T., Xia, W., Rahmati, T., Wolfe, M.S., and Selkoe, D.J. (2000). The transmembrane aspartates in presenilin 1 and 2 are obligatory for gamma-secretase activity and amyloid beta-protein generation. *J. Biol. Chem.* 275, 3173-3178.
- Kipanyula, M.J., Contreras, L., Zampese, E., Lazzari, C., Wong, A.K., Pizzo, P., Fasolato, C., and Pozzan, T. (2012). Ca²⁺ dysregulation in neurons from transgenic mice expressing mutant presenilin 2. *Aging Cell.* 11, 885-893.
- Korzeniowski, M.K., Szanda, G., Balla, T., and Spat, A. (2009). Store-operated Ca²⁺ influx and subplasmalemmal mitochondria. *Cell Calcium* 46, 49-55.
- Krieger-Brauer, H.I., and Gratzl, M. (1983). Effects of monovalent and divalent cations on Ca²⁺ fluxes across chromaffin secretory membrane vesicles. *J. Neurochem.* 41, 1269-1276.
- Kwong, J.Q., Lu, X., Correll, R.N., Schwanekamp, J.A., Vagnozzi, R.J., Sargent, M.A., York, A.J., Zhang, J., Bers, D.M., and Molkentin, J.D. (2015). The Mitochondrial Calcium Uniporter Selectively Matches Metabolic Output to Acute Contractile Stress in the Heart. *Cell. Rep.* 12, 15-22.
- LaFerla, F.M. (2002). Calcium dyshomeostasis and intracellular signalling in Alzheimer's disease. *Nat. Rev. Neurosci.* 3, 862-872.
- LaFerla, F.M., Green, K.N., and Oddo, S. (2007). Intracellular amyloid-beta in Alzheimer's disease. *Nat. Rev. Neurosci.* 8, 499-509.
- LaPointe, N.E., Morfini, G., Pigino, G., Gaisina, I.N., Kozikowski, A.P., Binder, L.I., and Brady, S.T. (2009). The amino terminus of tau inhibits kinesin-dependent axonal transport: implications for filament toxicity. *J. Neurosci. Res.* 87, 440-451.
- Lazzari, C., Kipanyula, M.J., Agostini, M., Pozzan, T., and Fasolato, C. (2015). Abeta42 oligomers selectively disrupt neuronal calcium release. *Neurobiol. Aging* 36, 877-885.
- Leal, N.S., Schreiner, B., Pinho, C.M., Filadi, R., Wiehager, B., Karlstrom, H., Pizzo, P., and Ankarcrona, M. (2016). Mitofusin-2 knockdown increases ER-mitochondria contact and decreases amyloid beta-peptide production. *J. Cell. Mol. Med.* 20, 1686-1695.
- Lee, S.F., Shah, S., Li, H., Yu, C., Han, W., and Yu, G. (2002). Mammalian APH-1 interacts with presenilin and nicastrin and is required for intramembrane proteolysis of amyloid-beta precursor protein and Notch. *J. Biol. Chem.* 277, 45013-45019.
- Leissring, M.A., Akbari, Y., Fanger, C.M., Cahalan, M.D., Mattson, M.P., and LaFerla, F.M. (2000). Capacitative calcium entry deficits and elevated luminal calcium content in mutant presenilin-1 knockin mice. *J. Cell Biol.* 149, 793-798.
- Levy-Lahad, E., Wasco, W., Poorkaj, P., Romano, D.M., Oshima, J., Pettingell, W.H., Yu, C.E., Jondro, P.D., Schmidt, S.D., and Wang, K. (1995). Candidate gene for the chromosome 1 familial Alzheimer's disease locus. *Science* 269, 973-977.
- Lewis, R.S. (2007). The molecular choreography of a store-operated calcium channel. *Nature* 446, 284-287.
- Li, W., Shariat-Madar, Z., Powers, M., Sun, X., Lane, R.D., and Garlid, K.D. (1992). Reconstitution, identification, purification, and immunological characterization of the

110-kDa Na⁺/Ca²⁺ antiporter from beef heart mitochondria. *J. Biol. Chem.* *267*, 17983-17989.

- Li, X., Han, G., Li, X., Kan, Q., Fan, Z., Li, Y., Ji, Y., Zhao, J., Zhang, M., Grigalavicius, M., *et al.* (2017). Mitochondrial pyruvate carrier function determines cell stemness and metabolic reprogramming in cancer cells. *Oncotarget* *8*, 46363-46380.
- Lin, P., Yao, Y., Hofmeister, R., Tsien, R.Y., and Farquhar, M.G. (1999). Overexpression of CALNUC (nucleobindin) increases agonist and thapsigargin releasable Ca²⁺ storage in the Golgi. *J. Cell Biol.* *145*, 279-289.
- Linn, T.C., Pettit, F.H., and Reed, L.J. (1969). Alpha-keto acid dehydrogenase complexes. X. Regulation of the activity of the pyruvate dehydrogenase complex from beef kidney mitochondria by phosphorylation and dephosphorylation. *Proc. Natl. Acad. Sci. U. S. A.* *62*, 234-241.
- Liou, J., Kim, M.L., Heo, W.D., Jones, J.T., Myers, J.W., Ferrell, J.E., Jr, and Meyer, T. (2005). STIM is a Ca²⁺ sensor essential for Ca²⁺-store-depletion-triggered Ca²⁺ influx. *Curr. Biol.* *15*, 1235-1241.
- Lissandron, V., Podini, P., Pizzo, P., and Pozzan, T. (2010). Unique characteristics of Ca²⁺ homeostasis of the trans-Golgi compartment. *Proc. Natl. Acad. Sci. U. S. A.* *107*, 9198-9203.
- Lodish, H., Berk, A., and Zipursky, S. (2000). *Molecular Cell Biology*
- Lu, T., Aron, L., Zullo, J., Pan, Y., Kim, H., Chen, Y., Yang, T.H., Kim, H.M., Drake, D., Liu, X.S., *et al.* (2014). REST and stress resistance in ageing and Alzheimer's disease. *Nature* *507*, 448-454.
- Luo, W.J., Wang, H., Li, H., Kim, B.S., Shah, S., Lee, H.J., Thinakaran, G., Kim, T.W., Yu, G., and Xu, H. (2003). PEN-2 and APH-1 coordinately regulate proteolytic processing of presenilin 1. *J. Biol. Chem.* *278*, 7850-7854.
- Luongo, T.S., Lambert, J.P., Yuan, A., Zhang, X., Gross, P., Song, J., Shanmughapriya, S., Gao, E., Jain, M., Houser, S.R., *et al.* (2015). The Mitochondrial Calcium Uniporter Matches Energetic Supply with Cardiac Workload during Stress and Modulates Permeability Transition. *Cell. Rep.* *12*, 23-34.
- Ma, Q.H., Futagawa, T., Yang, W.L., Jiang, X.D., Zeng, L., Takeda, Y., Xu, R.X., Bagnard, D., Schachner, M., Furley, A.J., *et al.* (2008). A TAG1-APP signalling pathway through Fe65 negatively modulates neurogenesis. *Nat. Cell Biol.* *10*, 283-294.
- Magistretti, P.J., and Allaman, I. (2015). A cellular perspective on brain energy metabolism and functional imaging. *Neuron* *86*, 883-901.
- Mahapatra, N.R., Mahata, M., Hazra, P.P., McDonough, P.M., O'Connor, D.T., and Mahata, S.K. (2004). A dynamic pool of calcium in catecholamine storage vesicles. Exploration in living cells by a novel vesicle-targeted chromogranin A-aequorin chimeric photoprotein. *J. Biol. Chem.* *279*, 51107-51121.
- Mak, D.O., and Foskett, J.K. (2015). Inositol 1,4,5-trisphosphate receptors in the endoplasmic reticulum: A single-channel point of view. *Cell Calcium* *58*, 67-78.
- Mallilankaraman, K., Cardenas, C., Doonan, P.J., Chandramoorthy, H.C., Irrinki, K.M., Golenar, T., Csordas, G., Madireddi, P., Yang, J., Muller, M., *et al.* (2012). MCUR1 is an essential component of mitochondrial Ca²⁺ uptake that regulates cellular metabolism. *Nat. Cell Biol.* *14*, 1336-1343.

- Mammucari, C., Raffaello, A., Vecellio Reane, D., and Rizzuto, R. (2016). Molecular structure and pathophysiological roles of the Mitochondrial Calcium Uniporter. *Biochim. Biophys. Acta* 1863, 2457-2464.
- Manczak, M., Calkins, M.J., and Reddy, P.H. (2011). Impaired mitochondrial dynamics and abnormal interaction of amyloid beta with mitochondrial protein Drp1 in neurons from patients with Alzheimer's disease: implications for neuronal damage. *Hum. Mol. Genet.* 20, 2495-2509.
- Martin, L., Latypova, X., and Terro, F. (2011). Post-translational modifications of tau protein: implications for Alzheimer's disease. *Neurochem. Int.* 58, 458-471.
- McCarthy, J.V., Twomey, C., and Wujek, P. (2009). Presenilin-dependent regulated intramembrane proteolysis and gamma-secretase activity. *Cell Mol. Life Sci.* 66, 1534-1555.
- McCommis, K.S., Chen, Z., Fu, X., McDonald, W.G., Colca, J.R., Kletzien, R.F., Burgess, S.C., and Finck, B.N. (2015). Loss of Mitochondrial Pyruvate Carrier 2 in the Liver Leads to Defects in Gluconeogenesis and Compensation via Pyruvate-Alanine Cycling. *Cell. Metab.* 22, 682-694.
- McCormack, J.G., Halestrap, A.P., and Denton, R.M. (1990). Role of calcium ions in regulation of mammalian intramitochondrial metabolism. *Physiol. Rev.* 70, 391-425.
- Meldolesi, J., and Pozzan, T. (1998). The endoplasmic reticulum Ca²⁺ store: a view from the lumen. *Trends Biochem. Sci.* 23, 10-14.
- Mishra, P., and Chan, D.C. (2016). Metabolic regulation of mitochondrial dynamics. *J. Cell Biol.* 212, 379-387.
- Mitchell, K.J., Pinton, P., Varadi, A., Tacchetti, C., Ainscow, E.K., Pozzan, T., Rizzuto, R., and Rutter, G.A. (2001). Dense core secretory vesicles revealed as a dynamic Ca(2+) store in neuroendocrine cells with a vesicle-associated membrane protein aequorin chimaera. *J. Cell Biol.* 155, 41-51.
- Mitchell, P., and Moyle, J. (1967). Chemiosmotic hypothesis of oxidative phosphorylation. *Nature* 213, 137-139.
- Miyawaki, A., Llopis, J., Heim, R., McCaffery, J.M., Adams, J.A., Ikura, M., and Tsien, R.Y. (1997). Fluorescent indicators for Ca²⁺ based on green fluorescent proteins and calmodulin. *Nature* 388, 882-887.
- Morre, D.J., Merritt, W.D., and Lembi, C.A. (1971). Connections between mitochondria and endoplasmic reticulum in rat liver and onion stem. *Protoplasma* 73, 43-49.
- Murphy, E., Pan, X., Nguyen, T., Liu, J., Holmstrom, K.M., and Finkel, T. (2014). Unresolved questions from the analysis of mice lacking MCU expression. *Biochem. Biophys. Res. Commun.* 449, 384-385.
- Neumann, D., Buckers, J., Kastrup, L., Hell, S.W., and Jakobs, S. (2010). Two-color STED microscopy reveals different degrees of colocalization between hexokinase-I and the three human VDAC isoforms. *PMC Biophys.* 3, 4-5036-3-4.
- Nosek, M.T., Dransfield, D.T., and Aprille, J.R. (1990). Calcium stimulates ATP-Mg/Pi carrier activity in rat liver mitochondria. *J. Biol. Chem.* 265, 8444-8450.
- Nowikovsky, K., Pozzan, T., Rizzuto, R., Scorrano, L., and Bernardi, P. (2012). Perspectives on: SGP symposium on mitochondrial physiology and medicine: the pathophysiology of LETM1. *J. Gen. Physiol.* 139, 445-454.

- Oldershaw, K.A., and Taylor, C.W. (1990). 2,5-Di-(tert-butyl)-1,4-benzohydroquinone mobilizes inositol 1,4,5-trisphosphate-sensitive and -insensitive Ca²⁺ stores. *FEBS Lett.* *274*, 214-216.
- Oules, B., Del Prete, D., Greco, B., Zhang, X., Lauritzen, I., Sevalle, J., Moreno, S., Paterlini-Brechot, P., Trebak, M., Checler, F., Benfenati, F., and Chami, M. (2012). Ryanodine receptor blockade reduces amyloid-beta load and memory impairments in Tg2576 mouse model of Alzheimer disease. *J. Neurosci.* *32*, 11820-11834.
- Palmieri, L., Pardo, B., Lasorsa, F.M., del Arco, A., Kobayashi, K., Iijima, M., Runswick, M.J., Walker, J.E., Saheki, T., Satrustegui, J., and Palmieri, F. (2001). Citrin and aralar1 are Ca²⁺-stimulated aspartate/glutamate transporters in mitochondria. *Embo j.* *20*, 5060-5069.
- Palty, R., Silverman, W.F., Hershinkel, M., Caporale, T., Sensi, S.L., Parnis, J., Nolte, C., Fishman, D., Shoshan-Barmatz, V., Herrmann, S., Khananshvil, D., and Sekler, I. (2010). NCLX is an essential component of mitochondrial Na⁺/Ca²⁺ exchange. *Proc. Natl. Acad. Sci. U. S. A.* *107*, 436-441.
- Pan, X., Liu, J., Nguyen, T., Liu, C., Sun, J., Teng, Y., Fergusson, M.M., Rovira, I.I., Allen, M., Springer, D.A., *et al.* (2013). The physiological role of mitochondrial calcium revealed by mice lacking the mitochondrial calcium uniporter. *Nat. Cell Biol.* *15*, 1464-1472.
- Pardo, B., Contreras, L., Serrano, A., Ramos, M., Kobayashi, K., Iijima, M., Saheki, T., and Satrustegui, J. (2006). Essential role of aralar in the transduction of small Ca²⁺ signals to neuronal mitochondria. *J. Biol. Chem.* *281*, 1039-1047.
- Parihar, M.S., and Hemnani, T. (2004). Alzheimer's disease pathogenesis and therapeutic interventions. *J. Clin. Neurosci.* *11*, 456-467.
- Parks, A.L., and Curtis, D. (2007). Presenilin diversifies its portfolio. *Trends Genet.* *23*, 140-150.
- Pastorino, J.G., and Hoek, J.B. (2008). Regulation of hexokinase binding to VDAC. *J. Bioenerg. Biomembr.* *40*, 171-182.
- Pastorino, J.G., Shulga, N., and Hoek, J.B. (2002). Mitochondrial binding of hexokinase II inhibits Bax-induced cytochrome c release and apoptosis. *J. Biol. Chem.* *277*, 7610-7618.
- Patron, M., Raffaello, A., Granatiero, V., Tosatto, A., Merli, G., De Stefani, D., Wright, L., Pallafacchina, G., Terrin, A., Mammucari, C., and Rizzuto, R. (2013). The mitochondrial calcium uniporter (MCU): molecular identity and physiological roles. *J. Biol. Chem.* *288*, 10750-10758.
- Paupe, V., Prudent, J., Dassa, E.P., Rendon, O.Z., and Shoubridge, E.A. (2015). CCDC90A (MCUR1) is a cytochrome c oxidase assembly factor and not a regulator of the mitochondrial calcium uniporter. *Cell. Metab.* *21*, 109-116.
- Pera, M., Larrea, D., Guardia-Laguarta, C., Montesinos, J., Velasco, K.R., Agrawal, R.R., Xu, Y., Chan, R.B., Di Paolo, G., Mehler, M.F., *et al.* (2017). Increased localization of APP-C99 in mitochondria-associated ER membranes causes mitochondrial dysfunction in Alzheimer disease. *Embo j.* *36*, 3356-3371.
- Perl, D.P. (2010). Neuropathology of Alzheimer's disease. *Mt. Sinai J. Med.* *77*, 32-42.

- Perocchi, F., Gohil, V.M., Girgis, H.S., Bao, X.R., McCombs, J.E., Palmer, A.E., and Mootha, V.K. (2010). MICU1 encodes a mitochondrial EF hand protein required for Ca²⁺ uptake. *Nature* 467, 291-296.
- Perrin, R.J., Fagan, A.M., and Holtzman, D.M. (2009). Multimodal techniques for diagnosis and prognosis of Alzheimer's disease. *Nature* 461, 916-922.
- Pinton, P., Pozzan, T., and Rizzuto, R. (1998). The Golgi apparatus is an inositol 1,4,5-trisphosphate-sensitive Ca²⁺ store, with functional properties distinct from those of the endoplasmic reticulum. *Embo j.* 17, 5298-5308.
- Pitter, J.G., Maechler, P., Wollheim, C.B., and Spat, A. (2002). Mitochondria respond to Ca²⁺ already in the submicromolar range: correlation with redox state. *Cell Calcium* 31, 97-104.
- Pizzo, P., Lissandron, V., Capitanio, P., and Pozzan, T. (2011). Ca²⁺ signalling in the Golgi apparatus. *Cell Calcium* 50, 184-192.
- Pozzan, T., and Rizzuto, R. (2000). The renaissance of mitochondrial calcium transport. *Eur. J. Biochem.* 267, 5269-5273.
- Prakriya, M., Feske, S., Gwack, Y., Srikanth, S., Rao, A., and Hogan, P.G. (2006). Orai1 is an essential pore subunit of the CRAC channel. *Nature* 443, 230-233.
- Querfurth, H.W., and LaFerla, F.M. (2010). Alzheimer's disease. *N. Engl. J. Med.* 362, 329-344.
- Raffaello, A., De Stefani, D., Sabbadin, D., Teardo, E., Merli, G., Picard, A., Checchetto, V., Moro, S., Szabo, I., and Rizzuto, R. (2013). The mitochondrial calcium uniporter is a multimer that can include a dominant-negative pore-forming subunit. *Embo j.* 32, 2362-2376.
- Raffaello, A., Mammucari, C., Gherardi, G., and Rizzuto, R. (2016). Calcium at the Center of Cell Signaling: Interplay between Endoplasmic Reticulum, Mitochondria, and Lysosomes. *Trends Biochem. Sci.* 41, 1035-1049.
- Rasola, A., and Bernardi, P. (2011). Mitochondrial permeability transition in Ca²⁺-dependent apoptosis and necrosis. *Cell Calcium* 50, 222-233.
- Raychaudhury, B., Gupta, S., Banerjee, S., and Datta, S.C. (2006). Peroxisome is a reservoir of intracellular calcium. *Biochim. Biophys. Acta* 1760, 989-992.
- Rizzuto, R., Pinton, P., Carrington, W., Fay, F.S., Fogarty, K.E., Lifshitz, L.M., Tuft, R.A., and Pozzan, T. (1998). Close contacts with the endoplasmic reticulum as determinants of mitochondrial Ca²⁺ responses. *Science* 280, 1763-1766.
- Rizzuto, R., and Pozzan, T. (2006). Microdomains of intracellular Ca²⁺: molecular determinants and functional consequences. *Physiol. Rev.* 86, 369-408.
- Rizzuto, R., Simpson, A.W., Brini, M., and Pozzan, T. (1992). Rapid changes of mitochondrial Ca²⁺ revealed by specifically targeted recombinant aequorin. *Nature* 358, 325-327.
- ROBERTSON, J.D. (1960). The molecular structure and contact relationships of cell membranes. *Prog. Biophys. Mol. Biol.* 10, 343-418.
- Robey, R.B., and Hay, N. (2006). Mitochondrial hexokinases, novel mediators of the antiapoptotic effects of growth factors and Akt. *Oncogene* 25, 4683-4696.

- Roche, T.E., and Hiromasa, Y. (2007). Pyruvate dehydrogenase kinase regulatory mechanisms and inhibition in treating diabetes, heart ischemia, and cancer. *Cell Mol. Life Sci.* **64**, 830-849.
- Roos, J., DiGregorio, P.J., Yeromin, A.V., Ohlsen, K., Lioudyno, M., Zhang, S., Safrina, O., Kozak, J.A., Wagner, S.L., Cahalan, M.D., Velicelebi, G., and Stauderman, K.A. (2005). STIM1, an essential and conserved component of store-operated Ca²⁺ channel function. *J. Cell Biol.* **169**, 435-445.
- Rowland, A.A., and Voeltz, G.K. (2012). Endoplasmic reticulum-mitochondria contacts: function of the junction. *Nat. Rev. Mol. Cell Biol.* **13**, 607-625.
- Rutter, G.A., Burnett, P., Rizzuto, R., Brini, M., Murgia, M., Pozzan, T., Tavares, J.M., and Denton, R.M. (1996). Subcellular imaging of intramitochondrial Ca²⁺ with recombinant targeted aequorin: significance for the regulation of pyruvate dehydrogenase activity. *Proc. Natl. Acad. Sci. U. S. A.* **93**, 5489-5494.
- S, K., C, S., Cs, K., and S, W. (2014). Clotrimazole as a Cancer Drug: A Short Review. *Med. Chem. (Los Angeles)* **4**, 722-724.
- Sampson, M.J., Decker, W.K., Beaudet, A.L., Ruitenbeek, W., Armstrong, D., Hicks, M.J., and Craigen, W.J. (2001). Immobile sperm and infertility in mice lacking mitochondrial voltage-dependent anion channel type 3. *J. Biol. Chem.* **276**, 39206-39212.
- San Martin, A., Ceballo, S., Ruminot, I., Lerchundi, R., Frommer, W.B., and Barros, L.F. (2013). A genetically encoded FRET lactate sensor and its use to detect the Warburg effect in single cancer cells. *PLoS One* **8**, e57712.
- Sancak, Y., Markhard, A.L., Kitami, T., Kovacs-Bogdan, E., Kamer, K.J., Udeshi, N.D., Carr, S.A., Chaudhuri, D., Clapham, D.E., Li, A.A., *et al.* (2013). EMRE is an essential component of the mitochondrial calcium uniporter complex. *Science* **342**, 1379-1382.
- Satrustegui, J., Pardo, B., and Del Arco, A. (2007). Mitochondrial transporters as novel targets for intracellular calcium signaling. *Physiol. Rev.* **87**, 29-67.
- Scherer, P.E., Lederkremer, G.Z., Williams, S., Fogliano, M., Baldini, G., and Lodish, H.F. (1996). Cab45, a novel (Ca²⁺)-binding protein localized to the Golgi lumen. *J. Cell Biol.* **133**, 257-268.
- Scheuner, D., Eckman, C., Jensen, M., Song, X., Citron, M., Suzuki, N., Bird, T.D., Hardy, J., Hutton, M., Kukull, W., *et al.* (1996). Secreted amyloid beta-protein similar to that in the senile plaques of Alzheimer's disease is increased in vivo by the presenilin 1 and 2 and APP mutations linked to familial Alzheimer's disease. *Nat. Med.* **2**, 864-870.
- Schonfeld, P., and Reiser, G. (2013). Why does brain metabolism not favor burning of fatty acids to provide energy? Reflections on disadvantages of the use of free fatty acids as fuel for brain. *J. Cereb. Blood Flow Metab.* **33**, 1493-1499.
- Seidler, N.W., Jona, I., Vegh, M., and Martonosi, A. (1989). Cyclopiazonic acid is a specific inhibitor of the Ca²⁺-ATPase of sarcoplasmic reticulum. *J. Biol. Chem.* **264**, 17816-17823.
- Sherrington, R., Rogaev, E.I., Liang, Y., Rogaeva, E.A., Levesque, G., Ikeda, M., Chi, H., Lin, C., Li, G., Holman, K., *et al.* (1995). Cloning of a gene bearing missense mutations in early-onset familial Alzheimer's disease. *Nature* **375**, 754-760.

- Shimojo, M., Sahara, N., Murayama, M., Ichinose, H., and Takashima, A. (2007). Decreased Abeta secretion by cells expressing familial Alzheimer's disease-linked mutant presenilin 1. *Neurosci. Res.* 57, 446-453.
- Shoshan-Barmatz, V., Krelin, Y., and Shteinifer-Kuzmine, A. (2017). VDAC1 functions in Ca²⁺ homeostasis and cell life and death in health and disease. *Cell Calcium*
- Shoshan-Barmatz, V., and Mizrachi, D. (2012). VDAC1: from structure to cancer therapy. *Front. Oncol.* 2, 164.
- Smith, I.F., Boyle, J.P., Vaughan, P.F., Pearson, H.A., Cowburn, R.F., and Peers, C.S. (2002). Ca²⁺ stores and capacitative Ca²⁺ entry in human neuroblastoma (SH-SY5Y) cells expressing a familial Alzheimer's disease presenilin-1 mutation. *Brain Res.* 949, 105-111.
- Stoica, R., De Vos, K.J., Paillusson, S., Mueller, S., Sancho, R.M., Lau, K.F., Vizcay-Barrena, G., Lin, W.L., Xu, Y.F., Lewis, J., *et al.* (2014). ER-mitochondria associations are regulated by the VAPB-PTPIP51 interaction and are disrupted by ALS/FTD-associated TDP-43. *Nat. Commun.* 5, 3996.
- Stoica, R., Paillusson, S., Gomez-Suaga, P., Mitchell, J.C., Lau, D.H., Gray, E.H., Sancho, R.M., Vizcay-Barrena, G., De Vos, K.J., Shaw, C.E., *et al.* (2016). ALS/FTD-associated FUS activates GSK-3beta to disrupt the VAPB-PTPIP51 interaction and ER-mitochondria associations. *EMBO Rep.* 17, 1326-1342.
- Stone, S.J., and Vance, J.E. (2000). Phosphatidylserine synthase-1 and -2 are localized to mitochondria-associated membranes. *J. Biol. Chem.* 275, 34534-34540.
- Stutzmann, G.E., Caccamo, A., LaFerla, F.M., and Parker, I. (2004). Dysregulated IP3 signaling in cortical neurons of knock-in mice expressing an Alzheimer's-linked mutation in presenilin1 results in exaggerated Ca²⁺ signals and altered membrane excitability. *J. Neurosci.* 24, 508-513.
- Sun, L., Shukair, S., Naik, T.J., Moazed, F., and Ardehali, H. (2008). Glucose phosphorylation and mitochondrial binding are required for the protective effects of hexokinases I and II. *Mol. Cell. Biol.* 28, 1007-1017.
- Sun, L., Shukair, S., Naik, T.J., Moazed, F., and Ardehali, H. (2008). Glucose phosphorylation and mitochondrial binding are required for the protective effects of hexokinases I and II. *Mol. Cell. Biol.* 28, 1007-1017.
- Supnet, C., Grant, J., Kong, H., Westaway, D., and Mayne, M. (2006). Amyloid-beta-(1-42) increases ryanodine receptor-3 expression and function in neurons of TgCRND8 mice. *J. Biol. Chem.* 281, 38440-38447.
- Suter, M., Riek, U., Tuerk, R., Schlattner, U., Wallimann, T., and Neumann, D. (2006). Dissecting the role of 5'-AMP for allosteric stimulation, activation, and deactivation of AMP-activated protein kinase. *J. Biol. Chem.* 281, 32207-32216.
- Suzuki, T., Bridges, D., Nakada, D., Skiniotis, G., Morrison, S.J., Lin, J.D., Saltiel, A.R., and Inoki, K. (2013). Inhibition of AMPK catabolic action by GSK3. *Mol. Cell* 50, 407-419.
- Szabadkai, G., Bianchi, K., Varnai, P., De Stefani, D., Wieckowski, M.R., Cavagna, D., Nagy, A.I., Balla, T., and Rizzuto, R. (2006). Chaperone-mediated coupling of endoplasmic reticulum and mitochondrial Ca²⁺ channels. *J. Cell Biol.* 175, 901-911.

- Taylor, E.B. (2017). Functional Properties of the Mitochondrial Carrier System. *Trends Cell Biol.* *27*, 633-644.
- Teague, W.M., Pettit, F.H., Wu, T.L., Silberman, S.R., and Reed, L.J. (1982). Purification and properties of pyruvate dehydrogenase phosphatase from bovine heart and kidney. *Biochemistry* *21*, 5585-5592.
- Territo, P.R., Mootha, V.K., French, S.A., and Balaban, R.S. (2000). Ca(2+) activation of heart mitochondrial oxidative phosphorylation: role of the F(0)/F(1)-ATPase. *Am. J. Physiol. Cell. Physiol.* *278*, C423-35.
- Thangaratnarajah, C., Ruprecht, J.J., and Kunji, E.R. (2014). Calcium-induced conformational changes of the regulatory domain of human mitochondrial aspartate/glutamate carriers. *Nat. Commun.* *5*, 5491.
- Thestrup, T., Litzlbauer, J., Bartholomaeus, I., Mues, M., Russo, L., Dana, H., Kovalchuk, Y., Liang, Y., Kalamakis, G., Laukat, Y., *et al.* (2014). Optimized ratiometric calcium sensors for functional in vivo imaging of neurons and T lymphocytes. *Nat. Methods* *11*, 175-182.
- Thinakaran, G., and Koo, E.H. (2008). Amyloid precursor protein trafficking, processing, and function. *J. Biol. Chem.* *283*, 29615-29619.
- Tolia, A., and De Strooper, B. (2009). Structure and function of gamma-secretase. *Semin. Cell Dev. Biol.* *20*, 211-218.
- Trenker, M., Malli, R., Fertschai, I., Levak-Frank, S., and Graier, W.F. (2007). Uncoupling proteins 2 and 3 are fundamental for mitochondrial Ca2+ uniport. *Nat. Cell Biol.* *9*, 445-452.
- Trimmer, P.A., and Borland, M.K. (2005). Differentiated Alzheimer's disease trans-mitochondrial cybrid cell lines exhibit reduced organelle movement. *Antioxid. Redox Signal.* *7*, 1101-1109.
- Trushina, E., Nemutlu, E., Zhang, S., Christensen, T., Camp, J., Mesa, J., Siddiqui, A., Tamura, Y., Sesaki, H., Wengenack, T.M., Dzeja, P.P., and Poduslo, J.F. (2012). Defects in mitochondrial dynamics and metabolomic signatures of evolving energetic stress in mouse models of familial Alzheimer's disease. *PLoS One* *7*, e32737.
- Tu, H., Nelson, O., Bezprozvanny, A., Wang, Z., Lee, S.F., Hao, Y.H., Serneels, L., De Strooper, B., Yu, G., and Bezprozvanny, I. (2006). Presenilins form ER Ca2+ leak channels, a function disrupted by familial Alzheimer's disease-linked mutations. *Cell* *126*, 981-993.
- Vais, H., Mallilankaraman, K., Mak, D.D., Hoff, H., Payne, R., Tanis, J.E., and Foskett, J.K. (2016). EMRE Is a Matrix Ca(2+) Sensor that Governs Gatekeeping of the Mitochondrial Ca(2+) Uniporter. *Cell. Rep.* *14*, 403-410.
- Vanderperre, B., Herzig, S., Krznar, P., Horl, M., Ammar, Z., Montessuit, S., Pierredon, S., Zamboni, N., and Martinou, J.C. (2016). Embryonic Lethality of Mitochondrial Pyruvate Carrier 1 Deficient Mouse Can Be Rescued by a Ketogenic Diet. *PLoS Genet.* *12*, e1006056.
- VASINGTON, F.D., and MURPHY, J.V. (1962). Ca ion uptake by rat kidney mitochondria and its dependence on respiration and phosphorylation. *J. Biol. Chem.* *237*, 2670-2677.

- Verfaillie, T., Garg, A.D., and Agostinis, P. (2013). Targeting ER stress induced apoptosis and inflammation in cancer. *Cancer Lett.* 332, 249-264.
- Vigueira, P.A., McCommis, K.S., Schweitzer, G.G., Remedi, M.S., Chambers, K.T., Fu, X., McDonald, W.G., Cole, S.L., Colca, J.R., Kletzien, R.F., Burgess, S.C., and Finck, B.N. (2014). Mitochondrial pyruvate carrier 2 hypomorphism in mice leads to defects in glucose-stimulated insulin secretion. *Cell. Rep.* 7, 2042-2053.
- Wakabayashi, T., Craessaerts, K., Bammens, L., Bentahir, M., Borgions, F., Herdewijn, P., Staes, A., Timmerman, E., Vandekerckhove, J., Rubinstein, E., *et al.* (2009). Analysis of the gamma-secretase interactome and validation of its association with tetraspanin-enriched microdomains. *Nat. Cell Biol.* 11, 1340-1346.
- Waldeck-Weiermair, M., Duan, X., Naghdi, S., Khan, M.J., Trenker, M., Malli, R., and Graier, W.F. (2010). Uncoupling protein 3 adjusts mitochondrial Ca²⁺ uptake to high and low Ca²⁺ signals. *Cell Calcium* 48, 288-301.
- Walker, E.S., Martinez, M., Brunkan, A.L., and Goate, A. (2005). Presenilin 2 familial Alzheimer's disease mutations result in partial loss of function and dramatic changes in Aβ_{42/40} ratios. *J. Neurochem.* 92, 294-301.
- Walsh, D.M., Klyubin, I., Fadeeva, J.V., Cullen, W.K., Anwyl, R., Wolfe, M.S., Rowan, M.J., and Selkoe, D.J. (2002). Naturally secreted oligomers of amyloid beta protein potently inhibit hippocampal long-term potentiation in vivo. *Nature* 416, 535-539.
- Wang, P.T., Garcin, P.O., Fu, M., Masoudi, M., St-Pierre, P., Pante, N., and Nabi, I.R. (2015). Distinct mechanisms controlling rough and smooth endoplasmic reticulum contacts with mitochondria. *J. Cell. Sci.* 128, 2759-2765.
- Wang, P.T., Garcin, P.O., Fu, M., Masoudi, M., St-Pierre, P., Pante, N., and Nabi, I.R. (2015). Distinct mechanisms controlling rough and smooth endoplasmic reticulum contacts with mitochondria. *J. Cell. Sci.* 128, 2759-2765.
- Wang, X., Su, B., Lee, H.G., Li, X., Perry, G., Smith, M.A., and Zhu, X. (2009). Impaired balance of mitochondrial fission and fusion in Alzheimer's disease. *J. Neurosci.* 29, 9090-9103.
- Wang, X., Su, B., Siedlak, S.L., Moreira, P.I., Fujioka, H., Wang, Y., Casadesus, G., and Zhu, X. (2008). Amyloid-beta overproduction causes abnormal mitochondrial dynamics via differential modulation of mitochondrial fission/fusion proteins. *Proc. Natl. Acad. Sci. U. S. A.* 105, 19318-19323.
- Wang, Y., Deng, X., and Gill, D.L. (2010). Calcium signaling by STIM and Orai: intimate coupling details revealed. *Sci. Signal.* 3, pe42.
- Weingarten, M.D., Lockwood, A.H., Hwo, S.Y., and Kirschner, M.W. (1975). A protein factor essential for microtubule assembly. *Proc. Natl. Acad. Sci. U. S. A.* 72, 1858-1862.
- Wibom, R., Lasorsa, F.M., Tohonen, V., Barbaro, M., Sterky, F.H., Kucinski, T., Naess, K., Jonsson, M., Pierri, C.L., Palmieri, F., and Wedell, A. (2009). AGC1 deficiency associated with global cerebral hypomyelination. *N. Engl. J. Med.* 361, 489-495.
- Wiederkehr, A., Szanda, G., Akhmedov, D., Mataka, C., Heizmann, C.W., Schoonjans, K., Pozzan, T., Spat, A., and Wollheim, C.B. (2011). Mitochondrial matrix calcium is an activating signal for hormone secretion. *Cell. Metab.* 13, 601-611.
- Wojda, U., Salinska, E., and Kuznicki, J. (2008). Calcium ions in neuronal degeneration. *IUBMB Life* 60, 575-590.

- Wong, A.K., Capitanio, P., Lissandron, V., Bortolozzi, M., Pozzan, T., and Pizzo, P. (2013). Heterogeneity of Ca²⁺ handling among and within Golgi compartments. *J. Mol. Cell. Biol.* 5, 266-276.
- Woods, A., Johnstone, S.R., Dickerson, K., Leiper, F.C., Fryer, L.G., Neumann, D., Schlattner, U., Wallimann, T., Carlson, M., and Carling, D. (2003). LKB1 is the upstream kinase in the AMP-activated protein kinase cascade. *Curr. Biol.* 13, 2004-2008.
- Wu, S., Sampson, M.J., Decker, W.K., and Craigen, W.J. (1999). Each mammalian mitochondrial outer membrane porin protein is dispensable: effects on cellular respiration. *Biochim. Biophys. Acta* 1452, 68-78.
- Wu, Y., Rasmussen, T.P., Koval, O.M., Joiner, M.L., Hall, D.D., Chen, B., Luczak, E.D., Wang, Q., Rokita, A.G., Wehrens, X.H., Song, L.S., and Anderson, M.E. (2015). The mitochondrial uniporter controls fight or flight heart rate increases. *Nat. Commun.* 6, 6081.
- Xia, D., Watanabe, H., Wu, B., Lee, S.H., Li, Y., Tsvetkov, E., Bolshakov, V.Y., Shen, J., and Kelleher, R.J.,3rd. (2015). Presenilin-1 knockin mice reveal loss-of-function mechanism for familial Alzheimer's disease. *Neuron* 85, 967-981.
- Xie, G.C., and Wilson, J.E. (1988). Rat brain hexokinase: the hydrophobic N-terminus of the mitochondrially bound enzyme is inserted in the lipid bilayer. *Arch. Biochem. Biophys.* 267, 803-810.
- Yao, J., Irwin, R.W., Zhao, L., Nilsen, J., Hamilton, R.T., and Brinton, R.D. (2009). Mitochondrial bioenergetic deficit precedes Alzheimer's pathology in female mouse model of Alzheimer's disease. *Proc. Natl. Acad. Sci. U. S. A.* 106, 14670-14675.
- Yeromin, A.V., Zhang, S.L., Jiang, W., Yu, Y., Safrina, O., and Cahalan, M.D. (2006). Molecular identification of the CRAC channel by altered ion selectivity in a mutant of Orai. *Nature* 443, 226-229.
- Yoo, A.S., Cheng, I., Chung, S., Grenfell, T.Z., Lee, H., Pack-Chung, E., Handler, M., Shen, J., Xia, W., Tesco, G., *et al.* (2000). Presenilin-mediated modulation of capacitative calcium entry. *Neuron* 27, 561-572.
- Yu, G., Nishimura, M., Arawaka, S., Levitan, D., Zhang, L., Tandon, A., Song, Y.Q., Rogava, E., Chen, F., Kawarai, T., *et al.* (2000). Nicastrin modulates presenilin-mediated notch/glp-1 signal transduction and betaAPP processing. *Nature* 407, 48-54.
- Zaid, H., Abu-Hamad, S., Israelson, A., Nathan, I., and Shoshan-Barmatz, V. (2005). The voltage-dependent anion channel-1 modulates apoptotic cell death. *Cell Death Differ.* 12, 751-760.
- Zampese, E., Fasolato, C., Kipanyula, M.J., Bortolozzi, M., Pozzan, T., and Pizzo, P. (2011). Presenilin 2 modulates endoplasmic reticulum (ER)-mitochondria interactions and Ca²⁺ cross-talk. *Proc. Natl. Acad. Sci. U. S. A.* 108, 2777-2782.
- Zampese, E., and Pizzo, P. (2012). Intracellular organelles in the saga of Ca²⁺ homeostasis: different molecules for different purposes? *Cell Mol. Life Sci.* 69, 1077-1104.
- Zatti, G., Burgo, A., Giacomello, M., Barbiero, L., Ghidoni, R., Sinigaglia, G., Florean, C., Bagnoli, S., Binetti, G., Sorbi, S., Pizzo, P., and Fasolato, C. (2006). Presenilin mutations linked to familial Alzheimer's disease reduce endoplasmic reticulum and Golgi apparatus calcium levels. *Cell Calcium* 39, 539-550.

- Zatti, G., Ghidoni, R., Barbiero, L., Binetti, G., Pozzan, T., Fasolato, C., and Pizzo, P. (2004). The presenilin 2 M239I mutation associated with familial Alzheimer's disease reduces Ca²⁺ release from intracellular stores. *Neurobiol. Dis.* *15*, 269-278.
- Zhang, S., Hulver, M.W., McMillan, R.P., Cline, M.A., and Gilbert, E.R. (2014). The pivotal role of pyruvate dehydrogenase kinases in metabolic flexibility. *Nutr. Metab. (Lond)* *11*, 10-7075-11-10.
- Zhang, Y.W., Wang, R., Liu, Q., Zhang, H., Liao, F.F., and Xu, H. (2007). Presenilin/gamma-secretase-dependent processing of beta-amyloid precursor protein regulates EGF receptor expression. *Proc. Natl. Acad. Sci. U. S. A.* *104*, 10613-10618.
- Zheng, H., and Koo, E.H. (2006). The amyloid precursor protein: beyond amyloid. *Mol. Neurodegener* *1*, 5.